ELyT Workshop 2018

9th annual workshop

Satillieu, France – March 6th-8th 2018

Abstract Book

Acknowledgments

This workshop was partly supported by the JSPS Core-to-Core Program, A. Advanced Research Networks, “International research core on smart layered materials and structures for energy saving”.

This workshop was also partly supported by CNRS, INSA-Lyon, Ecole Centrale de Lyon, Université de Lyon and the French region Auvergne-Rhône-Alpes.

Program of ELyT Workshop 2018

	Tuesday, March 6th		
Time	***Title***	***Presenter***	***Project***
11:00	Arrival of the chartered bus		
12:00	Lunch		
13:30	Welcome address & presentation of ELyT Global	J. Fontaine, T. Uchimoto & D. Fabrègue	
13h50	Information on Core to Core program	T. Takagi	
14:00	Elaboration and characterization of porous FeCr obtained by liquid metal dealloying	M. Mokhtari	DeProMiNa
14:20	Consolidation Process of Cu from Powder to Plate by Compression Shearing Method	H. Miki & S. Takeda	COSMIC
14:40	The choice of Nd^{3+}/Yb^{3+} rare earth ions-doped Lu_2O_3 sesquioxide as a laser material	G. Boulon	LasMat
15:00	Study of the surface roughness measurement by ultrasonic scattering on a carbon steel block	P. Guy & H. Nakamoto	PYRAMID
15:20	Micromagnetic Non Destructive Testing: joining materials models and NDT experiment	B. Ducharne & T. Uchimoto	BeNTo
15:40	Coffee break		
16:10	J-F Collaborations of Materials related to CFRP, Actuators, Adhesion and EBI processes	Y. Nishi	
16:30	Miniature-Scale Energy Generation by Magnetic Shape Memory Alloys	M. Kohl	MISTRAL
16:50	Rolling Characteristics of Neutrophils on PDMS Surface Mimicking the Endothelial Topography: Effect of Pressing Force on Cell Trajectories	J.P. Rieu & A. Shirai	MicroCell
17:10	Endovascular research and training using PVA-H models	S. Tupin	FMMD
17:30	In-situ techniques in electron microscopy	L. Joly-Pottuz	
17:50	Information about ELyT School 2018	V. Fridrici & N. Wada	
18:00	End of session		
	Poster session (see last page) & free discussions		
19:30	Dinner		

	Wednesday, March 7th		
Time	***Title***	***Presenter***	***Project***
7:30	Breakfast (last order at 8:30)		
9:00	*Invited talk:* Ab Initio Modeling of Dislocation Cores in Metals	D. Rodney	
9:30	Additive manufacturing of 3D architectured metal/ceramic biomaterials by robocasting	M. Coffigniez	
9:50	Rubber-Ice Friction mechanisms: Multi-Physical and multi-scale approach	S. Hemette	EliceTrib
10:10	Influence of the composition on properties of Co based alloys	A. Chiba & D. Fabrègue	DECCOBABA
10:30	Coffee break		
10:50	Experiments and simulations on wear mechanisms of DLC and ceramics	Y. Long & M. Kubo	SuperLub
11:10	New metallic glasses for biomedical applications	O. Baulin	
11:30	Low and ultralow friction of microcrystalline diamonds films: towards smart and tribo-resistant coatings	M. Belin & H. Miki	lofDIAMS
11:50	Robust shape optimization under squeal noise response of brake systems	F. Gillot & K. Shimoyama	MuORode
12:10	End of session		
12h30	Lunch		
14:00	*Invited talk:* Ultrahigh-temperature materials research in Tohoku University	K. Yoshimi	
14:30	Design of interface structure of fiber-reinforced polymer blend	H. Kosukegawa	DESIRE
14:50	Mechanical characterization of Inter-particle sintering of Ultra High Molecular Weight Polyethylene (UHMWPE)-Fumed nano-alumina (FNA) composites processed under different interfacial loading conditions	K. Ogawa & O. Lame	PolymCold SprayCoat
15:10	Effects of temperature elevation on drilling of acrylic composite materials for bone biomodel	Y. Muramoto	BoneDrill
15:30	Piping sYstem, Risk management based on wAll thinning MonItoring and preDiction	T. Takagi & P. Guy	PYRAMID
15:50	Coffee break		
16:20	Experimental Study on Active Control of Protein Mass Flux	A. Komiya	
16:40	Nonlinear Ultrasonic Phased Array for Imaging Closed Cracks	Y. Ohara	
17:00	Surface Integrity and Structural Integrity	T. Shoji	
17:20	Magneto-mechanical energy conversion in magneto-rheological elastomers: effect of matrix change	G. Sebald	MARECO
17:40	Numerical Analysis for Ultrasonic Testing using EMAT under Extremely High Temperature	F. Kojima	
18:00	End of session		
	Free discussions		
19:00	Dinner		

	Friday 8th		
Time	***Title***	***Presenter***	***Project***
7:30	Breakfast (last order at 8:30)		
9:00	Wall turbulence nature and its control aimed at laminar wing technology	A. Yakeno	
9:20	Mechanism Analysis Technique for Fuel Diversification: In-situ Observation of Tribo-chemical Reaction in Methanol Blended Gasoline	K. Yoshida	
9:40	Application of big data analysis to NDT data pool	T. Soma	
10:00	Optimizing surface finish to Prevent SCC initiation in energy industries	H. Abe, B. Ter-Ovanessian	OPSCC
10:20	Coffee break		
10:50	Thermofluid characteristics of a flow channel with finger-stacked structure	S. Ebara	
11:10	Thermomechanical modelling of High Molecular Weight semi-crystalline polymers - Application to Cold-Spray simulation	C. Bernard	PolymCold SprayCoat
11:30	Concluding remarks		
11:50	Wrap up		
12:00	Lunch		
13:30	Gathering for departure		
14:00	Departure of the chartered bus		

List of posters

Number	***Title***	***Presenter***	***Project***
1	Consolidation Process of Cu from Powder to Plate by Compression Shearing Method	S. Takeda	COSMIC
2	Texturation multi-échelle des surfaces et effet sur le comportement tribologique d'un cartilage artificiel	L. Jay	TriArtiJoints
3	MIP NDT Characterization and Modelling	B. Gupta	BeNTo
4	Topology optimization for intracranial stent based on computational fluid dynamics	M. Ohta	
5	Study on experimental evaluation of repassivation condition of chloride stress corrosion cracking	T. Ohira	

Tuesday, March 6th – Afternoon

First session – 13:30-15:40

Elaboration and characterization of porous FeCr obtained by liquid metal dealloying

Project **DeProMiNa :** De alloying to produce micro and nano porous metal

KATO Hidemi
WADA Takeshi
MOKHTARI Morgane

IMR
Tohoku University
Japan

MAIRE Eric
LE BOURLOT Christophe
MOKHTARI Morgane

MATEIS
INSA LYON
France

Abstract :

1. Introduction

Nanoporous metals have attracted considerable attention for their excellent functional properties [1]. The most promising technique used to prepare such nanoporous metals is dealloying in aqueous solution. Nanoporous noble metals including *Au* have been prepared from binary alloy precursors [2]. The less noble metals, unstable in aqueous solution, are oxidized immediately when they contact water at a given potential so this process is only possible for noble metals. Porous structures with less noble metals such as *Ti* or *Fe* are highly desired for various applications including energy-harvesting devices [3]. To overcome this limitation, a new dealloying method using a metallic melt instead of aqueous solution was developed [4]. Dealloying in the metallic melt is a selective dissolution phenomenon of a mono-phase alloy solid precursor: one component (referred as soluble component) being soluble in the metallic melt while the other (referred as targeted component) is not. When the solid precursor contacts the metallic melt, only atoms of the soluble component dissolve into the melt inducing a spontaneously organized bi-continuous structure (targeted+sacrificial phases), at a microstructure level. This sacrificial phase can finally be removed by chemical etching to obtain the final nanoporous materials. Because this is a water-free process, it has enabled the preparation of nanoporous structures in less noble metals such as *Ti*, *Si*, *Fe*, *Nb*, *Co* and *Cr*.

2. Experimentation, discussion

In this study, $(Fe_{80}Cr_{20})_{30}Ni_{70}$, $(Fe_{80}Cr_{20})_{50}Ni_{50}$ and $(Fe_{80}Cr_{20})_{70}Ni_{30}$ precursors ingots were dealloyed 1h at 1093K for 1h in a *Mg* melt bath under a high-purity *He* atmosphere to give *FeCr-Mg* bicontinous structure. The selective etching step was carried out using highly concentrated nitric acid to dissolve the solid-state solution of *Mg*, resulting in microporous $Fe_{80}Cr_{20}$. Porous samples obtained from $(Fe_{80}Cr_{20})_{30}Ni_{70}$, $(Fe_{80}Cr_{20})_{50}Ni_{50}$ and $(Fe_{80}Cr_{20})_{70}Ni_{30}$ precursor will be referred as respectively 30%FeCr, 50%FeCr and 70%FeCr. To characterized the microstructure samples were 3D imaged by Xray tomography.

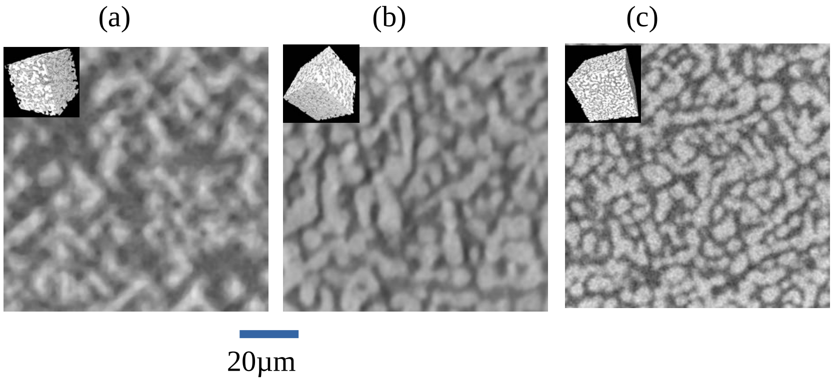

Figure 1 : Images extracted from Xray tomography scan and 3D view in inset of (a) 30%FeCr (b) 50%FeCr (c) 70%FeCr

Figure 1 shows one reconstructed slice for each sample extracted from the reconstruction and a 3D in inset. Two phases are visible. The lighter phase corresponds to the *FeCr* phase and the darker phase to the air.

From theses images morphological parameters can be extracted. Figure 2 presents the phase thickness distributions of *FeCr* and *Air* phases for all samples. The phases display a unimodal thickness distribution. *FeCr* phase thickness distribution are similar for all samples : *i.e.* ligaments size are independent of precursor composition. Because *FeCr* phase thickness distribution are similar and materials density are different, pores distributions must be dependent of precursor composition as shown on Figure 2. The average ligaments size is 4.8±0.3µm for 1h dealloying at 1093K and this value depends only of dealloying time and temperature.

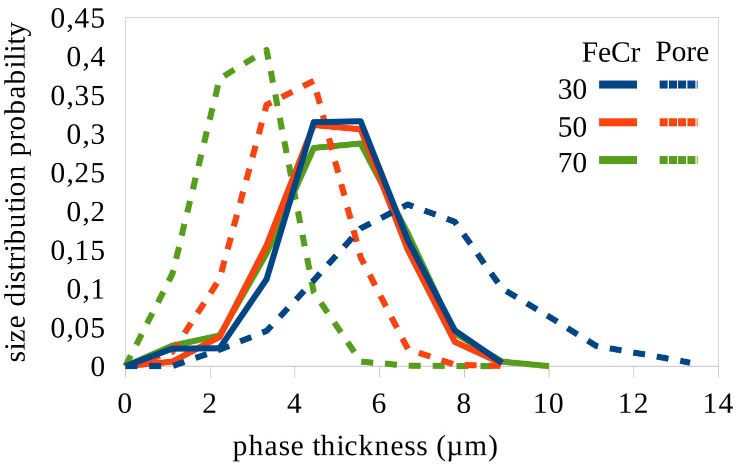

Figure 2: Evolution of phase thickness for different precursor composition

References

[1] J. Snyder, T. Fujita, M. Chen, J. Erlebacher. Nat. Mater., 9 (2010) 904-907
[2] A.J. Forty. Nature, 282 (1979) 597-598
[3] K. Sivula, R. Zboril, F.L. Formal, R. Robert, A. Weidenkaff, J. Tucek, J. Frydrych, M. Grätzel. J. Am. Chem. Soc., 132 (2010) 7436-7444
[4] T. Wada, K. Yubuta, A. Inoue, H. Kato. Mater. Lett., 65(2011) 1076-1078

COmpression-Shearing Method – understanding Interfaces in metal Composites

ELyT Global Project COSMIC

Surface and interfaces
Materials and structure design

	*FONTAINE Julien, Dr. Laboratoire de Tribologie et Dynamique des Systèmes, Ecole Centrale de Lyon, 36 avenue Guy de Collongue, 69134 Ecully cedex, France*		*MIKI Hiroyuki, Assoc Prof. Frontier Research Institute for Interdisciplinary Sciences (FRIS), Tohoku University, Aramaki aza Aoba 6-3, Aoba-ku, Sendai, 980-8578, Japan*
	*MIYAZAKI Takamichi, Dr. School of Engineering, Tohoku University, 6-6 Aramaki aza Aoba, Aoba-ku, Sendai, 980-8579, Japan*		*GUIBERT Matthieu, Laboratoire de Tribologie et Dynamique des Systèmes, École Centrale de Lyon, 36 avenue Guy de Collongue, 69134 Ecully cedex, France*
	*TAKEDA Sho, Graduate school of engineering, Tohoku University, 6-6 Aramaki aza Aoba, Aoba-ku, Sendai, 980-8579, Japan École Centrale de Lyon 36 Avenue Guy de Collongue, Écully, 69134, France*		

Abstract :

1. Introduction

In recent years, requirements for the material property such as a high strength and/or high toughness are increasing with development of machine and mechanical system. Materials processing is one of the important technique to improve those properties. Many scientists are working in this field and several processing for manufacturing metal and composite such as casting and powder metallurgy have been proposed.

Our research group has been focusing on a novel powder molding technique, COmpression Shearing MEthod at Room Temperature (COSME-RT) as the method to consolidate metal powder into thin plate directly. COSME-RT is the method for forming a thin plate using biaxial force which gives compression stress and shearing strain to raw metal powder simultaneously at room temperature in ambient atmosphere. In this method, dissolving at high temperature is not required and metal plate can be formed without coarsening of crystal grain and making compound. Consolidated metal plates indicate high mechanical strength according to refined crystal grains.

2. Scope

COSME-RT has attracted attention as the novel method of solidifying metal powder. The metal powders are solidified by the enforced plastic flow, and external heating is not required. Therefore, COSME-RT is considered as susceptible to form composite material which is keeping each of the individual characteristic of the original powder materials.

In this project, the possibility of compacting the metal powder and the composite between metal and other material, polymer, ceramics and compound etc., using COSME-RT will be investigated, to clarify the interparticle bonding of powder particles during the compression and shearing process. With development of this technique, we would like to form the multifunction material which shows the good electrical and friction properties by a simple solidifying process as a practical material.

In relation to this project, Mr. Sho TAKEDA attends a Double Doctoral Degree (DDD) program between the Graduate School of Engineering, Tohoku University, Japan and École Centrale de Lyon (Laboratoire de Tribologie et Dynamique des Systèmes), France from 2015. He recently finished writing his thesis based on our collaboration research and two research papers published [1] and accepted [2] in 2017. At this workshop, we would like to make presentation about the part of his work as our latest collaboration results.

Acknowledgments

Extensive studies on the COSME-RT by Prof. Takeishi (Chiba Institute of Technology), Prof. Nakayama and Dr. Horita (Shinshu University) are gratefully acknowledged.

This work was partly supported by the JSPS KAKENHI Grant Number 16H04504, the JSPS Core-to-Core Program, A. Advanced Research Networks, "International research core on smart layered materials and structures for energy saving" and the International Collaborative Research Project of Frontier Research Institute for Interdisciplinary Sciences, Tohoku University, Japan.

References :

[1] Sho Takeda, Hiroyuki Miki, Hiroyuku Takeishi, Toshiyuki Takagi, *Tribology Online* **12**(2017) 29-36.

[2] Sho Takeda, Hiroyuki Miki, Julien Fontaine, Hiroyuku Takeishi, Toshiyuki Takagi, *Tribology Online*, (Accepted).

The choice of Nd^{3+}/Yb^{3+} rare earth ions-doped Lu_2O_3 sesquioxide as a laser material

George Boulon
iLM, Université Claude Bernard Lyon 1

No abstract

A study of surface roughness measurement on a carbon steel block by ultrasonic scattering from the opposite side

Project ELyT lab : PYRAMID
(Piping system, risk management based on wall thinning monitoring and prediction)

	*Hiroyuki NAKAMOTO, Graduate School of System Informatics, Kobe University (1-1 Rokkodai-cho, Nada, Kobe 657-8501, Japan) and Laboratoire Vibrations Acoustique, INSA-Lyon (25 bis, av. J. Capelle F-69621 Villeurbanne Cedex, Lyon, France)*		*Philippe GUY, Laboratoire Vibrations Acoustique, INSA-Lyon (25 bis, av. J. Capelle F-69621 Villeurbanne Cedex, Lyon, France)*

Abstract :

1. Introduction

Piping system in nuclear power plants is one of important components. Since liquids flow in the piping system, Flow Accelerated Corrosion (FAC) occurs pipe-wall thinning through many years of use. To evaluate the pipe-wall thinning, thickness measurement is performed by ultrasonic testing devices. In the thickness measurement, the pulse-echo method determines thickness from time-of-flight and ultrasonic velocity. Although the pulse-echo method uses only the receiving time of the ultrasonic signal, the signal amplitude has also the information of ultrasonic attenuation. The attenuation depends on propagation distance, backscattering, grain size of carbon steel and so on. If one effect varies and the others are constant, we can evaluate the effect from the amplitude.

The surfaces thinned by FAC have been reported to have various roughness [1]. The roughness provides us with detail characteristics of FAC. In this study, we aim to measure not only thickness but also roughness of pipe-wall thinning from ultrasonic signal.

2. Theory, experimentation, discussion

The following theory is based on Nagy's work [2]. We consider a randomly rough surface of a solid $h(x,y)$ positioned in the z=0 plane of an x, y, z coordinate system as shown in Fig. 1. The rough surface is supposed to be geometrically flat over an area A, and the surface quality is characterized by a roughness parameter h:

$$h^2 = \frac{1}{A}\int_A \int h^2(x,y)dxdy, \qquad (1)$$

where h is a root-mean-squared roughness parameter. When a plane wave propagates and reflects at the rough surface on the opposite side, the wave is perturbed by random phase modulation $\phi_r(x,y)$. The coherent specular wave is given as

$$R = \frac{R_0}{A}\int_A \int e^{i\phi_r(x,y)}dxdy, \qquad (2)$$

where R_0 is the complex amplitude without surface roughness. According to the phase perturbation approximation, the roughness induced phase modulation is expressed by $\phi_r(x, y) = -2h(x, y)k$, where k denotes the wavenumber in the carbon steel. Here, we presumed that the correlation length of the rough surface is high with respect to the wavelength. In addition, presuming that the surface profile is an ergodic random process, we obtain the following equation by the probability density function $p(\phi)$ of the random phase modulation.

$$R = R_0 \int_{-\infty}^{\infty} e^{i\phi} p(\phi) d\phi. \tag{3}$$

When the probability density function is the Gaussian distribution, the solution is given by

$$R = R_0 e^{-\phi_r^2/2}. \tag{4}$$

If the related attenuation R/R_0 is obtained, the roughness parameter is determined by Eq. (4).

In an experiment, we obtained reflected waves on 5 specimens by an ultrasonic device (Prisma, Sonatest co.). The specimens are carbon-steel rectangular blocks with 20 mm thickness and 40×40 mm^2 area. Each specimen has a roughness surface with periodical flaws. The specimens are called #1, #2, #3, #4, #5, and their roughness parameters are 13.26, 21.48, 24.91, 34.12 and 52.80 μm, respectively. The ultrasonic longitudinal velocity was 5800 m/s and the actual frequency was 4.88 MHz. The probe was placed on the flat surface of the specimen through a contact medium and detected the first reflected wave from the opposite rough surface. The detection was conducted for 10 times. The average amplitude was normalized by the average amplitude of a specimen without roughness. The relationship between the roughness parameter value and the attenuation is shown in Fig. 2. The line denotes a theoretical relation by Eq. (4). The experimental results have a good agreement with the theory. Assuming that we estimated the roughness value from the attenuation, the ratios of errors to true roughness values were 58.8, 18.0, 34.6, 2.1, 1.2% to #1, #2, #3, #4, #5, respectively. Since the gradient of the theoretical cave in the range of low roughness value was low, the error ratios of #1, #2 and #3 were relatively high. These correlation lengths are too low for the theoretical assumption. In addition, the high error ratios indicate that the estimate of low roughness requires high-precision amplitude measurement. Normally, ultrasonic devices and probes measure thickness by inspector's hand. The high-precision amplitude measurement in this study is difficult for ultrasonic devices.

In future works, we use an electromagnetic acoustic transducer (EMAT) instead of ultrasonic devices. The EMAT fixed on a specimen has a potential of a high-precision amplitude measurement. The EMAT also has a wide-range frequency which is suitable for the theoretical presumption.

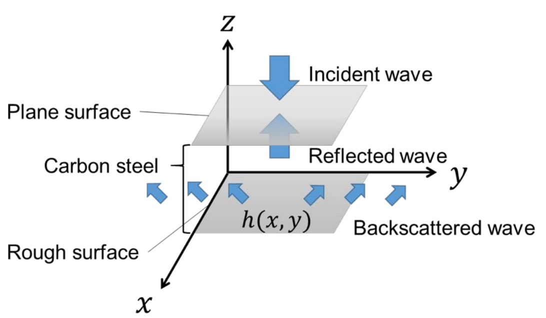

Fig. 1 Coordinate system with rough surface for wave reflection.

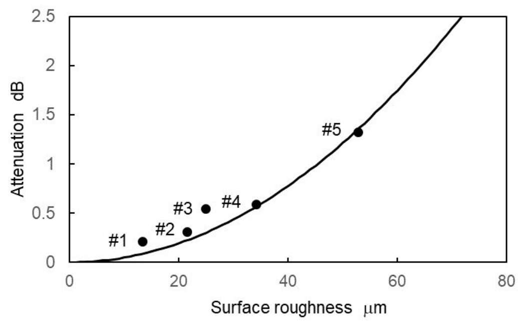

Fig. 2 Relationship between surface roughness and surface roughness induced attenuation.

References :

[1] B. Poulson, *Int. J. of Nuclear Energy*, **2014**(2014), Article ID 423295.
[2] P. B. Nagy and L.o Adler, *J. Acoust. Soc. Am.* **82**(1987) 193-197.

Micro-magnetic non-destructive needle probes technique for materials characterization.

Project ELyTGlobal BENTO

	TENE DEFFO YVES ARMAND _ *Université de Lyon, INSA-Lyon, LGEF EA682* _ Buéa University, Cameroun	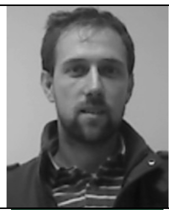	DUCHARNE Benjamin *Université de Lyon, INSA-Lyon, LGEF EA682*
	*GUPTA Bhaawan* *- ELyTMaX UMI 3757, CNRS - Université de Lyon - Tohoku University, International Joint Unit,* *- Université de Lyon, INSA-Lyon, LGEF EA682*		*UCHIMOTO Tetsuya* *- ELyTMaX UMI 3757, CNRS - Université de Lyon - Tohoku University, International Joint Unit* *- Institute of Fluid Science, Tohoku University*
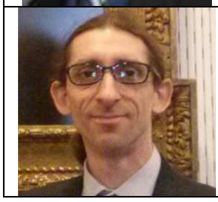	*SEBALD Gael* *ELyTMaX UMI 3757, CNRS - Université de Lyon - Tohoku University, International Joint Unit, Tohoku University*		*TAKAGI Toshiyuki* *- ELyTMaX UMI 3757, CNRS - Université de Lyon - Tohoku University, International Joint Unit* *- Institute of Fluid Science, Tohoku University*

The constant increase in inline production rates, along with an improvement of quality standards have revealed a huge industrial need for precise and systematic inspection of steel products. Different techniques such as destructive or nondestructive testing for the control of the manufactured products quality already exist. The objective of nondestructive testing (NDT) is to evaluate both internal and external fatigue states of the inspected parts without affecting their integrity. Nondestructive testing & evaluation (NDT&E) using electromagnetic techniques is based on the micromagnetic response of material properties such as microstructure and residual stress under application of external magnetic fields [1][2].

Several years ago Japanese researchers [3]-[5] returned to an old Austrian patent of Werner [6]. Werner proposed to form a one-turn coil by using two pairs of needles, but the application of his invention was difficult, due to relatively small (less than mV) output signal of the sensor. Experimental and theoretical analyses [6] proved that today this method can be used with satisfactory results. This point probe method consists in application of probe needles to a conductive sheet of magnetic material, forming two point contacts. Based on the potential difference produced by eddy currents generated by ac magnetization, it is possible to measure the flux density in the area surrounded by points 1-2-3-4 shown in Figure 1.

In a uniform magnetization model (a model having a structure without magnetic domains), the voltage detected by the needle probes is equivalent to half that measured by a search coil (one turn) wound around the 1-2-3-4 area. Assuming that the specimen structure has 180° magnetic domains, the voltage displays a stepped behavior depending on the locations of measurements in the form of deviations from the average magnetization. Such deviations can reach considerable magnitudes, especially if the span of the probe needles is small or if the ratio of the 180°-domain wall spacing to the sheet thickness is large. According to an analysis of eddy current distribution, the measurement error in the point probe method is slightly greater than in measurements made by a search coil, but not so great as to create problems from the standpoint of practical use. It is stated that when the span between probes is about 10 mm, it is possible to evaluate localized flux densities in grain-oriented electrical steel sheets.

However, due to limitations in the technical developments, this technique has never been used as a micro magnetic sensor principle for nondestructive evaluation. The recent improvements in the field of analog electronics and numeric analysis enabled this method to produce reliable results. Due to the potential for making localized measurements associated to its directional behavior, this technique is well suited to NDT applications. Hence, it is legitimate to assume that by changing the orientation of the two point probe techniques, micro-residual stresses can be detected directionally and from a set of experimental results, the depth defect could be determined.

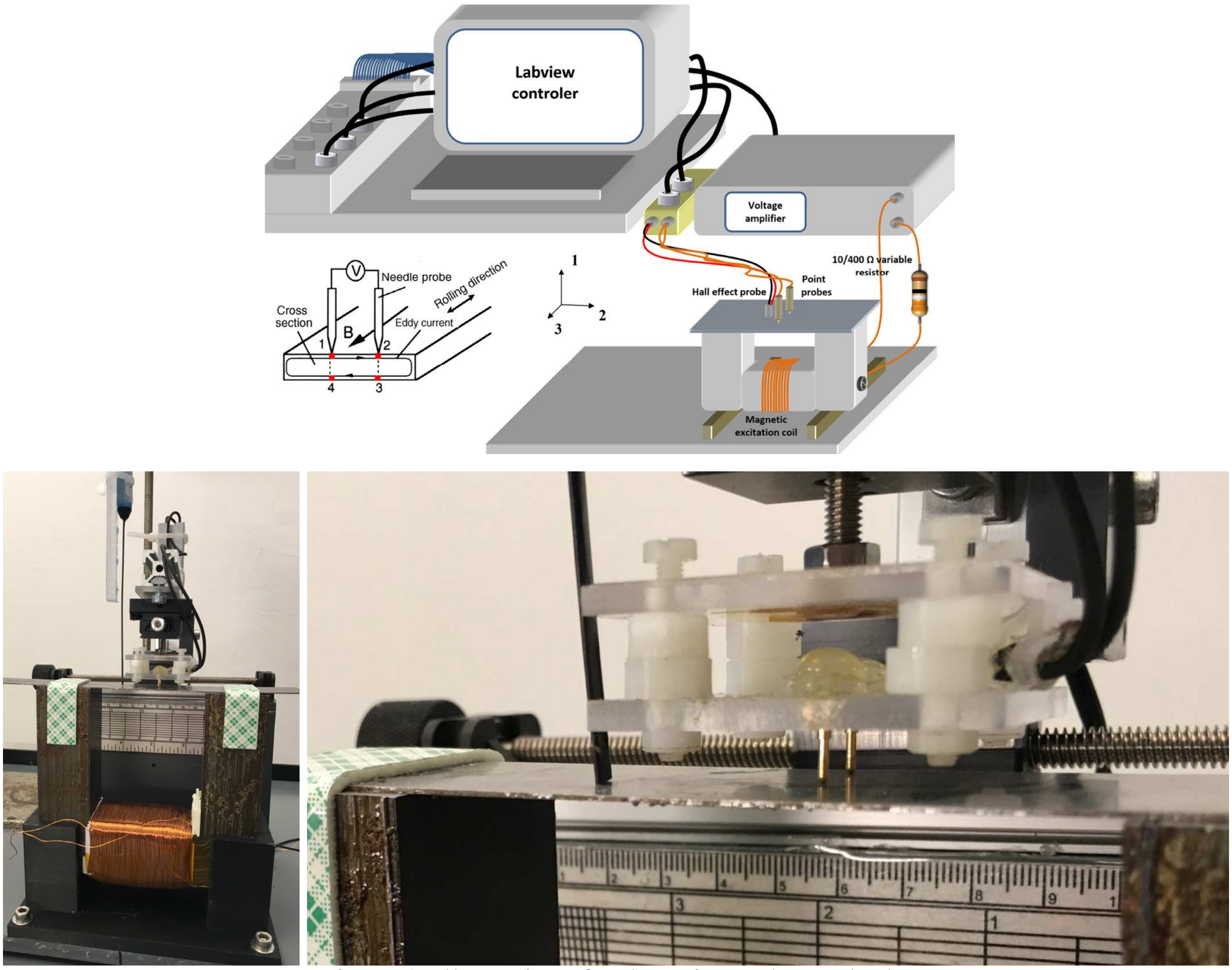

Figure 1: Illustrations for the point probe method.

References:

[1] B. Gupta, B. Ducharne, G. Sebald, T. Uchimoto, “A space discretized ferromagnetic model for non-destructive eddy current evaluation”, IEEE Trans. on. Mag, vol. 54 Iss. 3, 2018.

[2] B. Ducharne, MQ. Le, G. Sebald, PJ. Cottinet, D. Guyomar, Y. Hebrard, “Characterization and modeling of magnetic domain wall dynamics using reconstituted hysteresis loops from Barkhausen noise”, J. of Mag. And Mag. Mat., pp. 231-238, 2017.

[3] T. Yamaguchi, K. Senda, M. Ishida, K. Sato, A. Honda and T. Yamamoto, “Theoretical analysis of localized magnetic flux measurement by needle probe”, J. Physique IV, 8 717–20 Pr2, 1998.

[4] K. Senda, M. Ishida, K. Sato, M. Komatsubara and T. Yamaguchi, “Localized magnetic properties in grain-oriented silicon steel measured by stylus probe method”, Trans. IEEE Japan, pp. 941–50, 1997.

[5] K. Senda, M. Ishida, K. Sato, M. Komatsubara and T. Yamaguchi, “Localized magnetic properties in grain-oriented electrical steel measured by needle probe method”, Electr. Eng. Japan, 126 942–9, 1999.

[6] E. Werner, ‘Einrichtung zur Messung magnetischer Eigenschaften von Blechen bei Wechselstrom magnetisierung (The device for testing of electrical steel magnetized by AC field)’, Austrian patent no. 191015, 1957.

[7] H. Pfützner and G. Krismanic, ‘The needle method for induction tests – sources of error’, IEEE Trans. Mag., 40 1610–6, 2004.

Tuesday, March 6th – Afternoon

Second session – 16:10-18:00

J-F Collaborations of Materials related to CFRP, Actuators, Adhesion and EBI processes

Project ELyT lab : MX2– Study of Effects of HLEBI on safety of CFRP-J-F-3(Tokai U./*ECL,*), M13 – High strain electrostrictive polymers: elaboration modeling: J-F-2(Tokai/ LGEF, *INSA Lyon,*), MX1– Study of Effects of HLEBI on properties of Polymers- J-F-1(Tokai/ *MATEIS, INSA Lyon*)

	***Yoshitake Nishi**, Dr. Engi., Prof. Tokai University, Hiratsuka, JAPAN, Address:west@keyaki.cc.u-tokai.ac.jp*		***Kaori Yuse**, Ph.D.Associate Prof. INSA Lyon, LGEF, FRANCE Address: kaori.yuse@insa-lyon.fr*
	***Masae Kanda**, Ph.D.(INSA Lyon) Assistant Prof. Chubu University, JAPAN, Address: kanda@isc.chubu.ac.jp*		***Daniel Guyomar**, Ph.D.Prof. INSA Lyon, LGEF,France, Address: daniel.guyomar@insa-lyon.fr*
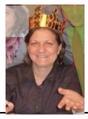	***Michelle Salvia**, Ph.D. Associate Prof. Ecole Centrale de Lyon, Ecully Cedex 69134, France,*		***Jean-Yves CAVAILLE**, Ph.D. Prof. INSA Lyon, MATEIS, Jean Capelle, 69621 Villeurbanne cedex FRANCE*

Our target of the projects since 1998 has been the rising the international activities of Research & corresponding Education of finally getting PhD in INSA Lyon, France, for my former master course student, Assistant Prof. Kanda.

Based on the collaboration with ECL (M. Salvia), the CFRPs (fiber reinforced polymer) have been investigated. They are ①Enhanced Tensile Strength of Titanium/Polycarbonate Joint Connected by Electron Beam Activated Cross-Weave Carbon Fiber Cloth Insert (H. Hasegawa, M. C. Faudree, Y. Enomoto, S. Takase, H. Kimura, A. Tonegawa, Y. Matsumura, I. Jimbo, M. Salvia and Y. Nishi , Mater. Trans. 58(11) (2017) 1606-1615).② Improvement of Bending Modulus and Impact Value of Injection-Molded Short Carbon Fiber Reinforced Polyetheretherketone (PEEK) with Homogeneous Low-Voltage Electron Beam Irradiation (Y. Nishi, R. Ourahmoune, M. Kanda, J.H. Quan, M.C. Faudree and M. Salvia; *Mater. Trans.*, **55** (8) (2014) 1304-1310), ③Effects of Electron Beam Irradiation on Elasticity of CFRTP (CF/PEEK), (H. TAKEI, M. Salvia, A. Vautrin, A.Tonegawa, Y.Nishi; Mater. Trans. **52** (4) 2011 pp734-739), ④ Effects of Electron Beam Irradiation on Impact Value of Novolak-Type Phenol CFRTP（Y. Nishi, H. Takei, K. Iwata, M. Savia, A. Vautron；Mater.Trans.51 (12) (2010) 2259-2265）and ⑤ Effects of Electron Beam Irradiation on Impact Value of Carbon Fiber Reinforced Thermoplastic Polyetheretherketone (Y. Nishi, H. Takei, K. Iwata, M.Salvia, A. Vautrin; Mater.Trans.**50** (12) (2009) 2826-2832).

Based on the collaboration with LGEF, INSA de Lyon (D. Guyomar & K. Yuse), the Sensor and Actuators have been investigated and constructed with ①Effect of 100 keV Class Electron Beam Irradiation on Impact Fatigue Behavior of PZT Ceramics (N. Tsuyuki，A. Takahashi，S. Takase，D. Kitahara，M. Kanda，N. Inoue，K. Yuse, D. Guyomar, A. Tonegawa, Y. Matsumura and Y. Nishi; Materials Trans.Vol.59, No3(2018) in press), ②An Improved H_2-Gas Pressure Operated $LaNi_5$ Powder-Dispersed Polyurethane/Titanium 2-Layer Actuator with Reversible Giant and Rapid Expansion by Hydrogenation (Y. Nishi, J. Ohkawa, M. C. Faudree, M. Kanda, K. Yuse, D. Guyomar, H-H. Uchida; Materials Transactions, Vol.59 No.01 (2018) pp.129-135), ③Improvement of Electric Field Induced Compressive Electrostriction of Polyurethane Composites Film Homogeneously Dispersed with Carbon Nanoparticles, (M. Kanda, K. Yuse, B. Guiffard, L. Lebrun, Y. Nishi, D. Guyomar: Materials Transactions,Vol.56 No.12 (2015) pp.2029-2033.), ④Actuation abilities of multiphasic electroactive polymeric systems, (M. Lallart, J.-F. Capsal, A. K. Mossi Idrissa, J. Galineau, M. Kanda, D. Guyomar; Journal of Applied Physics,Vol.112 (2012) 094108), ⑤Solidification Thickness Dependent Electrostriction of Polyurethane Films (M. Kanda, K. Yuse, B. Guiffard, L. Lebrun, Y. Nishi, D. Guyomar: Materials Transactions, Vol.53 (2012) pp1806-1809), ⑥ Modeling of thickness effect and polarization saturation in electrostrictive polymers,(M. Lallart, J.-F. Capsal, M. Kanda, J. Galineau, D. Guyomar, K. Yuse, B. Guiffard: Sensors and Actuators B: Chemical, Vol.171-172 (2012) pp739-746), ⑦The compressive electrical field electrostrictive coefficient M_{33} of electroactive polymer composites and its saturation versus electrical field, polymer thickness, frequency and fillers, (D. Guyomar, P.-J. Cottinet, L. Lebrun, C. Putson, K. Yuse, M. Kanda, Y. Nishi: Polym. Adv. Technol, (2011) DOI 10.1002/pat.1993), ⑧Thickness effect on electrostrictive polyurethane strain performances: A three-layer model, (D. Guyomar, K. Yuse, M. Kanda , Sensors and Actuators A,Vol.168 (2011) pp307-312.), ⑨ Development of large-strain and low-powered electro-active polymers (EAPs) using conductive fillers, (K. Yuse, D. Guyomar, M. Kanda, L. Seveyrat, B. Guiffard: Sensors and Actuators A,Vol.165 (2011) pp147-154.), ⑩ Focus on the electrical field-induced strain of electroactive polymers and the observed saturation, (D. Guyomar, K. Yuse, P.-J. Cottinet, M. Kanda, L. Lebrun, J. Applied Physics,Vol.108 (2010) 114910.), ⑪ Reversible Bending Motion of Unimorph Composites Driven by Combining $LaNi_5$ Alloy Powders Dispersed Polyurethane and Thin Supporting Copper Sheet under Partial Hydrogen Gas Pressure, (J. Okawa, M. Kanda, K. Yuse, H-H. Uchida, D. Guyomar, Y. Nishi , Materials Transactions Vol.51 (2010) pp994-1001.), and ⑫ Giant Bending Strain of Reversible Motion of Uni-Morph Soft Mover Composites Driven by Hydrogen Storage Alloy Powders Dispersed in Polyurethane Sheet, (Y. Nishi, S. Ohkawa, M. Kanda, A. Shimazu, R. Suenaga, Y. Ebihara, D. Kubo, H.H. Uchida, K. Yuse, D. Guyomar: Materials Transactions, Vol.50 (2009) pp2460-2465).

Based on the collaboration with MATEIS, INSA de Lyon (J-Y Cavaille), the Adhesion and strengthening of polymers induced by EBI process have been investigated and constructed with ①Adhesion of Polyethylene/Polyethylene Terephthalate (PE/PET) Laminated Sheets by Homogeneous Low Potential Electron Beam Irradiation (HLEBI) Prior to Assembly and Hot-Press above Melting Point, (S. Takase, H. T. Uchida, A. Yagi, M. Kanda, O. Lame, J.-Y. Cavaille, Y. Matsumura, Y. Nishi: Materials Transactions, Vol.58 No.07 (2017) pp.1055-1062), ② Effects of Homogeneous Low Energy Electron Beam Irradiation (HLEBI) on Adhesive Force of Peeling Resistance of Laminated Sheet with Polyethylene (PE) and Austenitic 18-8 Stainless Steels (C. Kubo, M. Kanda, O. Lame, J-Y. Cavaille, Y. Nishi: *Materials Transactions*, 57(3) (2016) 373-378), ③Evaluation of the Tensile Strength of Electron Beam Irradiated Powdered Ultra High Molecular Weight-Polyethylene (UHMWPE) Prior to Sintering (M. Kanda, T. Deplancke, O. Lame, Y. Nishi and J-Y. Cavaille, *Materials Transactions*, 56 (9) (2015) 1505-1508), ④High Electric Conductive PMMA Composites without Impact Value Decay by Dispersion of Copper Powder, (Y. Nishi, Y. Ebihara, N. Kunikyoh, M. Kanda, K. Iwata, K. Yuse, B. Guiffard, L. Lebrun, D. Guyomar, Materials Transactions, Vol.51 (2010) pp1437-1442.), ⑤Impact Value of High Electric Conductive ABS Composites with Copper Powder Dispersion Prepared by Solution-Cast Method, (Y. Nishi, N. Kunikyo, M. Kanda, L. Lebrun, D. Guyomar: Materials Transactions, Vol.51 (2010) pp165-170), and ⑥ Effects of Homogeneous Low Voltage Electron Beam Irradiation on Brazilian Bending Strength of Liquid Quenched Ten Mega Molecular Weight-Polyethylene (TMMW-PE) (Y. Nishi, M. Kanda, K. Shiraishi, S. Ishii, M. Uyama, S. Inui, M. C. Faudree, O. Lame and J-Y. Cavaille, unpublished data).

Future contribution to J-F Collaboration: Our Research unit is constructed with Tokai U. < A. Prof. Uchida (CFRP and polymer adhesion), Prof. Tsuchiya (PZT film, fine needle), Prof. Kimura (Solar car), Prof. Takashiri (Thermoelectric power device), Prof. Kikugawa (Bioadaptable materials), Profs. Horisawa, Shibuya & Tonegawa (plasma electrode engine for interplanetary space ship)> and Prof. H-H. Uchida (Hydrogen Storage alloy), as well as Ibaraki University <Prof. Ohta & A.Prof.Nishi (Thermal conductivity and viscosity) and Chubu University <Prof. Inoue & A. Prof. Kanda (Direct current system for Superconducting wire)>.

MIniature-Scale Energy GeneraTion by Magnetic Shape MemoRy ALloys

ELyT Global Project MISTRAL

Materials and structure design
Simulation and modeling

	*Manfred KOHL, Prof. Institute of Microstructure Technology(IMT), Karlsruhe Institute of Technology(KIT), Hermann-von-Helmholtz-Platz 1 76344 Eggenstein-Leopoldshafen*		*Hiroyuki MIKI, Assoc Prof. Frontier Research Inst. for Interdisc. Sci. (FRIS), Tohoku University, Aramaki asa Aoba 6-3, Aoba-ku, Sendai, Japan*
	*Mickaël Lallart, Assoc Prof. Laboratory of Electrical Engineering and Ferroelectricity (LGEF - EA 682), INSA-Lyon, F-69621 Villeurbanne, France*		*Marcel GUELTIG, Dr. Institute of Microstructure Technology(IMT), Karlsruhe Institute of Technology(KIT), Hermann-von-Helmholtz-Platz 1 76344 Eggenstein-Leopoldshafen*
	*Makoto OHTSUKA, Assoc Prof. Institute of Multidisciplinary Research for Advanced Materials(IMRAM), Tohoku University, Katahira 2-1-1, Aoba-ku, Sendai, Japan*		

Abstract :

1. Introduction

Recently, attaining multi-functionality and improving functionality for the conventional mechanical system have been required with the development of science and technology. However, the performance enhancement usually brings complication and enlargement of the system. Our research group have focused on the "smart" concept as a keyword of function improvement. It aims at improving reliability and stability of the system by functional advancement of composing elements.

Functional materials are the novel material, which provide a new function and realize simplification and miniaturization for the mechanical system alternatively. Examples of the functional materials are described in the following: Shape memory alloys, piezoelectric material, liquid crystal and magnetic material, etc. These show the property variation and/or the special function on certain conditions, such as temperature change, and electric field applied, and so on. At the present, there are few materials put to practical use. The research of development and application on these materials will become more important in the near future.

The shape memory alloy is a material with the function of the shape memory effect and the superelasticity, which originates from the martensitic transformation. Shape recovery force and shape reversibility are the typical properties of the shape memory alloy. From these functions, the shape memory alloys are applied over industrial machinery, such as an automobile, an electrical equipment, and a medical equipment.

Recently, ferromagnetic shape memory alloy (FSMA) attract attention as a new SMA with the magnetically induced shape memory effect [1]. Using FSMA as the actuator element, it is expected that high-speed operation and high stress load become the possible. As the example of the shape memory alloy in which magnetic property is greatly related to mechanism of the generation of shape memory effect, Ni-Mn-X (X = In, Sn) type FSMAs have been found and their meta-magnetic phase transition (MT) has been observed from ferromagnetic austenitic (A) phase to antiferromagnetic or paramagnetic martensitic (M) phase [2]. FSMAs are expected to exhibit the shape memory effect (SME) associated with the reverse MT induced by a magnetic field [3]. For the properties described above, metamagnetic shape memory alloys (MSMAs) are attractive for micro-actuation due to their multifunctional properties [4, 5].

2. Outline of the research

The project MISTRAL exploits the potential of magnetic shape memory alloys (MSMAs) for use in energy generation on a miniature scale. The objectives are two-fold: (1) The Villari effect in single crystalline NiMnGa will be implemented in a new generation of vibration energy harvesting devices. (2) The temperature-induced change of magnetization in Ni-Mn-X (X = In, Sn) films and plates will implemented in novel thermomagnetic energy generators. In both cases, resonance effects will be exploited to maximize energy conversion and efficiency. Experiments include material characterization (thermal, magnetic, mechanical properties) as well as characterization of device performance (force-/temperature-induced change of magnetization, mechanical performance, generation of electrical energy). Based on obtained empirical data, finite element and lumped element models will be developed to simulate coupled physical properties and device characteristics in order to enable performance prediction as well as efficiency improvement.

References :

[1] M. Matsumoto, M. Ohtsuka, H. Miki and T. Takagi, *J. JSAEM*, 8 (2000) 445-453.

[2] Y. Sutou, Y. Imano, N. Koeda, T. Omori, R. Kainuma, K. Ishida and K. Oikawa, *Appl. Phys. Lett.*, 85 (2004) 4358-4360.

[3] R. Kainuma, Y. Imano, W. Ito, Y. Sutou, H. Morito, S. Okamoto, O. Kitakami, K. Oikawa, A. Fujita, T. Kanomata, K. Ishida, *Nature*, 439 (2006) 957-960.

[4] M. Gueltig, H. Ossmer, M. Ohtsuka, H. Miki, K. Tsuchiya, T. Takagi and M. Kohl. *Adv, Ener. Mater.*4 (2014) 751-758.

[5] Marcel Gueltig, Frank Wendler, Hinnerk Ossmer, Makoto Ohtsuka, Hiroyuki Miki, Toshiyuki Takagi, Manfred Kohl, *Adv. Energy Mater.* (2016), 1601879.

Rolling Characteristics of Neutrophils on PDMS Surface Mimicking the Endothelial Topography: Influence of Pressing Force on Cell Trajectories

Project ELyT lab B3 : **MicroCell (**Microsystems for Cell Engineering)

SHIRAI Atsushi
Institute of Fluid Science, Tohoku Univ.
2-1-1 Katahira, Aoba-ku, Sendai 980-8577, Japan

RIEU Jean-Paul
Univ. Claude Bernard Lyon 1, CNRS, Institut Lumière Matière
F-69622, Villeurbanne, France

1. Introduction

Neutrophils' rolling on endothelium of blood vessels is the earliest event of their immune response to initiate the subsequent events for their extravasation. It is known that this process is predominantly observed in post-capillary venules namely mediated by binding of P-selectin on the endothelial cells and PSGL-1 on the neutrophils [1]. In the post-capillary venules, erythrocytes aggregate to axis of the vessels to displace neutrophils toward the vessel wall [2]. Since the endothelial cells are nucleated cells, inner lumen of the vessels is bumpy due to their convex shape. And thus, neutrophils are expected to roll along borders of the endothelial cells under a pressing force by the red blood cells. Furthermore, it is known that P-selectin is expressed along border of the endothelial cells by a stimulation of histamine [3]. The cells tracing the borders have high possibility to bind with the selectin during their rolling. To summarize, the neutrophil rolling is mediated both by selectin/ligand binding, the pressing force toward the vessel wall, surface topography of the endothelium and the localized expression of the selectin. The aim of this study is elucidation of correlative effects of the pressing force and the surface topography on the rolling characteristics of the cells among these four factors. For this purpose, we fabricated a patterned PDMS substrate which mimics the surface topography of the endothelium. We observed behavior of HL-60 cells, which are widely accepted as a model cell of neutrophils, on the substrate under a variety of pressing forces using a homemade inclined centrifuge microscope system [4] that was already used to test unspecific HL-60 cells/substrate adhesion recently [5].

2. Fabrication of patterned PDMS substrate

We assumed the endothelial cells are tiled inner lumen of the blood vessels in a zigzag [6]. We reproduced this topography by a hexagonal pattern, i.e., short hexagonal poles with a height of 2.3 µm and 16 µm a side arranged with a clearance of 12 µm. The resultant apical cell area which is a hexagonal area connecting centerlines between adjacent hexagons is 1,365.8 μm^2. This was designed considering the size of HUVECs, i.e., the height is around 2 µm and the apical area is 1,238±52 μm^2 [7, 8]. A Si mold for fabricating the substrate was made by the reactive ion etching with *NanoLyon* facility (ILM, UCBL). PDMS (Sylgard® 184, Dow Corning) was pourd onto the mold with the thickness of 1 mm and cured in a oven. The PDMS sheet was peeled off from the mold and stuck onto a flat glass plate after 1 min. absorption to air plasma. Figure 1 shows an example of the fabricated patterned substrate. Here, for comparison of the motion of HL-60 cells on the hexagonal pattern, a stripe pattern with the width of 12 µm is also arranged.

3. Rolling experiment of HL-60 cells

The HL-60 cells (supplied by Center for Biomedical Research, Institute of Development, Aging and Cancer Tohoku University) are suspended in a medium RPMI-1640 (Wako) supplemented with 15% FBS (HyClone) at the concentration of 3×10^5 cells/ml. The rolling experiment of the HL-60 cells was performed usin the inclined centrifuge microscope system [4]. This system has a container bottom of which the PDMS substrate is settled and filled with the suspension of the HL-60 cells. The container is mounted on a rotor of a centrifuge to apply a centrifugal force F. Here, since the container is inclined from the rotational plane, initially buoyant cells are driven in radial directiona, and the cells land on the substrate is driven by the tangential component, F_T, of F to the substrate while being pressed onto the substrate by the normal component F_N. We can control F_N and F_T arbitrarily by choosing appropriate combination of the inclination angle of the container and the rotational speed.

In this study, we observed motion of the cells at $F_T = 30$ pN under a variety of F_N from 23.5 to 70.5 pN. To characterize the cells behavior, we introduced two parameters; mean velocity, U, of the cell velocity in the direction of F_T and circular variance ,CV, of instantaneou cell velocity vectors. Figure 2 shows influence of F_N on U and CV on the the hexagonal pattern normalized by those on the stripe pattern, i.e., $U_{\mathrm{hexagon}}/U_{\mathrm{stripe}}$ and $CV_{\mathrm{hexagon}} - CV_{\mathrm{stripe}}$, respectively. As shown in this figure, they both approach 0.4 as the increase in F_N, which is the analytical limit when all the cells trace valley of the pattern by pure geometrical considerations. This figure indicates importance of F_N in characterizing the cell behavior. For $F_N \leq 20$ pN, the cells mostly go straight above the hexagonal surface.

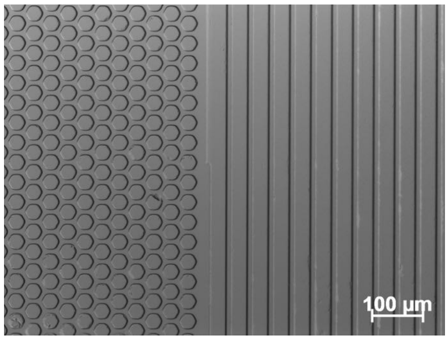

Fig. 1 Microscopic view of PDMS substrate

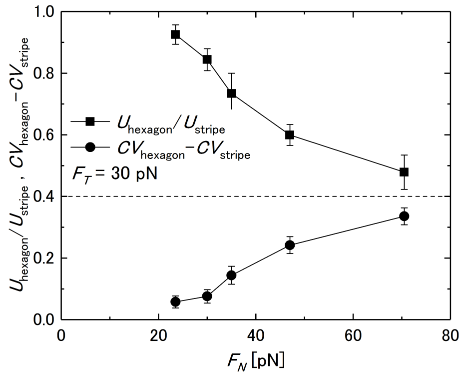

Fig. 2 Influence of pressing force F_N on normalized mean velocity and circular variance of HL-60 cells. They approach 0.4 as the increase in F_N.

4. On-going project

We are now struggling in functionalization of the PDMS substrate to coat the valleys of the patten with P-selectin mimicing localized expression of the selectin. For this purpose, we apply the micro-contact printing to coat BSA on hump part of the pattern in advance, and immerse in a P-selectin solution to coat the hollow part. Figure 3 shows an example of immunofluorescent image of the functinoalized PDMS substrate shown in Fig. 1. P-selectin was labeled by AlexaFluor 555, and the bright parts indicates existence of P-selectin. At the present state, the yield ratio is up to about 70%, and it is not good to comfirm success of the functionalization by the labeling P-selectin before the experiment. We are looking for a better way of the functionalization and confirmation of the success.

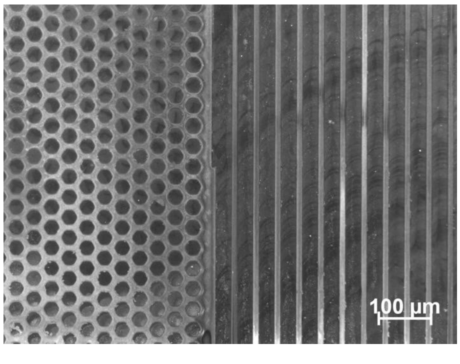

Fig. 3 Immunofluorescent image of functionalized PDMS substrate. Bright parts indiate existence of P-selectin.

References:

[1] Kolaczkowska, E. and Kubes, P., *Nature reviews Immunol.*, **13** (2013), 159-175.

[2] Schmid-Schonbein, G.W. et al., *Microvasc. Res.*, **19** (1980), 45-70.

[3] Burns, A.R. et al., *J. Leukoc. Biol.*, **65** (1999), 299-306.

[4] Kandori, T. et al., *J. Biomech. Eng.*, **130** (2008), #51007.

[5] Shirai, A. et al., *Tech. Health Care*, **26** (2018), in Printing.

[6] Ye, M. et al., Scientific Reports, 4 (2014) #4681.

[7] Shojaei, S. et al., *Cell Biology International*, **39** (2015)741-749.

[8] Oberleithner, H., *Kidney International*, **67** (2005), 1680-1682.

Endovascular research and training using PVA-H models

TUPIN Simon [1]
YU Kaihong [1]
MATSUURA Masami [1]
SHIMIZU Yasutomo [1]
OHTA Makoto [1,2]

[1] *Institute of Fluid Science Tohoku University 2-1-1 Katahira, Aoba-ku, Sendai, Japan*

[2] *ELyTMaX UMI 3757, CNRS – Université de Lyon – Tohoku University, International Joint Unit, Tohoku University, Sendai, Japan*

Abstract :

1. Introduction

Over last two decades, endovascular repair became the standard for intracranial aneurysm management. As the number of endovascular devices increased, training of clinician is important to ensure the right selection of device and a smooth operation. Such training is usually performed on an *in vitro* model made of silicone, which main problem is its bad friction with medical devices. Poly-vinyl alcohol hydrogel (PVA-H) was proposed previously as a vascular models base material [1] as it combines several advantages: transparency, low friction [4] and mechanical properties similar to vascular tissues [2-3]. As a proof of concept, a sensory test and a pre-operative training performed by trained medical doctors using such vascular models are presented in this study.

2. Material & methods

Vascular models were manufactured based on a previously described lost-wax technique [1,3], using patient specific artery and aneurysm geometries. For the sensory test, a tubular type model filled with saline was equipped with customized connectors and fixed on the support frame as shown in fig.1a. Tests were performed in an angiography room, in where model side, angiography image and operator side can be monitored and recorded at the same time (fig.1). For the pre-operative training, a flow circuit (fig.2a) was built to recreate steady cerebral flow conditions (250ml/min and 90mmHg) in a box type vascular model. Pressure sensors and flowmeter were used to record the evolution of flow conditions during the training. Moreover, two cameras were used to record the device deployment in frontal and lateral view, as an usual angiographic system (fig.2a).

3. Experimentations and discussion

3.1 Sensory test (in collaboration with Pr Shojima, Saitama Medical University, Japan)

A sensory test was performed by comparing artery mimicking tubular models made of silicone and PVA-H. A clinician carried out the evaluation by inserting a micro-catheter and a guide wire in each model. In the doctor's opinion, PVA-H model better mimicked the real operation sensation due to its low friction properties. However, the experiment revealed that poor fixation of the model inducing shaking and deformation that affect the medical device manipulation. Fixation that mimics the surrounding tissues mechanical properties needs to be developed for future experiments.

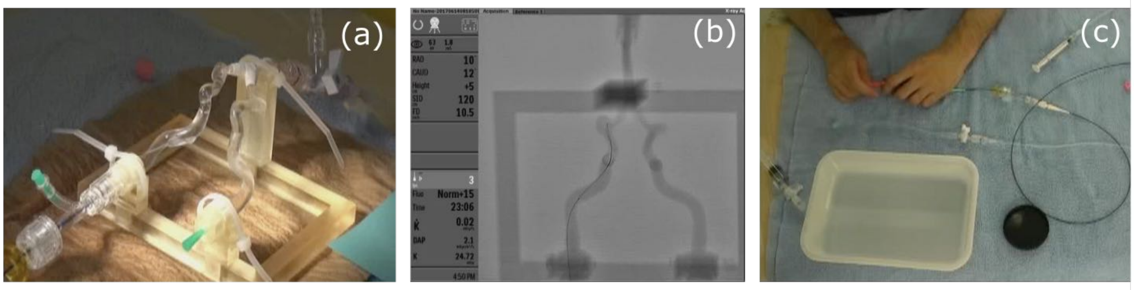

Fig.1: Sensory test: (a) PVA-H model, (b) model angiography, (c) clinician operation (from [5])

3.2 Pre-operative training (in collaboration with Pr MATSUMOTO, Kohnan Hospital, Japan)

A training experiment was performed using a PVA-H box model representing a patient aneurysm located on the internal carotid artery (ICA) (fig.2b) into which a medical doctor deployed a flow diverter (Pipeline, Medtronic, USA) (fig.2c). During the experiment, change of pressure and flow rate were recorded (fig.2a) and correlated to doctor's manipulation. The flow diverter was found too short to cover the whole aneurysm, which would have required the deployment of a second device during a real operation. This revealed the difficulty for clinician to choose the right device and the benefit of such pre-operative training. Moreover, impacts of medical device on the hemodynamic conditions can be evaluated with such system.

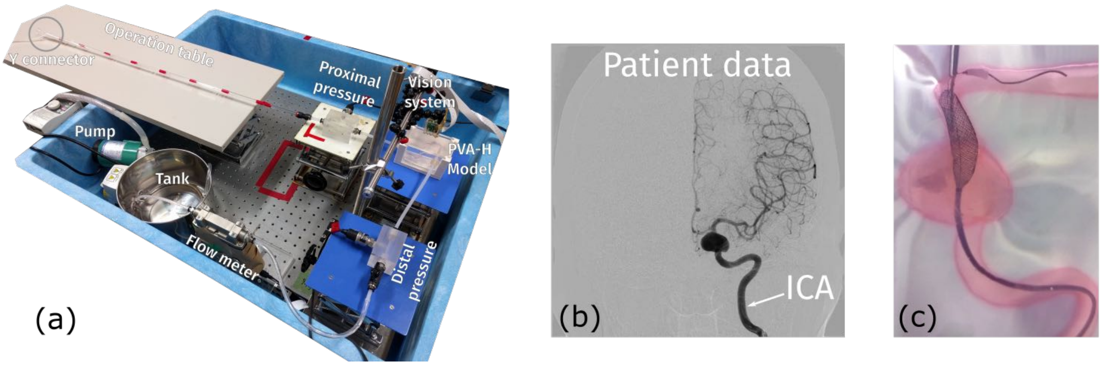

Figure 2: Pre-operative training: (a) flow circuit, (b) patient angiography, (c) device deployment in PVA-H model.

Acknowledgment

This research was funded by ImPACT Program of Council for Science, Technology and Innovation (Cabinet Office Government of Japan).

References :

[1] Ohta, Makoto, et al. "Poly-vinyl alcohol hydrogel vascular models for in vitro aneurysm simulations: the key to low friction surfaces." Technology and Health Care 12.3 (2004): 225-233.

[2] Kosukegawa, Hiroyuki, et al. "Measurements of dynamic viscoelasticity of poly (vinyl alcohol) hydrogel for the development of blood vessel biomodeling." Journal of Fluid Science and Technology 3.4 (2008): 533-543.

[3] Liu, Lei, et al. "Anisotropic in vitro vessel model using poly (vinyl alcohol) hydro gel and mesh material." Journal of applied polymer science 116.4 (2010): 2242-2250.

[4] Kosukegawa, Hiroyuki, et al. "Friction properties of medical metallic alloys on soft tissue–mimicking poly (vinyl alcohol) hydrogel biomodel." Tribology Letters 51.3 (2013): 311-321.

[5] Yu, Kaihong, et al. "Sensory Evaluation of Cerebral Artery Blood Vessel Model using PVA-H." 30th BioEngineering Conference of the JSME. (2017)

In-situ techniques in electron microscopy

Lucile Joly-Pottuz[1], T; Epicier[1], I. Issa[1,2], J. Réthoré[2], C. Esnouf[1], V. Garnier[1], J. Amodeo[1], J. Morthomas[1], D. Stauffer[3], K. Masenelli-Varlot[1]

1 Université de Lyon, INSA-Lyon, MATEIS UMR5510, Bât. Blaise Pascal, 7 Avenue J. Capelle, 69621 Villeurbanne Cedex, France
2 Université de Lyon, INSA-Lyon LaMCoS CNRS UMR5259, 69621 Villeurbanne, France
3 Hysitron Inc, 9625 W 76th St., Minneapolis, MN 55344, USA

Abstract :

Characterization of nanomaterials or materials at the nanoscale has drastically increased during the last decades. This increase can be explained by (i) the necessity to obtain materials with nanometer-size grains, for instance nanocomposites, and by (ii) the use of nanoparticles in different fields, for instance lubrication applications. A challenge lies in the in situ microstructural characterization of such materials as it can give access to valuable pieces of information regarding the microstructural changes induced by their use.

Dedicated TEM (Transmission Electron Microscopy) holders equipped with force and displacement sensors have been developed and are of a very high interest to test, in situ, the mechanical properties of nanometer-sized objects [1,2]. On crystalline nano-objects, Molecular Dynamics simulations have shown that dislocations nucleate at the surface [3]. Coupling TEM nanocompression and numerical simulations can be of much interest to determine the mechanical porpoerties at the nanometer scale and to study the deformation mechanisms.

The innovative mechanical observation protocol of nanoparticles in the 100nm size range is presented in Figure 1. It consists of in-situ TEM nano-compression tests of isolated nanoparticles Load–real displacements curves, obtained by Digital Image Correlation, are analyzed and these analyses are correlated with Molecular Dynamics simulations. A constitutive law with the mechanical parameters (Young modulus, Yield stress...) of the studied material at the nano-scale can be obtained [2]. In-situ TEM nano-compression tests were performed on ceramic MgO nanocubes. Magnesium oxide is a model material and its plasticity is very well known at bulk. The MgO nanocubes show large plastic deformation, more than 50% of plastic strain without any fracture [4].

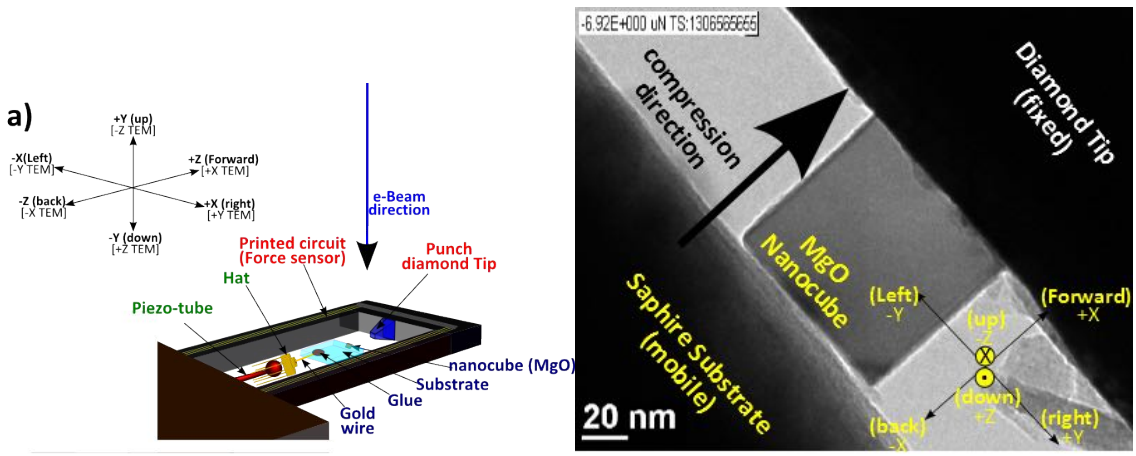

Figure 1: a) Schematic representation of the front piece of the sample holder used for in-situ testing, b) MgO nanocube just before in-situ nanocompression test. Arrows show possible movements of the sample

References :

[1] Q. Yu, M. Legros, A.M. Minor, MRS Bulletin 40, 62-70 (2015).
[2] E. Calvié, L. Joly-Pottuz, C. Esnouf, P. Clément, V. Garnier, J. Chevalier, Y. Jorand, A. Malchère, T. Epicier, K. Masenelli-Varlot, J. Eur. Ceram. Soc. 32 2067-2071 (2012).
[3] S. Lee, J. Im, Y. Yoo, E. Bitzek, D. Kiener, G. Richter, B. Kim, S.H. Oh, Nature Communications 5:3033 (2014).
[4] I. Issa, J. Amodéo, J. Réthoré, L. Joly-Pottuz, C. Esnouf, J. Morthomas, M. Perez, J. Chevalier, K. Masenelli-Varlot, Acta Materialia 86, 295-304 (2015).
[5] This work is performed within the framework of the LABEX iMUST (ANR-10-LABX-0064) of Université de Lyon, within the program "Investissements d'Avenir" (ANR-11-IDEX-0007). The authors thank the CLYM (Consortium Lyon-Saint Etienne de Microscopie, www.clym.fr) for the access to the microscope and A.K.P. Mann, Z. Wu and S.H. Overbury (ORNL, USA) for having provided the samples.

Tuesday, March 6th – Afternoon

Poster session – 18:00-19:30

Consolidation Process of Cu from Powder to Plate by Compression Shearing Method

Project ELyT lab : Poster session

	*TAKEDA Sho, Graduate school of engineering, Tohoku University, 6-6 Aramaki aza Aoba, Aoba-ku, Sendai, 980-8579, Japan*		*MIKI Hiroyuki Frontier Research Institute for Interdisciplinary Sciences, Tohoku University, 6-3 Aramaki aza Aoba, Aoba-ku, Sendai, 980-8578, Japan*		*FONTAINE Julien Laboratoire de Tribologie et Dynamique des Systèmes, École Centrale de Lyon, 26 avenue Guy de Collongue, 69134 Écully cedex, France*
	*GUIBERT Matthieu Laboratoire de Tribologie et Dynamique des Systèmes, École Centrale de Lyon*		*TAKEISHI Hiroyuku Chiba Institute of Technology, 2-17-1 Tsudanuma, Narashino, 275-0016, Japan*		*TAKAGI Toshiyuki Institute of Fluid Science Tohoku University, 2-1-1 Katahira, Aoba-ku, Sendai, 980-8577, Japan*

Abstract :

1. Introduction

There are many inhabitations to making sustainable development in human society, such as depletion of resources, environmental pollution, and mass production. In order to overcome these problems, the development of new materials and new ways of applying materials are investigated in the field of materials science. As a method to develop metals, we focus on a novel powder molding technique, compression shearing method at room temperature (COSME-RT) [1, 2].

COSME-RT is a molding method in which metal powder is consolidated into a thin plate material by applying biaxial forces at room temperature and ambient atmosphere. The most notable feature of this method is it can fabricate materials without heat treatment. Therefore, by this method, it is possible to fabricate materials which are easily affected by heating and practical use of this method is expected.

However, there are some issues to be solved to put COSME-RT into a practical use. In particular, clarification of the consolidation mechanism of a metal by COSME-RT is a fundamental issue for ensuring the reliability of COSME-RT. One of the major reasons behind lack of progress in the mechanism clarification is the difficulty in controlling and visualization of the process of COSME-RT. To solve this issue, the author conduct the unidirectional friction experiment and try to clarify the bonding mechanism of powder particles.

2. Experimentation, discussion

The material used in this study is powder of 99.9% purity Cu. The average particle size of this powder was 38 μm. This powder was compressed under a uniaxial normal stress of 1000 MPa to get a compressed sample. Target size of a sample was 20 × 20 × 0.25 mm^3.

Figure 1 shows a schematic illustration of a unidirectional friciton experiment. The following four steps are defined as one cycle, and this cycle was repeated. (1) The ball was placed on a sample and a normal load was applied to the sample through the ball. (2) A tangential force was applied to the ball whilst maintaining the compressive load. The ball was sliding on the sample and a tangential force was applied to the sample. (3) The ball was pulled offthe sample. (4) The ball was moved to the initial position of the first step. The experimental conditions were set to correspond with the forming conditions of the pure Cu plate by COSME-RT apparatus (DRD-NNK-002, DIP Co., Ltd., Gunma,

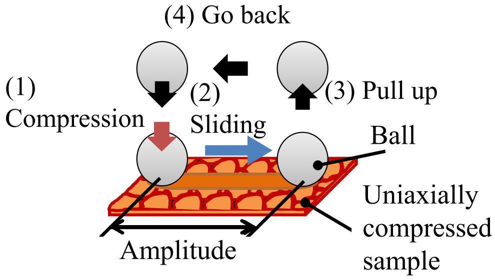

Figure 1 : Schematic illustration of unidirectional friction experiment.

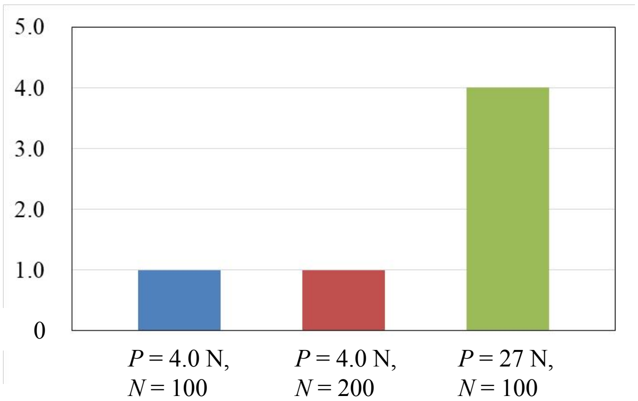

Figure 2 : Thickness of deformed zone of samples after friciton experiments.

Japan) [3]. In order to avoid the oxidation of the sliding surface of the samples, all the tests were performed with 5.0 l/min nitrogen blowing around the contact surface. A ZrO_2 ball of a half-inch diameter was chosen as a counter material to avoid wear of the sliding surface. The amplitude and the sliding velocity were programmed to be 10 mm and 5.0 mm/min, respectively. The normal load P was set to be 4.0 and 27 N, which correspond to the theoretical maximum Hertzian contact pressure of 500 and 1000 MPa, respectively. The number of the sliding cycles N was programmed 100 and 200. Allthe friciton experiments were performed at room temperature.

The fracture surfaces of the samples after the friction experiments were observed by using a scanning electron microscope. In all the samples, the part of the powder particles near the sample surface deformed along the sliding direction. Figure 2 shows the measured thicknesses of the deformed zones of powder particles on the samples after the friciton experiments. For a normal load of $P = 4.0$ N, the thickness of the deformed zone was almost 1.0 μm regardless of the number of the sliding cycles N. When the normal load was $P = 27$ N, the thickness of the deformed zone was approximately 4.0 μm. The stress applied to the particles increases when the applied normal load increases, and the strain applied to the particles may increase when the number of sliding cycles increases. Therefore, we clarified that the applied stress had a greater effect on the deformation of the powder particles than the applied strain. For the future work, the applied stress will be evaluate qualitatively to investigate how stress is required to proceed the bonding process of the particles.

Acknowledgements :

Extensive studies on the COSME-RT by Prof. N. Nakayama and Dr. M. Horita of Shinshu University are gratefully acknowledged. This work was partly supported by JSPS KAKENHI Grant Number 16H04504 and the JSPS Core-to-Core Program, A. Advanced Research Networks, "International research core on smart layered materials and structures for energy saving". Part of the work was carried out under the International Collaborative Research Project of Frontier Research Institute for Interdisciplinary Sciences, Tohoku University.

References :

[1] H. Miki, N. Nakayama, H. Takeishi, *Materials Science Forum*, **706-709** (2012) 1955-1960
[2] M. Horita, N. Nakayama, H. Miki, T. Miyazaki, H. Takeishi, *Journal of JSTP*, **54**, **625** (2013) 186-190
[3] S. Takeda, H. Miki, H. Takeishi, T. Takagi, *Tribology Online*, **12**, **2** (2017) 29-36

Multi-scale surface texturing and effect on the tribological behavior for artificial cartilage

Pr. Hassan ZAHOUANI (LTDS – ENISE – ECL / FRANCE)	*JAY Laura*
Pr. Philippe KAPSA (LTDS – ENISE – ECL / FRANCE)	*Laboratory of Tribology and Systems Dynamics*
Pr. Koshi ADACHI (Tohoku University / JAPAN)	*Central School of Lyon*
Pr. Koki KANDA (Tohoku University / JAPAN)	*36 avenue Guy de Collongues 69134 Ecully, France*

Abstract:

Over the last ten years, the use of artificial joint for hip or knee is significantly increased. In France for example, around 140 000 hip prostheses were implanted in 2013 [1] because of arthrosis or fracture. Due to the aging of population, eventually leading to an increase of natural joint dysfunction by arthrosis [2], this tendency is expected to grow.

Through the years, the design of artificial joints has been improved, with the introduction of ceramic-ceramic contact, and titanium based coatings. Indeed, as the artificial joints are implanted in human body, the use of non-aggressive materials such as titanium is highly required. These solutions are presenting drawbacks on patient's health. The main disadvantage can be summarized in the resulting wear particles that can be scattered in the patient body and potentially causing damages because of their high hardness.

In order to limit wear in artificial joints, harder coatings such as DLC are investigated. A biomimetic approach for this problem is proposed, this method is based on the use of a soft material to prevent the appearance of hard particle. Indeed, in natural joints, bones are coated by soft cartilage immerged in synovial fluid. This soft cartilage presents nonetheless remarkable friction coefficient [3]. Among the soft friction materials, the polymer gels are attractive as potential replacement for titanium in artificial joints, especially since the elaboration of double-network hydrogel by Pr. Gong et al. from Hokkaido University [3].

The material being studied for this application is the double network gel (DN gel). This kind of polymer gel, containing high water proportion, has shown several advantages as friction material, such as low friction ($\mu << 0.1$) [4] with water lubrication, biocompatibility and mechanical strength clearly higher than usual polymer gels. The DN gel is considered as an efficient material that can replace for titanium coating based in artificial joints, but it can now also be considered for various machine designs. In order to do so, many aspects of gel friction should be studied and improved.

The purpose of our study is to adapt and verify the rubbing performance of the DN gel in order to have a comparable friction coefficients to the ones in the human case. To understand the

general behavior of the material, we propose a rheological model of the DN gel by performing mechanical tests. This later will also give us information about the role of each mechanical property on the friction behavior.

In a second time, we will investigate the previous limits by using a multi-scale texturing on subtract materials or on the gel surface with the help of a femtosecond laser. A static and a dynamic contact analysis between subtract and textured gel for several speeds and loads will be proposed. A complimentary study based on the numerical simulation in order to understand the gel – subtract contact for different shapes of textures and the pressure repartition.

References :

[1] Agence Nationale de la sécurité du Médicament et des Produits de Santés (ANSM) website (2017) available at: http://ansm.sante.fr/

[2] J. Caton, P. Papin, Typologie et épidémiologie des prothèses totales de hanche en France, e-memoires de l'Académie Nationale de Chirurgie, 11 ,2 (2012) 001-007.

[3] J. P. Gong, Friction and Lubrication of Hydrogels—its Richness and Complexity, The Royal Society of Chemistry, Soft Matter, 2, 7 (2006) 544-552.

[4] Gong J. P. and Y. Osada, Surface friction of polymer gels, Progress in polymer science 27 (2002) 3-38

Magnetic incremental permeability for the non-destructive evaluation: Characterisation and Modelling

Project ELyTGlobal BENTO

	DUCHARNE Benjamin *Université de Lyon, INSA-Lyon, LGEF EA682*		*UCHIMOTO Tetsuya* *- ELyTMaX UMI 3757, CNRS - Université de Lyon - Tohoku University, International Joint Unit - Institute of Fluid Science, Tohoku University*
	*GUPTA Bhaawan* *- ELyTMaX UMI 3757, CNRS - Université de Lyon - Tohoku University, International Joint Unit, - Université de Lyon, INSA-Lyon, LGEF EA682*		*TAKAGI Toshiyuki* *- ELyTMaX UMI 3757, CNRS - Université de Lyon - Tohoku University, International Joint Unit - Institute of Fluid Science, Tohoku University*
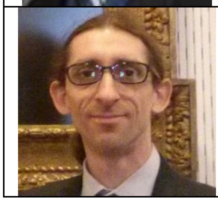	*SEBALD Gael* *ELyTMaX UMI 3757, CNRS - Université de Lyon - Tohoku University, International Joint Unit, Tohoku University*		

Abstract: A modified Jiles-Atherton model has been used to numerically reproduce experimental Magnetic Incremental Permeability (MIP). The small alternating magnetic field creates local changes in the magnetic state of the sample which can be considered as extremely weak minor loops. Even if the frequency of this alternating excitation is high, the rate dH/dt remains sufficiently low to limit the model as a quasi-static contribution. Jiles-Atherton model exhibits issue to reproduce in simulation closed minor cycles. This is corrected here assuming that the excitation is sufficiently weak to consider minor loops just as anhysteretic rate.

1. Introduction

In ferromagnetic materials, magnetic domain walls interact with microstructure over similar mechanisms as dislocations do [1, 2, and 3]. This fundamental observation is the basis of micro-magnetic materials characterization. Coupling between the stress and magnetic field is the main and important feature of the ferromagnetic materials consisting of various small magnetic domains in its microstructure [4]. Conventional Eddy current testing has been extensively used for the ferromagnetic materials characterization but when it comes to creep damage detection, it becomes difficult to distinguish between the changes caused by the actual creep damage and from the signals generated by other sources, like microstructure, surface roughness, hardness etc.

Magnetic Incremental Permeability (MIP), as shown by experiments in this research, because of its high sensitivity to stress, is used to investigate samples in this study. When a ferromagnetic material is exposed to a steady and static magnetic field, the reversible permeability measured with a small alternative magnetic field is defined as the magnetic incremental permeability [5]. MIP is calculated by measuring the minor loop magnetic flux density during the process of magnetization. MIP is very efficient in understanding the degradation/creep in the materials which also gives a lot of information about the microstructure of the ferromagnetic materials. Moreover, as the microstructure of a ferromagnetic material, e.g. the magnetic domain etc., is easily affected by the technical damage such as plastic deformation and fatigue damage, MIP method is considered as a promising NDT technique to evaluate the residual stress [Chen].

2. Discussions

Figure 1 demonstrates the experimental set-up for the measurement of magnetic incremental permeability on 12 Cr-Mo-W-V steel creep test samples. The samples are magnetically excited using a sinusoidal magnetic field with the help of a U-shaped electromagnet. The excitation frequency chosen for these measurements is 0.1Hz after comparing the effect of different frequencies. The excitation magnetic field has been chosen as 100 $A.cm^{-1}$. The sensor also consists of a Hall sensor which is used to measure the tangential magnetic field strength H. The sensor used is a Transmitter-Receiver type, the transmitting coil of which is used to provide a small alternating magnetic field, ΔH, which is superimposed on the steady large magnetic field (definition of Magnetic Incremental Permeability). The frequency chosen for the small alternating field is finalized as 50 kHz. The output of the Receiver coil in the sensor is fed to LI 5640 (NF Corporation) Digital lock-in amplifier. A modified Jiles-Atherton model has been used to numerically reproduce the experimental situation. The small alternating magnetic field creates local changes in the magnetic state of the sample which can be considered as extremely weak minor loops. Even if the frequency of this alternating excitation is high, the rate dH/dt remains sufficiently low to limit the model as a quasi-static contribution. Jiles-Atherton model exhibits issue to reproduce in simulation closed minor cycles. This will be corrected here assuming that the excitation is sufficiently weak to consider minor loops just as anhysteretic rate.

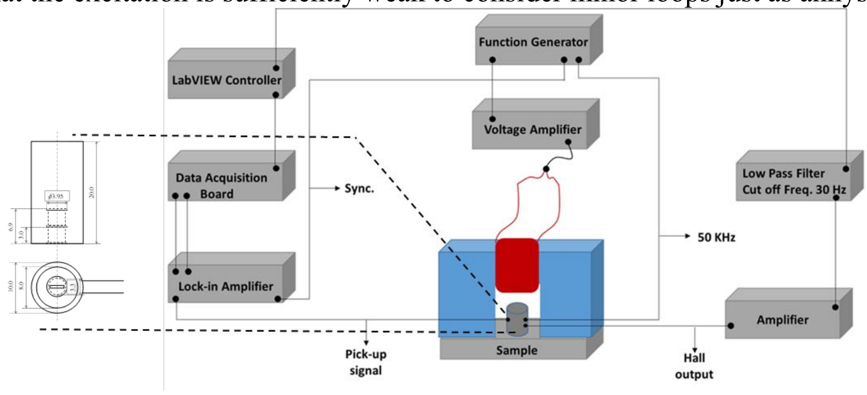

Figure 1:Set-up for the Magnetic Incremental Permeability testing (Schematic)

A large number of comparisons between simulations and experimental results will be presented as well as detailed explanation as to how this numerical tool can be used to interpret experimental results. Figure 2 below demonstrates the MIP signature of ruptured samples from each of the three categories of difference in temperature treatments. It is well distinguishable that the cross points and Hc value of each of the curves are variable to each other. The coercivity of samples decreases with the increase in the temperature. The value of cross point which represents the remanence, increases with the increase in temperature.

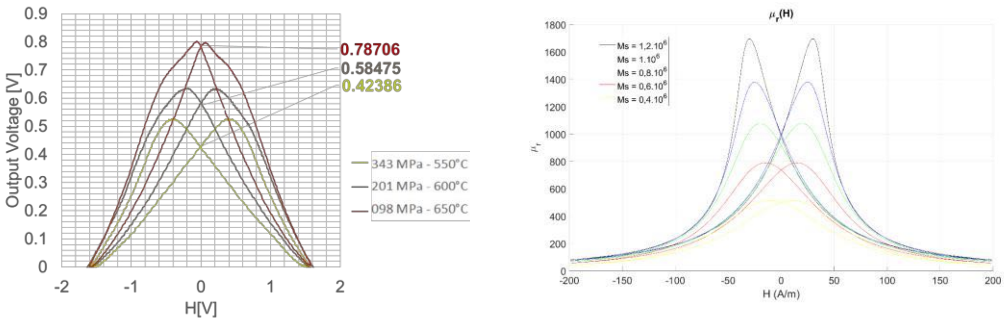

Figure 2: MIP signatures for varied temperature treated samples (L) and some simulated results with Jiles-Atherton model for MIP curves (R)

References :

[1] Bozorth R.M.; Ferromagnetism. Van Nordstrand, Princeton. 1951.
[2] Cullity B. D.; Introduction to magnetic materials. Addison-Wesley. 1972.
[3] Jiles D.; Introduction to magnetism and magnetic materials. Chapman and Hall.1991.
[4] Schull P.J.; Non-destructive evaluation: theory, techniques and applications. New York. Marcel Dekker,Inc.2002.
[5] Chen H., Numerical simulation of magnetic incremental permeability for ferromagnetic material, International Journal of Applied Electromagnetics and Mechanics 45 (2014) 379–386,2014

Topology optimization for intracranial stent based on computational fluid dynamics

Hitomi Anzai
Frontier Institute of Interdisciplinary Sciences, Tohoku University
6-3 Aramaki-Aza, Aoba, Aoba-ku, Sendai, Miyagi, Japan

Mingzi Zhang
Institute of Fluid Science, Tohoku University
Katahira 2-1-1, Aoba-ku, Sendai, Miyagi, Japan

Narendra Kurnia Putra
Graduate School of Engineering, Tohoku University
6-6-4 Aramaki-Aza, Aoba, Aoba-ku, Sendai, Miyagi, Japan

Kazuhiro Watanabe
Graduate School of Biomedical Engineering, Tohoku University
6-6 Aramaki-Aza, Aoba, Aoba-ku, Sendai, Miyagi, Japan

Makoto Ohta
ELyTMaX UMI 3757, CNRS – Université de Lyon – Tohoku University, International Joint Unit, Tohoku University, Sendai, Japan

Abstract : Stent insertion aims at reducing the flow in an aneurysm. To minimize the average velocity in an aneurysm, we applied optimization technique to explore the stent geometry to lead better treatment outcomes based on computational fluid dynamics.

1. Introduction

A modern technique treating cerebral aneurysm is the insertion of a medical device called a flow diverter (FD) stent, which is a tubular mesh made of NiTi wire. The aim of FD implantation is to reduce the flow in an aneurysm by covering an aneurysm orifice. Given that the aim of stent insertion is to reduce flow, optimization is applied using computational fluid dynamics (CFD) analysis in recent years [1,2]. However, owing to some limitation on computational resource and complexity of bio-system in our body, there are still problems remaining to explore the clinical optimal.

Here, we present several approaches to optimize a FD stent for intracranial aneurysm based numerical studies.

2. Automatic optimization using lattice Boltzmann method and simulated annealing

The first issue for optimization is a number of numerical models. Indeed, optimization method may require a huge number of flow simulations to determine the best stent geometry. To solve this problem, we consider the possibility to use lattice Boltzmann (LB) bloodflow simulations in combination with an optimization algorithm that can explore the design space of FD stents, in a fully automated way.

A set of struts as FD stent model was represented into mathematical equations on D3Q19 lattice topology (Fig. 1). Automatic optimization procedure gradually improves flow-reduction with probabilistic modification of mathematical equations. Improve ratio depends on geometry (2.6-28.1%), however, the optimal geometries for each aneurysm geometry show similar tendency to block the inflow.

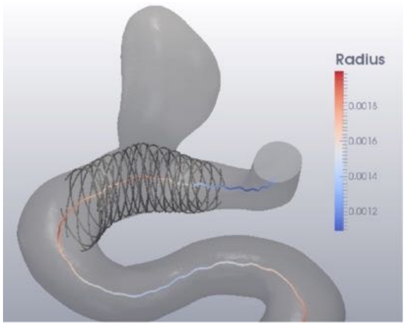

Figure 1: Mathematical representation of stent based on 8 helixes.

3. Surrogate-based optimization of stent in Fluid-Solid Interaction analysis

Secondly, optimization study for intracranial stent neglect the influence of wall deformation by stent deployment. As low wall shear stress (WSS) on the vessel wall surface and the excess force exerted from stent to the blood vessel are the two parameters which are believed to be the reason of these post-stenting problems [3], therefore, this phenomenon is considered important to be included in optimization as well.

In this study, we developed Kriging model based on response behavior of stent design variables towards objective function. With the aim of minimizing low WSS area on the vessel wall, we constructed 26 numerical models as initial sample points using Halton sequence sampling method. All simulations have been conducted as one-way coupled Fluid-Solid Interaction (FSI) simulation (Fig. 2). As the results, response surface suggests that strut with medium size around 100-250 micron with a relatively big inter-strut gap is suitable for achieving the optimize criteria in case of rectangular cross-section.

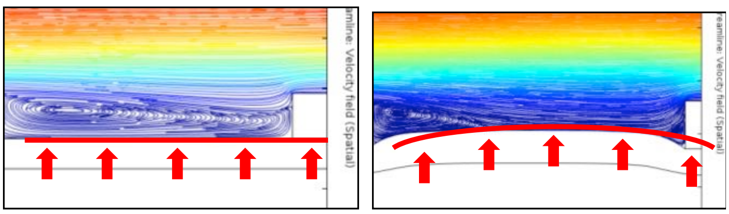

Figure 2: Flow pattern around the vicinity of stent struts (left: without vessel deformation, right: with vessel deformation)

References :

[1] Srinivas, K, et al., 2010, ASME J. Med. Devices 4(2), p. 021003.

[2] Nakayama, T., et al., 2010, Proceedings of the 3rd ASME 2010 Joint US-European Fluids Engineering Summer Meeting and 8th International Conference on Nanochannels, Microchannels, and Minichannels, Paper No. FEDSM/ICNMM 2010-30592.

[3] Chen YH, et al., J. Appl. Physiol., vol. 106, no. 5, pp. 1686-1691, 2009.

Experimental Evaluation of Repassivation Condition of Chloride Stress Corrosion Cracking

Takeyuki OHIRA Supervisors Professor Marion Fregonese Professor Yutaka WATANABE Senior Lecturer Hiroshi ABE	*Watanabe Laboratory , Department of Quantum Science and Energy Engineering (QSE), Graduate School of Engineering, Tohoku University* *MATEIS Lab, INSA-Lyon*	*Address: 〒980-8579 Main Building 320 Room Aramaki Aoba 6-6-01-2, Aoba-ku Sendai shi, Miyagi ken, Japan* *21 avenue Jean Capelle, 69621 Villeurbanne cedex, France*

1. Introduction

For light water reactors (LWR), it is necessary that structural materials have high corrosion resistance in addition to high mechanical properties such as strength,toughness and workability. For this reason, materials such as stainless steel are widely used as structural materials of LWR. However, passivation film tends to be broken in chloride-containing environment and localized corrosion can occur [1]. During the Great East Japan Earthquake that occurred on March 11, 2011, TEPCO Fukushima Daiichi Electric Power Plant was urgently shut downed, and all power supply was lost due to the subsequent tsunami. For cooling the fuel, seawater was injected in the reactor and in the spent nuclear fuel pools (SNFP)

Reduction of dissolved oxygen by hydrazine injection and removal of salt have been carried out in the spent fuel pool system as a countermeasure against corrosion. In the reactor system, switching to freshwater injection and nitrogen degassing have been carried out [2].

With these countermeasures, the possibility of further initiation of localized corrosion is now low. However, if localized corrosion has occurred in the highly corrosive environment right after the accident, the localized corrosion can possibly continue today to grow. There are many crevice structures such as regions of contact between components and locations under wreckages in the nuclear reactor and in the spent fuel pools. Therefore, there is a possibility that crevice corrosion has occurred inside such a crevice structure. In addition, when a certain amount of tensile stress exists on these parts, there is a possibility that the crevice corrosion is transitioning to stress corrosion cracking (SCC). In order to evaluate the effectiveness of the countermeasures taken, it is necessary to study the repassivation conditions. Type 304 stainless steel used for the Fukushima Daiichi Power Plant spent fuel pool liner is normally used in high-purity water conditions to cool the spent fuel, yet the corrosion resistance towards large amounts of sea water has never been considered. There are a few studies concerning the critical conditions for SCC of austenitic stainless steel in neutral chloride environment, but there is no study on the repassivation conditions [3].

In that context, this research is aimed at proposing an evaluation method to estimate the repassivation conditions in chloride environment for Type 304 stainless steel

2. Experimentation, discussion

2.1 Overview of the Experiment

In order to evaluate the conditions for repassivation of SCC, it is necessary to combine a method for measuring the crack length and electrochemical measurements at same time. Electrochemical tests were carried out using the three electrodes method. After sweeping from the Open Circuit Potential (OCP) to the critical potential of SCC and maintaining that potential, stepped polarization was conducted towards cathodic direction. The schematic diagram of the evaluation method of repassivation potential using electrochemical test and crack monitoring method is shown in the Fig.1

Moreover, it is generally known that the length of cracks caused by SCC differs between the inside and the surface of a specimen [4][5]. In order to evaluate the repassivation conditions more accurately, it is therefore important to combine several methods. That is why experiments were conducted with combining the Direct Current Potential Drop (DCPD) method, the Digital Image Correlation (DIC) method, and the Acoustic Emission (AE) method. The advantages of combining these methods are:

1. accurate evaluation of crack repassivation: even when it is measured that the crack propagation has stopped by the DIC method and the DCPD method, if the AE generated by SCC is still measured, there is a possibility that SCC propagation is still occurring inside the specimen.
2. difference in the crack propagation rate between surface and bulk: can be obtained by comparing DIC (surface information) and DCPD (surface + bulk) measurements.

2.2 Experimentation

The comparison of experimental conditions carried out at Tohoku University and INSA-Lyon is shown in the Table 1. Firstly, the test which generates crevice corrosion as the starting point of SCC by electrochemical measurement and makes the transition in pre-crack was conducted. It was confirmed that pre-crack can effectively act as a corrosion crevice and that SCC occurs and develops at the crack tip. Then the measurement of the crack length by DCPD method was successfully conducted.

From these methods, it appears that stress corrosion crack did not repassivate without sweeping the potential towards lower values.

The repassivation potential and the crack growth rate were measured by the combination of electrochemical measurement and DCPD method and DIC+AE performances are now investigated. In order to optimize the DIC measurements, adjustment of the position of the light, investigation of the noise source, reduction of vibrations, acquisition of conversion coefficient, etc… are currently carried out.

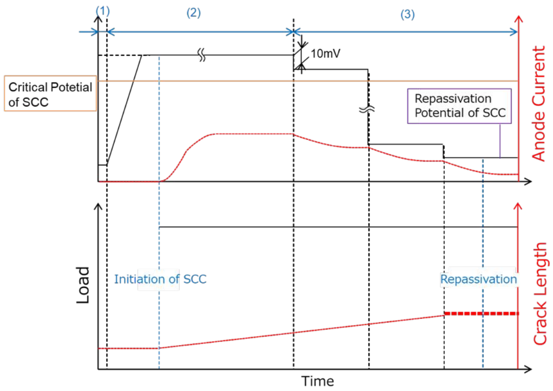

Fig.1 The schematic diagram of the evaluation method of repassivation potential

	Tohoku University	INSA-Lyon
Sample Material	Type 304 Stainless Steel	
Sensitization Rate	46%	13%
Solution	80±1°C, 3wt% NaCl, N_2 gas deaeration	70±1°C, 3wt% NaCl, N_2 gas deaeration
Specimen	CDCB(K Value is constant)	Flat type(K Value is not constant)
Crevice Geometry	Fatigue Crack	
Surface Treatment	SiC paper(#600)	SiC paper(#2400)+ Elecrochemical Polishing
Electrochemical Test	Constant Potential holding+Step Polarization(Cathode Direction)	
Evaluation Method	DCPD Method	DIC+AE Method
Crack mesureing position	Surface+Bulk	Surface

Fig.2 Comparison of experimental condition between Tohoku University and INSA-Lyon

References :

[1] Corrosion and corrosion prevention society ed., "Corrosion and corrosion protection handbook Part II corrosion phenomenon," pp. 49-149, 2000.
[2] TEPCO, "Medium- to Long-Term Roadmap for Decommissioning Fukushima Daiichi Nuclear Power Plant, etc. Review the process in removing fuel from the spent fuel pool," 2015.
[3] Gen Nakayama, Bei Seihiro, and Akashi Masato, "Stress corrosion crack initiation critical conditions in sensitized stainless steel · neutral chloride environment," Materials and environment, vol. 45, no. 5, pp. 298-304 , 1996.
[4] Masanori Aoki, Takuya Yamada, Yuki Miyamoto, "Investigation of SCC generation and evolution transition condition of stainless steel," INSS JJ Inst. Nucl. Saf. Syst., Vol. 21, pp. 144-153, 2014 .
[5] Nuclear Safety and NISA and Nuclear Safety Infrastructure Organization, "Summary of the findings up to the present on stress corrosion cracking (SCC)," 2006.

Wednesday, March 7th – Morning

Third session – 09:00-10:30

Ab Initio Modeling of Dislocation Cores in Metals

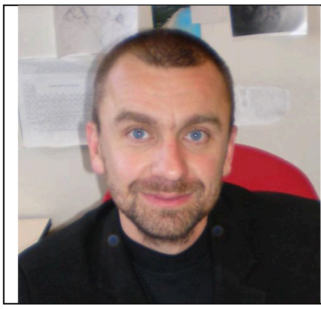

David Rodney
Institut Lumière Matière
Lyon University

The modeling of dislocations and their mobility using ab initio density functional theory (DFT) calculations has made tremendous progress these past few years, in part thanks to an increase in computing power, but also because of methodological developments, including methods to correct the energy for elastic interactions between periodic images. I will review recent advances in dislocation plasticity based on ab initio calculations, mainly in body centered cubic (BCC) and hexagonal close packed (HCP) metals.

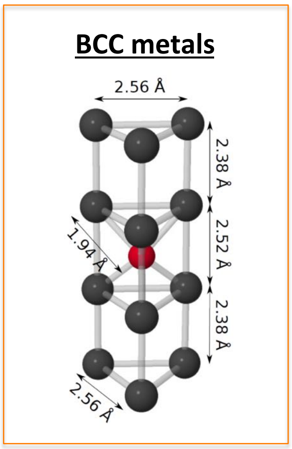

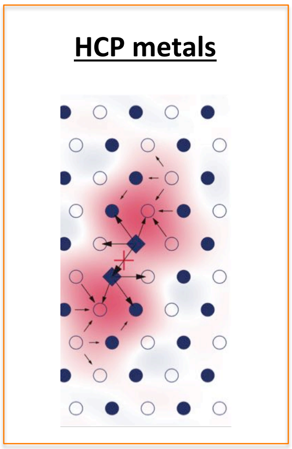

In BCC transition metals, I will discuss our new understanding of the screw dislocation two-dimensional Peierls potential and its close connection to the well-known deviations from the Schmid law. Alloying effects on the dislocation core structure and mobility will be addressed, highlighting how interstitial atoms can restructure the screw dislocation core. In HCP metals, I will show how DFT calculations identified stable and metastable dislocation cores, how these cores are related to slip in different slip systems and how an inversion of stability between a glissile and a sessile core explains the profoundly different plastic behaviors observed by in-situ TEM in Zr and Ti. I hope that this talk can serve as a basis for discussion on the challenges and opportunities to bridge these small-scale simulations with higher-scale models and simulations.

References:

- Rodney D., Clouet E., Ventelon L., Pizzagalli L., Willaime F. ‘Ab initio modeling of dislocation core properties in metals and semiconductors’ *Acta Materialia* **124** (2017) 63.
- Dezerald L., Rodney D., Clouet E., Ventelon L., Willaime F. ‘Plastic anisotropy and dislocation trajectory in BCC metals’ *Nature Communications* **7** (2016) 11695.
- Ventelon L., Lüthi B., Clouet E., Proville L., Legrand B., Rodney D., Willaime F. ‘Dislocation core reconstruction induced by carbon segregation in bcc iron’ *Physical Review B (Rapid Communications)* **91** (2015) 220102.
- Clouet E., Caillard D., Chaari N., Onimus F., Rodney D. ‘Dislocation locking versus easy glide in titanium and zirconium’ *Nature Materials* **14** (2015) 931.

Additive manufacturing of 3D architectured metal/ceramic biomaterials by robocasting

PhD started in October 2017, a collaboration with Tohoku University is desired

Coffigniez Marion *PhD Student* *MATEIS Laboratory* *INSA Lyon*	*Thesis supervisor:* *Gremillard Laurent* *MATEIS Laboratory* *INSA Lyon*	*Thesis co-supervisor:* *Boulnat Xavier* *MATEIS Laboratory* *INSA Lyon*

Abstract :

1. Introduction

Additive manufacturing allows the production of cellular structures. Bone cells thrive on porous surface, suggesting that bone cells could actually grow into scaffolds obtained by robocasting, to solidly anchor it or even to replace it in case of resorbable formulation.

This project aims at developping new metal/ceramic composite scaffolds for bone implants with improved properties. Two kinds of composite structures are studied:

- A non-resorbable metal/ceramic structure of Ti6Al4V / Hydroxyapatite, where the Ti6Al4V will improve ductility.
- A resorbable metallic/ceramic structure of Mg / HA (or Mg / ß-TCP) which implies to deal with Mg reactivity.

Those scaffolds are manufactured by robocasting. This process allows to build-up a structure layer by layer, from a powder-based ink. Then, the structure undergoes thermal treatments to be debinded and sintered.

2. Experimentation

As a first step and before the composites structures, scaffolds of each constitutive material are produced following the process detailed below, and characterised step by step.

The first important step is the ink formulation and the characterisation of its rheological behavior. As explained by M'Barki and al, a printable ink should present a dynamic yield stress high enough to compensate both the gravity and the capillary forces [1]. Then, during the whole process, the evolution of both macroscopic structure and microstructure, are followed by scanning electron microscopy, X-Ray diffraction and X-Ray tomography. The mechanical properties of the scaffolds are mesured through compressive tests.

Once the process optimised, a work on Mg biodegradation rate will be needed as it is known to be strongly impacted by both alloying elements and impurities level [2, 3].

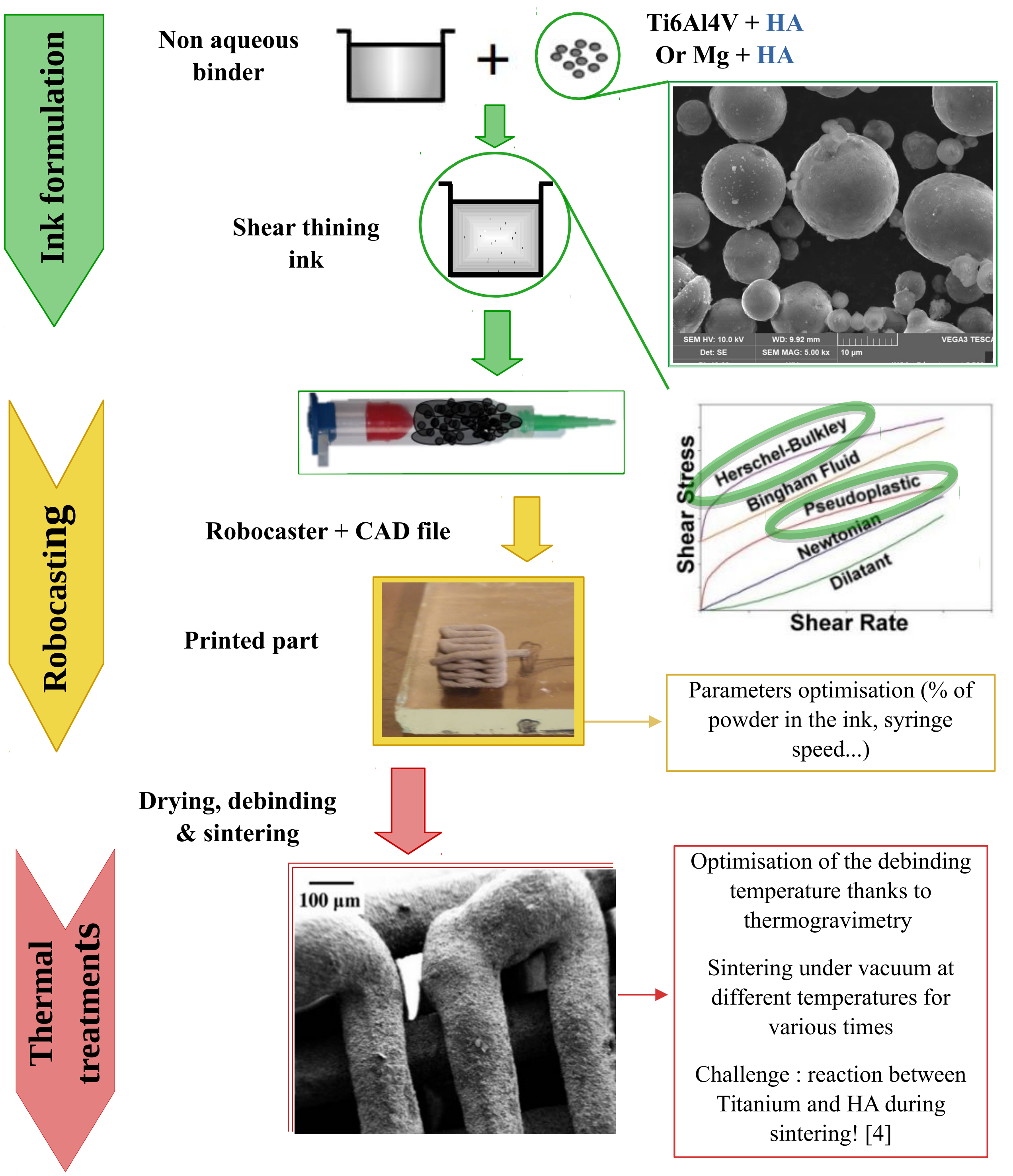

Ti6Al4V based scaffolds obtained by robocasting could be compared to those obtained by electron beam melting at Tohoku University.

References:

[1] M'barki, A., Bocquet, L., & Stevenson, A. (2017). Linking Rheology and Printability for Dense and Strong Ceramics by Direct Ink Writing. *Scientific Reports*, *7*(1), 6017.

[2] Shaw, B. A. (2003). Corrosion resistance of magnesium alloys. ASM handbook, 13, 692-696.

[3] Song, G. (2007). Control of biodegradation of biocompatable magnesium alloys. Corrosion Science, 49(4), 1696-1701.

[4] Yang, Y., Kim, K. H., Agrawal, C. M., & Ong, J. L. (2004). Interaction of hydroxyapatite–titanium at elevated temperature in vacuum environment. Biomaterials, 25(15), 2927-2932.

Rubber-Ice Friction mechanisms: Multi-Physical and multi-scale approach

Project ELyT lab: T5 – ELiceTrib Tribology of elastomer/ice contact from nm to mm scale

Sylvain HEMETTE
LTDS
Ecole Centrale de Lyon
Tohoku University

Kazue KURIHARA
NiChe
Tohoku University

Juliette CAYER-BARRIOZ
LTDS
Ecole Centrale de Lyon

Denis MAZUYER
LTDS
Ecole Centrale de Lyon

Abstract:

1. Introduction

Driving on ice is a delicate exercise due to the poor adherence of tire on ice and the use of studded tires is tightly regulated or forbidden in many countries. In this context of road safety improvement under severe climatic conditions, it is necessary to precisely study and investigate the sliding contact between rubber and ice and to determine the different key mechanisms governing the tribological behavior of the rubber-ice contact.

2. Strategy and collaboration

The strategy chosen here is to investigate the rubber-ice contact at different scales – macrometric (scale of apparent surface contact), micrometric (scale of group of contact between asperities) and nanometric (scale of a contact spot) – in order to link the physical process of friction and adhesion observed at the macrometric scale to their potential causes induced at subscale (micrometric and/or nanometric).

In this perspective a tri-partite collaboration was developed between the Laboratoire de Tribologie et Dynamique des Systèmes (LTDS), the Kurihara Laboratory from the

Tohoku University and Nihon Michelin, and especially around a PhD study in co-supervision between the Ecole Centrale de Lyon (ECL) and the Tohoku University.

3. Measurements and results

The adhesive properties at a contact spot scale were investigated by means of a Surface Force Apparatus (SFA) based system as a function of rubber mechanical properties and topography under negative temperature conditions. In parallel, the friction behavior was analyzed at the macro and micro scales for sliding velocities ranging from µm/s to m/s, temperatures ranging from -15°C to -2.5°C and various rubber mechanical properties and topography. The stiffer the material, the lower the friction. The topography also induced a variation of friction. Ice melting can appear as function of rubber-ice contact temperature and sliding velocity and then, impact friction behavior within contact. The friction mechanisms are discussed in terms of adhesion, viscoelasticity and thermal effect.

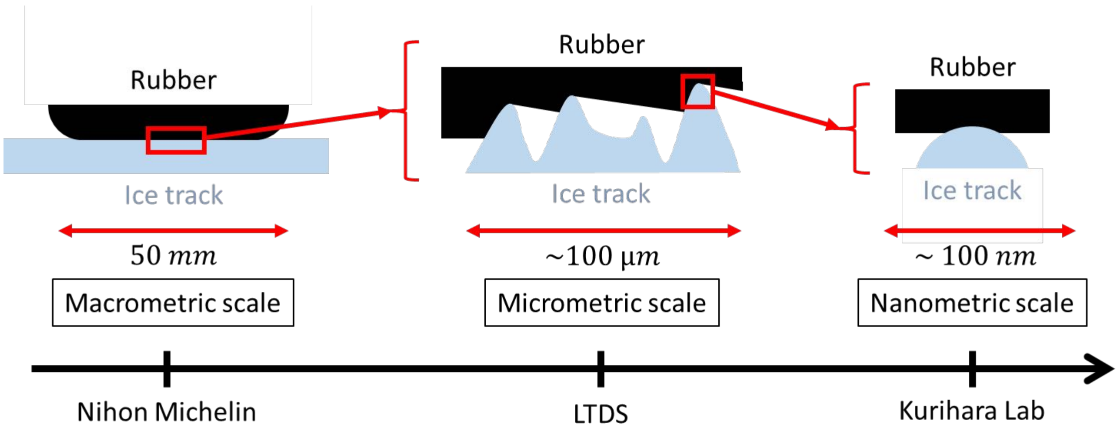

Schematic of rubber-ice contact from macro, micro and nanoscale points of view and experimental strategy

Influence of the composition on properties of Co based alloys

Project **DECCOBABA**

ELyT Global
Engineering for health
Materials and structure design

	**Prof. Chiba** **Deformation lab** **Institute for Materials Research** **Tohoku University**		**Prof. Fabrègue** **MATEIS** **INSA Lyon**

Abstract

The Cobalt based alloys are good candidates for biomedical applications such as implants. However for some specific case, their hardness should be improved. One possibility is to modify the carbon content. The higher the carbon content, the higher the fraction of carbide and usually the higher the strength. This study will focus on the influence of the carbon content on the microstructure and mechanical properties of Co based alloys with different carbon content and especially in the case where additive manufacturing is used to produce the implants.

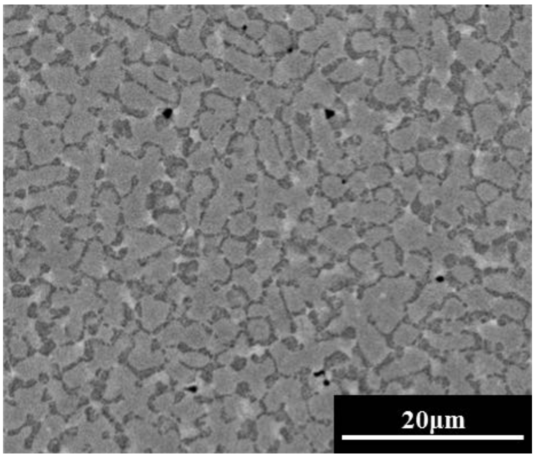

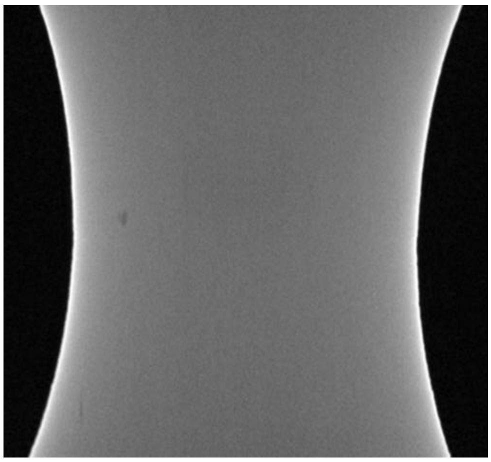

Microstructure of the initial Co based alloy without C and tomography of an alloy with C showing porosity after additive manufacturing

Wednesday, March 7th – Morning

Fourth session – 10:50-12:10

Experiments and Simulations on Wear Mechanism of Diamond-like Carbon and Ceramics

Project ELyT Lab : T2 –TRIBOCHEM : Mechanisms of lubrication of ta-C by hydrogen gas.

	Momoji Kubo IMR Tohoku University 2-1-1 Katahira, Aoba-ku Sendai 980-8577, Japan		Yusuke Ootani IMR Tohoku University 2-1-1 Katahira, Aoba-ku Sendai 980-8577, Japan
	Maria Isabel De Barros Bouchet LTDS Ecole Centrale de Lyon 69134, Ecully, France		Jean Michel Martin LTDS Ecole Centrale de Lyon 69134, Ecully, France

Abstract :

1. Introduction

Diamond-like carbon (DLC) is a promising protective coating to reduce the friction and wear of materials. It is known that the tribological properties of DLC coatings are strongly affected by the hydrogen gas environment due to the tribochemical reactions. Thus, the detailed tribochemical reaction dynamics with hydrogen gas are required to improve the tribological properties of DLC coatings.

2. Computer simulations

We performed molecular dynamics sliding simulations of DLC to investigate the effects of hydrogen gas environment on the tribological properties of amorphous carbon. The sliding simulations were performed with hydrogen-free DLC model in vacuum and hydrogen gas environment, respectively. We used reactive force field (ReaxFF) to take into account chemical reactions [1]. Figure 1 shows snapshots of the sliding simulations after 600 ps in the (a) vacuum and (b) hydrogen gas environment. We found two different wear mechanisms of DLC in our simulations: chemical wear as the generation of gaseous hydrocarbons and adhesive wear as the transfer of carbon atoms to the counter surface. Figure 2 shows the wear amount of DLC asperities in the (a) vacuum and (b) hydrogen gas environment. In the vacuum environment, adhesive wear is the dominant wear mechanism. Generally, the adhesion is directly determined by the number of interfacial C-C bonds connecting the two surfaces. In the vacuum environment, the hydrogen terminations were gradually depleted from the surface due to the generation of gaseous hydrocarbon molecules, leading to the formation of interfacial C-C bonds. On the other hand, the adhesive wear was largely suppressed in the hydrogen gas environment because hydrogen molecules have passivated the DLC surface and have inhibited the formation of interfacial C-C bonds. Therefore, the hydrogen gas environment prevents the DLC from deterioration and maintains the low wear behaviors during the whole lifespan of the coatings. In these simulations friction was not calculated.

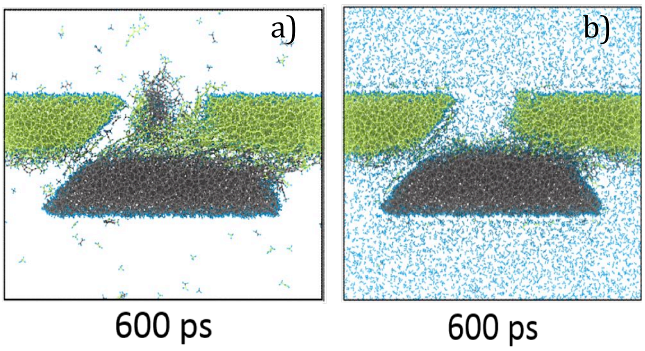

Figure 1 : Snapshots of DLC asperities in the (a) vacuum and (b) hydrogen gas environment at the end of the friction simulation.

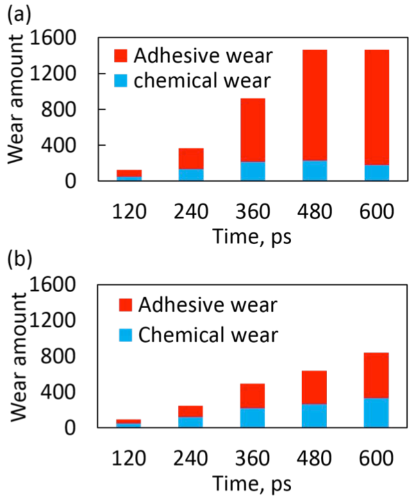

Figure 1 : Wear amount of DLC asperities in the (a) vacuum and (b) hydrogen gas environment.

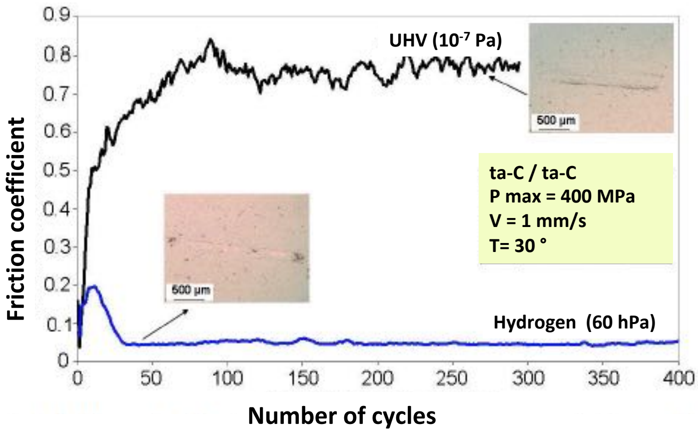

Figure 3 : Friction coefficient and optical wear tracks of ta-C/ta-C contact in vacuum (10 nPa) and hydrogen gas environment (60 hPa).

2. Tribological experiments

Tribological experiments with ta-C carbon film were performed first in ultrahigh vacuum (10 nPa) and then with introducing a partial pressure of hydrogen of 60 hPa. The results shown in Figure 3 are in good agreement with the simulations: In UHV, at the beginning of friction, passivation of ta-C by H/OH is removed by shear and friction increases drastically to high value (0.8). In presence of hydrogen, the friction decreases to a low value (below 0.05) and is stabilized. The wear scar in vacuum is well visible with black marks. In H_2, the wear scar is hardly visible.

It is interesting to notice that in the early stage of friction (the first 10 cycles) we have the removal of chemisorbed species by shearing process in both cases. Afterwards, it is necessary to have seizure and dangling bonds formation (friction increase at 0.2) for hydrogen molecules to react with the carbon. This suggests that only hydrogen atoms as radicals are able to passivate the surface. Compared to this, water vapor reacts much more quickly and easily and a much lowest partial pressure (about 10^{-3} hPa) is necessary

References :

[1] A. C. T. Van Duin, S. Dasgupta, F. Lorant, ReaxFF: A Reactive Force Field for Hydrocarbons. *J. Phys. Chem. A* **105** *(2001)* 9396-9409.

New, toxic element free metallic glasses for biomedical applications

Project ELyT lab

	*BAULIN Oriane MATEIS Laboratory, INSA Lyon, UMR CNRS 5510, 69621 Villeurbanne France*		*FABREGUE Damien MATEIS Laboratory, INSA Lyon, UMR CNRS 5510, 69621 Villeurbanne France*
	*KATO Hidemi, Tohoku University, 2-1-1 Katahira, Aoba Ward, Sendai 980-8577 Japan*		*TAKESHI Wada, Tohoku University, 2-1-1 Katahira, Aoba Ward, Sendai 980-8577 Japan*
	*PELLETIER Jean-Marc MATEIS Laboratory, INSA Lyon, UMR CNRS 5510, 69621 Villeurbanne France*		

Abstract :

Metallic glasses exhibit unique properties compared to crystalline alloys, high strength and low Young Modulus. This last feature is interesting to prevent bone osteolysis due to stress shielding. The biocompatible amorphous alloys could be of two kinds: reinforcement or biodegradable. To improve ductility or glass forming ability, most part of the glasses for biomedical applications contain non desirable elements such Be or Ni. In this work two new metallic glasses were elaborated, a Mg-based system : $Mg_{(85-x)}Ca_{(8+x)}$-Au_7 (with x=0, 2, 4) and $Mg_{(81-x)}Ca_{10}Au_7Yb_{(2+x)}$ (with x= 0, 8) and a Zr-based system : $Zr_{56}Co_{28}Ga_{16-x}(Si)_x(Sn)_x$.

From a first observation, the samples exhibit some ductility. The super-cooled liquid region was evaluated to be equal to 22 °C for the Mg-based metallic glass and can reach 29°C for the Zr-based system. The resistance to crystallization and thermal stability were investigated with different experimental methods. At 120°C, no crystallization was detected after 30 minutes, which is a crucial advantage for the process of sterilization in medicine for both samples. Cytotoxicity tests were done on the Zr-based sample to investigate the biocompatibility of the Gallium.

Mechanical properties has been also investigated by hardness and nanoindentation. The results are promising and now the effect of small addition of others elements is investigated to increase Delta T.

Low and ultralow friction of microcrystalline diamonds films

towards smart and tribo-resistant coatings

Project lofDIAMS

ELyT Global
Surface and interfaces
Materials and structure design

Dr. Hiroyuki MIKI

Frontier Research Inst. for Interdisc. Sci. (FRIS), Tohoku University Aramaki asa Aoba 6-3, Aoba-ku, Sendai, Japan

Michel BELIN

LTDS, CNRS Ecole Centrale de Lyon 36 rue Guy de Collongue, 69134 Ecully cedex, France

1. Introduction

In the field of tribology, the low and ultra-low friction is one of the most challenging subject [1, 2]. Different kinds of tribosystems are expected to exhibit low friction performances. One of them is some hard coatings, and especially the carbon-based coatings under dry lubrication. Interesting results have been reported previously, obtained on partly polished CVD diamond-films. Very low friction has been reached in air [3]. The authors have shown that the friction results were strongly influenced by contact conditions, especially the sliding speed and surface profile. These results are very promising, but not fully understood yet. Starting from that point, we are running a research program, dealing with low- and ultra-low friction obtained on thin films based on diamond coatings. In particular the group of H. Miki *et al.* at Tohoku University, has recently highlighted a milli-range order friction, with a contact of partly polished microcrystalline diamond layers. On the other side, LTDS has improved an experimental technique to qualify ultralow friction level, called “relaxation tribometer technique”, down to the level of 10^{-2} to 10^{-4}, if it happens. The complementary skills are joining in this project to go further in the knowledge of low-friction processes. In the previous ELyT-Lab project, we have explored the friction properties of partly-polished CVD diamond coatings in dry friction. Especially, we have first quantified different components of friction: especially a solid-type friction independent of the speed and also a velocity-dependent contribution of friction, identified through the use of this technique. It should be noticed that this approach has no equivalent today. The influence of roughness was the main parameter under investigation.

2. Experimental

Friction characterization has been achieved thanks to the oscillating relaxation tribometer, recently developed at LTDS, in order to measure the kinematic friction between two sliding surfaces [4]. This technique is based on the study of the dynamic free-response of a single degree-of-freedom mechanical oscillator, in which the sliding contact acts as a damper. It has been beneficially used to determine the velocity-independent and velocity-dependent friction contributions, with no need for any direct friction force measurement. The samples have been prepared at Tohoku University. The diamond coatings were deposited by the Hot Filament CVD method on SiC ceramics substrate.

Deposited microcrystalline diamond films were then carefully polished, inducing surface topography changes, see Fig. 1.a. Three levels of roughness have been investigated in the preliminary experiments: 1.0-1.5 µm, 0.4-0.7 µm and 0.1-0.2 µm. The normal load used here is ranging from 50 to 300 mN. The experiments have been run in air, temperature of 23°C and humidity 38 RH%.

3. Main results

As a result of experiments, a typical time-response of the loaded contact was obtained, during its evolution from the initial situation, up to the final stop, through a damped oscillating process. The normal load was set to 50 mN. In these mild conditions, the maximum Hertzian pressure was 270 MPa and no wear is expected to occur. The main results are the following:

- we can observe the decay of the amplitude, due to low-friction value at the interface, see Fig. 1.b. From a qualitative point of view, we also can notice that the decay curve of the envelope of the velocity is not strictly linear (Coulomb-type friction), giving evidence for a velocity-dependent contribution of friction;
- from these oscillations data, we can compute directly the friction law, giving the dependence of the friction coefficient with sliding velocity, see Fig. 1.c;
- the effect of roughness of the coating has been investigated. It is clearly shown that low-friction is occurring for highly polished surfaces [5,6].

1.a

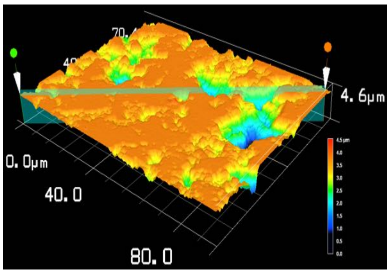

1.b

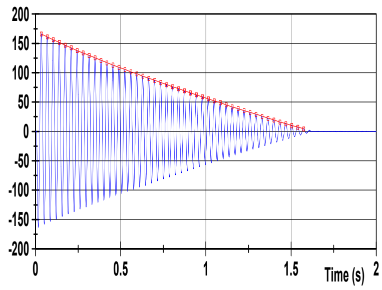

1.c

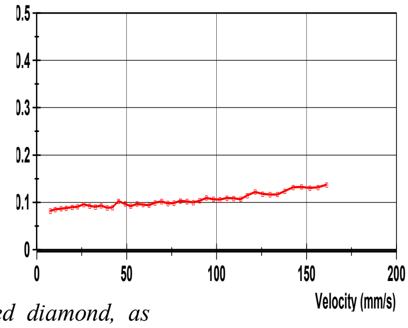

Fig. 1.a. Typical 3D topographic image obtained on a partially-polished diamond, as elaborated by CVD process. Different polishing features can be obtained. We can observe some plateaus, with initial grooves, coming from the elaboration process. Three different polish samples have been elaborated and tested: 0.1<Ra<0.2 µm, 0.4<Ra<0.7 µm, 1.0<Ra<1.5 µm. Fig. 1.b. Typical relaxation results of the friction oscillations obtained on zone 1: Ra: 0.1 to 0.2 µm, normal load: 50 mN. In blue, the velocity time-response of the test, dots in red: the detected envelope of the velocity maxima ; Fig. 1.c. Evolution of the friction coefficient as a function of velocity, so-called friction law, directly computed from oscillating data above.

4. Next steps

The next steps of this ELyT Global project will include the detailed modeling of friction laws obtained with the oscillating technique, and the comparison to those obtained on a classical tribometer configuration. We will also consider i/ the effect of an applied continuous sliding velocity component, in addition to the oscillating one, and ii/ the effect of surface topcoats of diamond films.

Acknowledgments

The authors acknowledge *Institut Carnot I@L, France* for partial funding the development of the experimental technique at LTDS, IFS and ELyT Lab. for their interest in this project. In addition, this work was partly supported by the JSPS Core-to-Core Program A. Advanced Research Networks, “International research core on smart layered materials and structures for energy saving”, the International Collaborative Research Project of Frontier Research Institute for Interdisciplinary Sciences, Tohoku University, Japan.

References

[1] Superlubricity, A. Erdemir & JM Martin Eds., Elsevier, (2007), ISBN: 978-0-444-52772-1.
[2] J. Fontaine, M. Belin, T. Le Mogne, A. Grill, Trib. Int., **37** (2004), pp. 869-877.
[3] H. Miki, A. Tsutsui, T. Takeno, T. Takagi, Diamond and Related Materials, **24** (2012), pp. 167–170.
[4] E. Rigaud, J. Perret-Liaudet, M. Belin, L. Joly-Pottuz, J.M. Martin, **43** (2010), pp. 320–329.
[5] M. Belin, H. Miki and T. Takagi, *World Tribology Congress 2017 Beijing, China, September 17 – 22, 2017*
[6] Belin, H. Miki and T. Takagi, to be submitted.

Robust shape optimization under squeal noise response for brake systems

Project ElyT Lab : R7 - Robust Multi Objective optimization design approaches

Koji SHIMOYAMA Institute of Fluid Science Tohoku University Sendai, Japan		 	Frédéric GILLOT Sébastien BESSET Laboratoire de Tribologie et Dynamique des Systèmes École Centrale de Lyon Écully, France

Abstract : In this project we focus on the robust shape optimization aiming at decreasing the squeal noise of a classical brake system. In the first steps a FEM of the pad and the disk have been modelized. Then stability diagrams have been generated to understand how geometrical parameters influence stability behavior of the structure. Next step will be to describe the pad as an iso-geometric element (IGA) in contact with the disk. Such formulation will enable fast and accurate shape optimization loop based on EGO approach, i.e. meta-heuristics optimizer on a meta-model surface response of the physical model.

1. Introduction

Squeal noise for brake systems is an industrial challenge addressed by many researchers. Among the research topics on squeal noise, squeal prediction is the basis. The shape optimization of a brake system under noise criteria is a quite new subject. Indeed, squeal noise prediction needs costly calculations that are not easy to include in optimization algorithms. Moreover, the remeshing step remains hard since the contact between the two structures strongly depends on their shapes.

2. Stability criteria

Robust optimization loops require dedicated stability criteria, as well as description of parameters incaccuracy impact on it. We proposed such stability criteria and studied deterministic parameter influence first (cf. Fig. 1). We intensively used parallelization to achieve such results, as full FEM model was used. Next step will consists in using IGA description of the pad as well as generated meta-models which will be used as basis models for the optimization, for example with meta-heuristics. Indeed reaching a robust shape design will request to consider statistical knowledge of the objectives functions.

Figure 1 : Left : SOM representation of stability criteria and 8 models parameters. Rigth : Classical FEA model of a brake system used for the SOM generation

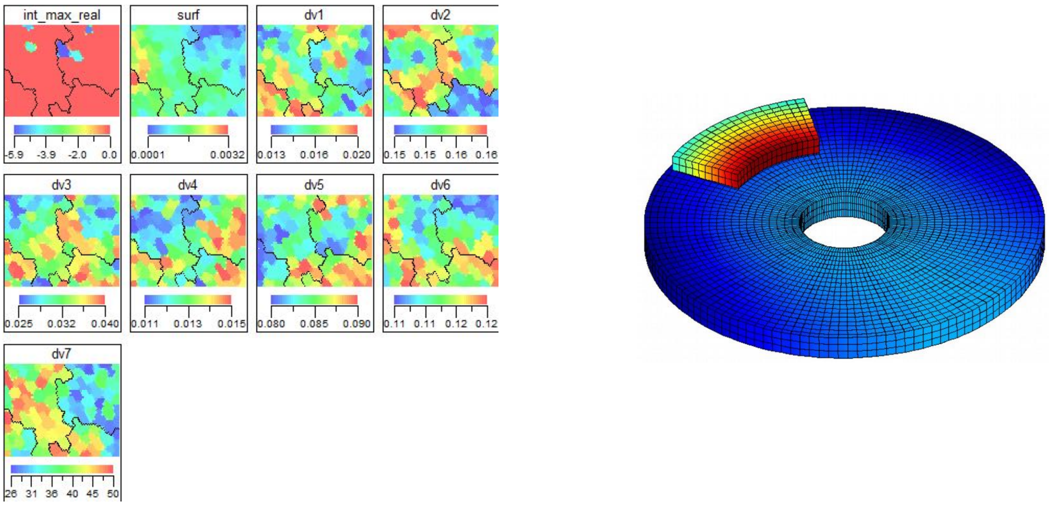

Such knowledge is hardly reachable without meta-modelizing. Robust optimal solutions belong then to a Pareto front usually provided by a specific meta-heuristic, as the proposed problem might expose a large number of parameters.

3. Originality

Shape optimization with iso-geometric models is a hot topic nowadays, as it will enable significant improvement in computing time cost and result accuracy. One the other hand nearly no results have been obtained on robust shape optimization of brake systems as such systems are very complex to simulate when considering non-linear behavior such as squeal noise. Black box optimization approaches have been successfully developed recently to address complex problems, such as robust optimization, where at least the first and second moment order of the cost function are to be considered. We aim at enabling practical systems such as brakes to benefit from such approach.

4. First Ph.d. work

A Ph.D. research grant has been awarded to Pradeep Mohannasundaram (three years from 10/2017). First work has consists in building a numerical framework for the optimization loop which involves Abaqus and Matlab, under a python script as parameters input leading block. Stability diagrams for different geometries have been generated.

Next steps will consist in using IGA description for the pad, which will require specific elements (virtual grid) for the contact problem involved. This kind of elements are not easy to use in the context of friction interfaces, since the surfaces are not defined through physical points.

5. International collaboration context

Ecole Centrale de Lyon and Tohoku University are collaborating within the International Associated Laboratory (LIA ElyTLab). French Ministry of Research has decided to move to the next step by creating on 1st April 2016 an International Mixted Unit, (UMI ElyTMax, UMI 3757) at Tohoku University. The 7th research topic of this research structure is dedicated to Multi objective robust design and is lead by Dr. Besset and Dr. Gillot for the French Side, and Dr. Shimoyama for the Japanese side.

Dr. Shimoyama has been awarded a position as Invited Professor in Ecole Centrale de Lyon for three months in 2013.

Dr. Gillot has received a position as Invited Professor for one month at Tohoku University, IFS, in May 2015.

A Ph. D. (Mss Mélina Ribaud), co-supervised by Dr. Gillot, has been invited at Tohoku University for two months (JSPS Summer Grant Program) to work under the supervision of Dr. Shimoyama.

A Carnot Grant to support this research activity has been awarded on the French side on June 2017 (to be used 01/2018 – 12/2019).

A french Ministry of Research and Education Ph.D. Grant has been awarded on the French side to support the Ph.D. of Pradeep Mohannasundaram (three years from 10/2017)

Next step is to deepen the collaboration work within this research topic through double diploma Ph.D. students, Post Doc and specific grants.

Wednesday, March 7th – Afternoon

Fifth session – 14:00-15:50

Ultrahigh-Temperature Materials and Processing Project in Tohoku University

Prof. YOSHIMI Kyosuke
Dept. Mater. Sci.
TOHOKU Univ.
Sendai
Miyagi 980-8579
JAPAN

Abstract :

In the graduate school of engineering, Tohoku University, there are three departments dedicating education and research on materials science and engineering (MSE). One is the Department of Metallurgy, the second one is the Department of Materials Science and the other is the Department of Materials Processing. Dept. Metallurgy consists of 5 research groups studying on steel making, casting and solidification processes, phase diagrams and alloy design, metal forming processes, and electro-chemical processes. Dept. Mater. Sci. has 7 research groups studying on corrosion and surface chemistry, spintronic materials, electronic materials, high-temperature materials, semiconductors, magnetic materials, and ionic conductors. Dept. Mater. Processing has 6 research groups studying on welding and joining, powder metallurgy and processing, non-destructive testing, biomolecular systems, and biomedical materials. In addition, 3 research groups studying on iron making, electro-magnetic processing, and surface and catalytic physics are involved from the graduate school of environmental studies. In total 21 research groups cooperatively engage in the MSE program at the Aobayama campus.

One of strong collaboration research projects among Dept. Metall., Mater. Sci. and Mater. Process. is on "Ultrahigh-temperature materials and processing". Ultrahigh-temperature materials beyond Ni-based superalloys are believed to play an important role to achieve sustainable societies in the world. We anticipate that they will improve the energy-conversion efficiency of heat engines such as gas turbines and jet engines and thus contribute to suppressing CO_2 gas emission. Quite recently, a novel ultrahigh-temperature material based on molybdenum has been developed in the high-temperature materials group of Dept. Mater. Sci. [1]. It is composed of molybdenum solid solution (Mo_{ss}), Mo_5SiB_2 (T_2), TiC, and a small amount of Mo_2C phases (Fig. 1) [1]. The Mo-based ultrahigh-temperature material, so-called "MoSiBTiC alloy", has a relatively low density comparable to that of Ni-based SX superalloys [2], excellent high-temperature creep strength (Fig. 2) [2], and acceptable room-temperature fracture toughness (Fig. 3) [3]. Therefore, the collaboration researches in the departments on the MoSiBTiC alloy have been performed relevant to phase diagram, microstructure analysis, fatigue, powder metallurgy and processing, application to the tool of friction stir welding oxidation-resistant coating, and so on.

In this presentation, the introduction about the Department of Metallurgy, Materials Science, and Materials Processing is briefly made first. Next, the material properties of the MoSiBTiC alloy is shown with recent hot topics. Finally, a couple of achievements obtained in the collaboration researches in the departments are presented.

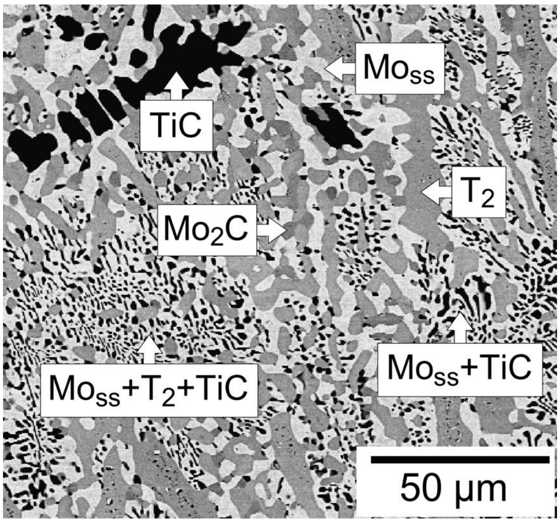

Fig. 1 A BSE-SEM micrograph of 1st generation MoSiBTiC alloy (Mo-10Ti-5Si-10C-10B (at.%))[1].

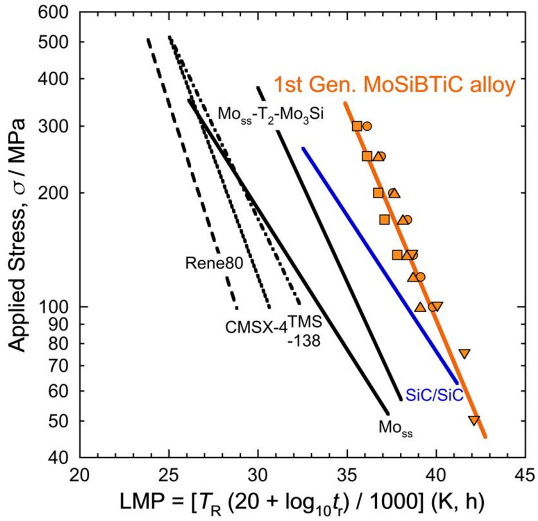

Fig. 2 Larson-Miller plots of high-temperature creep behavior of 1st generation MoSiBTiC alloy[2].

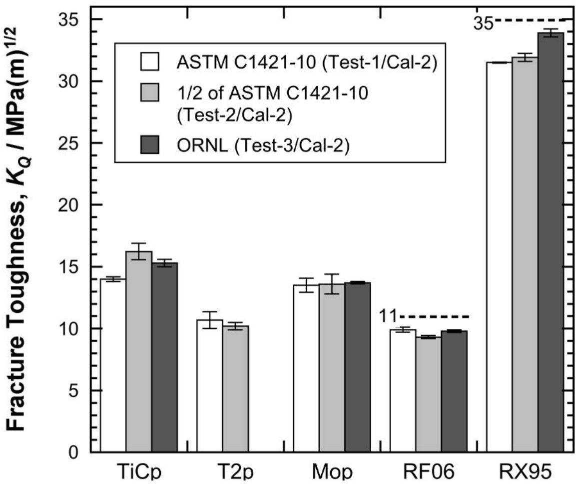

Fig. 3 Room-temperature fracture toughness values of 1st generation MoSiBTiC alloy (TiCp) and its derivatives (T2p and Mop) compared with that of commercial cemented carbides (RF06 and RX95[3]).

References :

[1] S. Miyamoto, K. Yoshimi, S.-H. Ha, T. Kaneko, J. Nakamura, T. Sato, K. Maruyama, R. Tu, T. Goto, *Metall. Mater. Trans. A* **45A**(2014) 1112-1123

[2] S.Y. Kamata, D. Kanekon, Y. Lu, N. Sekido, K. Maruyama, G. Eggeler, K. Yoshimi, submitted.

[3] T. Moriyama, K. Yoshimi, Mi Zhao, T. Masnou, T. Yokoyama, J. Nakamura, H. Katsui, T. Goto, *Intermetallics* **84**(2017) 92-102

Analysis of Interface Structure between Carbon Fiber and Immiscible Two-component Polymer Blend

Project ELyTGlobal: DESign of Interface structure of fiber-Reinforced polymer blEnd

	*KOSUKEGAWA, Hiroyuki* *Institute of Fluid Science, Tohoku University* *2-1-1 Katahira Aoba-ku, 980-8577 Sendai, Japan*		*DALMAS, Florent* *MATEriaux: Ingénierie et Science - CNRS UMR5510 INSA-Lyon* *7, avenue Jean Capelle, 69621 Villeurbanne cedex, France*
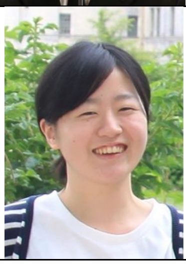	*HAYASHI, Riona* *Graduate School of Engineering, Tohoku University* *6-6 Aramaki-aza Aoba Aoba-ku, 980-8579 Sendai, Japan*		*CAVAILLE, Jean-Yves* *ELyTMaX UMI 3757, CNRS – Université de Lyon – Tohoku University, International Joint Unit, Tohoku University* *MaSC, room 502, 2-1-1 Katahira, Aoba-ku, 980-8577 Sendai,*
		*TAKAGI, Toshiyuki* *Institute of Fluid Science, Tohoku University* *2-1-1 Katahira Aoba-ku, 980-8577 Sendai, Japan*	

<u>Abstract :</u>

1. Introduction

Carbon fiber reinforced thermoplastic (CFRTP), which is a composite made of carbon fibers embedded in a thermoplastic matrix, has been studied for the applications to mass-production industries. CFRTP has some problems for practical applications. One problem is that adhesion between fiber and matrix can be weak, depending on the polymer matrix. For example, polypropylene (PP), which is generally used as the matrix of CFRTP, cannot be bonded well with carbon fiber because of hydrophobicity of PP [1]. Therefore, to improve this compatibility, the use of hydrophilic polymer such as polyamide (PA) has been studied. However, PA has disadvantages such as high hygroscopicity, high melting point and viscosity which make the material handling difficult.

The other problem of CFRTP is that impact resistance and strength of thermoplastic materials are generally incompatible. The use of polymer blends (made of two or more kinds of polymers) as matrix for CFRTP has attracted attention in order to combine two properties of component polymers at the same time. When blended polymers are immiscible, it is known that the polymer blend has a phase separation structure such as sea-island structure. The control of this phase separation structure can change the properties of the polymer blend. To reach properties for the polymer blend better than those of each polymer component, a compatibilizer is used to form stable phase structures. Even though hydrophobic PP and hydrophilic PA are incompatible, adding a compatibilizer makes the diameters of dispersed phase in PP/PA polymer blend smaller and stable, and also improves the mechanical properties of the blend. In the case of PP/PA polymer blend, maleic anhydride grafted polypropylene (MAgPP) is often investigated as a compatibilizer.

The purpose of this study is to evaluate whether CFRTP based on PP/PA polymer blend can be applied to a commercial product and to design the optimum interface structure of fiber/ polymer blend in CFRTP. As an initial stage, the interfacial shear strength (IFSS) and phase separation structure between carbon fiber and PP/PA polymer blend were evaluated. The values of the IFSS of the different combinations of fiber/polymer in surface characteristics were discussed by the observation of the phase separation at the interface by electron microscopy.

2. Experimentation

PP/PA polymer blends which have different concentration of PA were prepared by using a kneader (HAAKE Rheomix 600p, Thermo Scientific Inc.). All specimens have 10 wt% of MAgPP as a compatibilizer. PP/PA polymer blends were processed into thin films with a thickness of 100~200 μm by using a hot press (AH-203, AS ONE Co.). Two kinds of carbon fibers with different surface characteristics were prepared as follows: sizing reagent on commercial carbon fiber (T700SC, Toray Industries Inc.) was removed with a mixture of acetone and methyl-ethyl ketone (50/50, v/v), and the desized fiber was reduced by the reduction treatment by referring Gao's method [2]. Sized polar fiber (commercial one) and reduced nonpolar fiber are respectively named as "sCF" and "hCF".

A single filament of carbon fiber was embedded in molten PP/PA polymer blend film at 200ºC by using a hot press and then cooled to room temperature. Uniaxial tensile test of the single carbon fiber embedded films was conducted by a displacement of 1 mm, and the length of fragments of the broken fiber in the film was measured by using an optical microscope. The values of IFSS of the specimens were calculated by the Eq. (1);

$$\tau = \frac{3d\sigma_f}{8L_a} \qquad (1)$$

where, τ is IFSS (Pa), d is the diameter of carbon fiber (m), σ_f is the strength of fiber, L_a is the mean length of the fragments (m) [3].

The phase separation structure of the interface between fiber and polymer blend was observed by using a scanning electron microscope (SEM) (SUPRA 55VP, Carl Zeiss) and a transmission electron microscope (TEM) (JEM-2100F, JEOL Ltd.).

3. Results and Discussion

The tendency of IFSS according to the concentrations of PA in polymer blend was different depending on the surface characteristics of carbon fiber as shown in Fig. 1. IFSS of sCF, which is polar fiber, increased according to the concentrations of PA and reached about 12 MPa at 100wt% of PA. On the other hand, IFSS of hCF, which has nonpolar characteristic, becomes the maximum at 40wt% of PA showing about 12 MPa. This result indicates that the use of nonpolar fiber is sometimes more suited in terms of the adhesion between fiber and matrix than polar fiber when we use polymer blend of PP/PA as matrix.

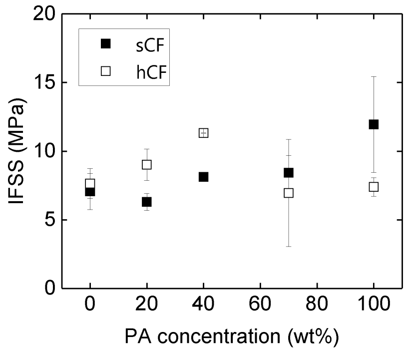

Figure 1 IFSS of carbon fibers and PP/PA polymer blends.

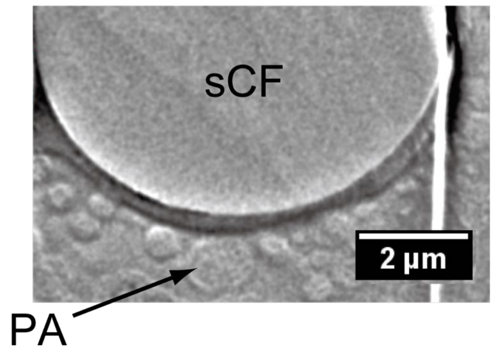

Figure 2 SEM image at the interface of sCF and PA40%.

By the observation of SEM and TEM, the phase separation of PP/PA polymer blend at the interface was different between sCF and hCF. At 40wt% of PA, PA was dispersed phase and distributed in the continuous phase of PP (Fig. 2). The dispersed phase of PA adhered on sCF at 40wt% of PA as shown in Fig. 2. However, PP was segregated on hCF, and the dispersed phase of PA did not adhere on hCF. These differences of the phase separation structures at the interface of fiber/matrix were reflected on the different tendency of IFSS of carbon fiber and PP/PA polymer blend. The adhesion of polar fiber (sCF) on PP/PA polymer blend is formed by hydrogen bonding between sCF and amide groups of PA, and the IFSS is dependent on the amount of PA dispersed phase surrounding the fiber. In addition, the shear stress on sCF may decrease due to the dispersed phase of PA adhered on sCF. On the other hand, the adhesion between nonpolar fiber (hCF) and polymer blend is formed by dispersion force, and the tendency of the IFSS is explainable by the dispersion component of surface free energy of polymer blend.

To improve and control the adhesion of fiber and matrix of CFRTP, it is required to design the optimum interface structure by adjusting the surface characteristics of fiber. Considering that the value of IFSS of carbon fiber and epoxy resin, which is the combination used in aircraft industry, is more than 20 MPa [4], it is needed to improve IFSS of CFRTP more for practical applications.

Acknowledgement

This work was partly supported by a JSPS KAKENHI Grant-in-Aid for Young Scientists (B) Grant Number 15K18219 and the JSPS Core-to-Core Program, A. Advanced Research Networks, “International research core on smart layered materials and structures for energy saving”.

References :

[1] N. Hirano, H. Muramatus, T. Inoue, *J Japan Soc Composite Mater*, **39** (2013) 113-119.
[2] W. Gao, et al., *Nature Chemistry*, **1** (2009) 403-408.
[3] A. Kelly and W. R. Tyson, *J Mech Phys Solids*, **13** (1965) 339-350.
[4] Y. Sawada and Y. Nakanishi, *Tanso*, **140**(1989) 248-254.

Mechanical characterization of Inter-particle sintering of Ultra High Molecular Weight Polyethylene (UHMWPE)-Fumed nano-alumina (FNA) composites processed under different interfacial loading conditions

	*Kesavan Ravi [1,2,3]*		*Olivier Lame [2]*
	*Kazuhiro Ogawa [1,3]*		*Jean-Yves Cavaillé [3]*

1) Fracture and Reliability Research Institute, Tohoku University
2) Material Engineering and Science lab, MATEIS, INSA Lyon
3) Engineering Science Lyon Tohoku joint Laboratory for Materials under Extreme Conditions, ELyTMaX, Tohoku University – CNRS – Université de Lyon

Abstract :

1. Introduction

UHMWPE, due to its molecular weight, is used in several applications like orthopedic implants, armor plates, ship rudders because of its high wear resistance, impact resistance, and cavitation erosion resistance [1–3]. Processing of UHMWPE via a technique called cold-spray was made possible [4] thanks to an understanding of classical compression sintering and the high-speed compaction of UHMWPE. Cold spray is a coating technology in which fine particles (5-100 μm) are impacted onto a target surface at high velocities (200-1000 m/s) to obtain thick coatings/sintered consolidates avoiding the traditional tools like monitored temperature presses [5]. In the case of UHMWPE, Ravi et al. reported that particle binding agents like FNA and particle temperature were the primary parameters that permitted the buildup of coating thickness [4]. This research work aims at understanding the effect of interfacial loading during the processing of UHMWPE interfaces because of effect of shot-peening seen during coating process. Thereby, helping to predict and understand the cold spray buildup mechanism. Hence, the study is a first step towards understanding the cohesive strength and physical properties of the cold-sprayed deposited material with respect to the interfacial loading conditions and effect of FNA particles.

2. Experimentation, discussion

UHMWPE volumes are processed at different compression loading by powder compression sintering to emulate various sections of cold-sprayed deposits. This study focuses on characterizing mechanical properties of UHMWPE-FNA composite consolidates as a function of (i) interfacial loading and (ii) percentage of FNA particles during processing. Two sintering protocols, namely half-sintering and full-sintering, under a low and a high compressive loading condition respectively were carried out. Tensile tests of the sintered samples were carried out to understand the strength of the interfaces. Figure 1 shows the conditions used to process sintered volumes.

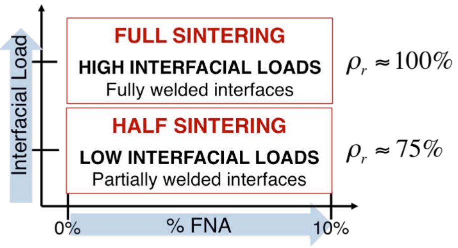

Figure 2 Illustration describing the full-sintering and half-sintering protocol and cross-section of the sintered product.

Firstly, while looking into the sintering of any two interfaces of nascent UHMWPE particles, it was understood that when the interface reaches melting point the chain diffusion and re-entanglement occurs through the interface. The results obtained with FNA content at high and low compressive loads showed that a sufficiently high interfacial load is necessary to embed FNA particles into the polymer matrix to promote wetting and continuity of polymer around FNA. Due to the consequential wetting of FNA particles by the UHMWPE chains, it was shown to reinforce the interfaces. Most likely phenomena for reinforcement is believed to be a percolating interfacial zone comprising of a co-continuous network of polymer chains and FNA particles wetted by polymer chains. In stark contrast, the low interfacial load was seen to be decreasing the mechanical property of the volume with the increase in the FNA content which suggested that interfacial load, during half-sintering, was not sufficient enough to provide the energy to press the interface against each other for a good wetting and a subsequent inter-diffusion. Figure 2 shows the tensile test results of the full sintered and the half sintered material containing different percentages of FNA content.

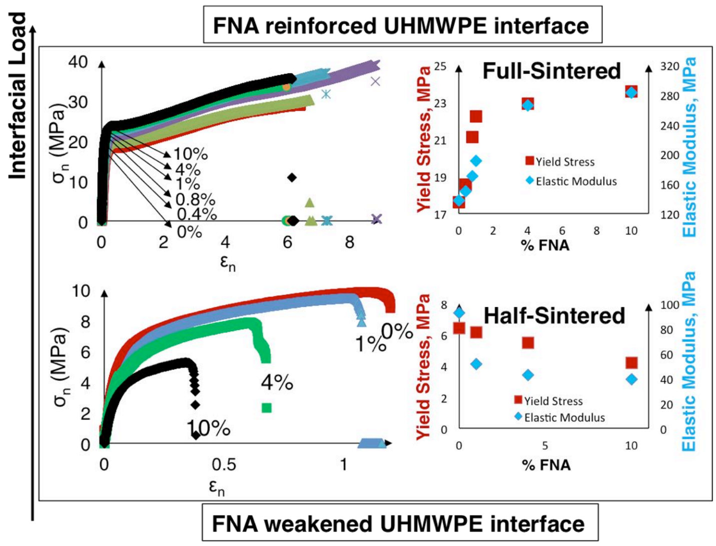

Fig. 2: The variation of the mechanical properties UHMWPE composites processed by full sintering and half sintering containing different percentages of FNA content.

References :

[1] S.M. Kurtz, Uhmwpe Biomaterials Handbook, 2009. doi:10.1016/B978-0-12-374721-1.X0001-6.

[2] T. Deplancke, O. Lame, F. Rousset, I. Aguili, R. Seguela, G. Vigier, Diffusion versus cocrystallization of very long polymer chains at interfaces: Experimental study of sintering of UHMWPE nascent powder, Macromolecules. 47 (2014) 197–207.

[3] S.B. Ratner, I.I. Farberova, O. V. Radyukevich, E.G. Lure, Connection between wear resistance of plastics and other mechanical properties, Sov. Plast. 12 (1964) 37.

[4] K. Ravi, Y. Ichikawa, T. Deplancke, K. Ogawa, O. Lame, J.-Y. Cavaille, Development of Ultra-High Molecular Weight Polyethylene (UHMWPE) Coating by Cold Spray Technique, J. Therm. Spray Technol. 24 (2015).

[5] V.K. Champagne, The cold spray materials deposition process Fundamentals and applications, Elsevier, 2007.

Effects of temperature elevation on drilling of acrylic composite materials for bone biomodel.

Project ELyT lab B6 / T:
Development and Friction Characterization of Biomodels of Bones, BoneDrill

	Yuta MURAMOTO Graduate School of Biomedical Engineering, Tohoku University / LTDS, Ecole Centrale de Lyon		Dominik Hüsener Department of Mechanical Engineering, RWTH Aachen University		Gaëtan BOUVARD, LTDS, Ecole Centrale de Lyon
	Makoto OHTA Institute of Fluid Science, Tohoku University / ELyTMaX UMI 3757, CNRS – Université de Lyon – Tohoku University		Vincent FRIDRICI LTDS, Ecole Centrale de Lyon		Philippe KAPSA, LTDS, Ecole Centrale de Lyon

Abstract :

1. Introduction

Drilling is one of the basic surgical skills in dentistry and orthopedics. Generally, bone biomodels play a role in doctors' training or evaluation of medical devices such as bone screw or pin. Compared to natural bone, biomodels have advantages such as reproducibility, and easiness of handling. However, mechanical properties of biomodels are too limited to reproduce mechanical / tribological response of natural bone. Existing bone biomodels can rarely provide clinically relevant data [1]. To the author's knowledge, a bone biomodel that can show the equal drilling behavior of natural bone has not been achieved yet. Therefore, the purpose of this study is development of a bone biomodel with realistic mechanical / tribological behavior. To obtain the target material, authors fabricated and studied acrylic composite materials. This report focuses on the drilling behavior considering the effect of temperature elevation during drilling on the work pieces.

2. Materials and methods

2. 1. Sample preparation

Poly(methyl methacrylate) (PMMA), so called acrylic resin, was chosen as a base of composite material. PMMA for dental application (Miky blue, Nissin Dental Products Inc.) was used. Then, cellulose fiber (CF), cellulose nano fiber (CNF), and wood fiber (WF) were obtained as additives. Additives were mixed with PMMA respectively, at each maximum soluble amount. In this research, the amount of each additive was 10% for CF, 20% CNF, 4% WF at weight ratio, which was defined as (Additive) / (PMMA + Additive). As a result, 4 samples including pure PMMA were fabricated. In addition, 2 types of conventional bone biomodels made of polyurethane (called PU20 and PU50 in this study) (Solid Rigid Polyurethane Foam, Pacific Research Laboratories, Inc., Vashon, WA, USA) were obtained as controls. Every sample was cut into a cube 20 mm on a side for drilling tests.

Porcine femoral bone was obtained by butcher. The bone shaft was taken out and cleaned. Then, the bone specimen was sunk in ethanol for a day, and dehydrated at room temperature. The authors estimated that storage in ethanol has no significant effect on mechanical behavior since it has been revealed by Linde and Sorensen that the storage in ethanol did not change the elastic properties of trabecular bone [2].

2. 2. Drilling tests

Experimental set-up consists of a tapping center (Brother TC-22A, Brother Industries, Ltd.), a dynamometer (Kistler Type 9125A, Kistler Co., Ltd.) for measurement of drilling properties such as thrust force and friction torque, and a clamp on a working table. Temperature was monitored with a thermographic camera (Infrared thermography FSV-2000, Apiste Corporation) during drilling. A tapered drill for dental surgery (Twist Drill, Nobel BioCare Japan Co., Ltd.) with a diameter of 2 mm was used in a series of tests. Rotation speed of the spindle was 1000 rpm, and feed rate 0.035 mm/rev.

3. Results and discussion

Figure 1 shows thrust force curve, averaged from 3 holes of drilling tests for all the materials. The results were smoothened by moving average filter. The curve for drilling on bone stands for mainly 3 phases [3]; first contact between the drill and the surface of samples, the start of material removal with continuous rise in thrust force until the full engagement of the drill-bit, and then penetration of the drill-bit where thrust force keeps the maximum value. Polymeric materials show equal trends on the elevation of thrust force, while materials except PU20 show gradual decrease after reaching its maximum force. The trend is not seen in porcine bone. Comparing the maximum values of thrust force, acrylic materials show almost half of porcine bone, where PU50 and PU20 show much smaller.

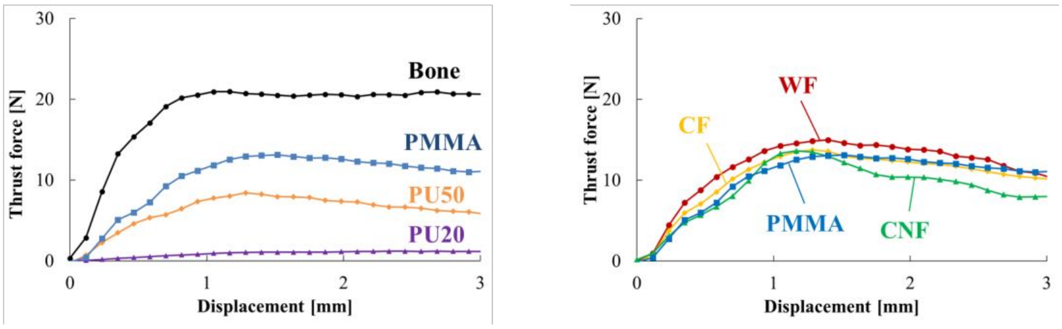

Figure 1: Thrust force profile for all the materials focusing on the difference of materials (left), additives (right)

The gradual decrease in thrust force especially for acrylic materials can be affected by temperature elevation due to friction heat during drilling. In order to see the effect of change in mechanical properties on thrust force profile, DMA measurement results reported previously [4] were combined with the recorded temperature distribution (Figure 2). Thrust force starts decreasing after 60ºC, where mechanical properties of PMMA is not largely changed. Considering the temperature gap between on the surface where infrared camera can monitor and on the drill tip inside the drilling hole, the effect of temperature elevation on drilling acrylic materials might not be ignored. Improvement of experimental set-up may be required for further analyzation,

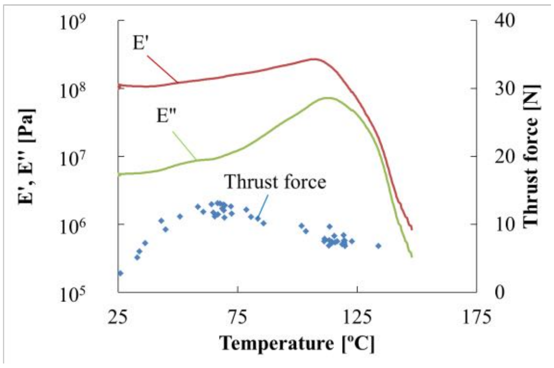

Figure 2: DMA curve and thrust force profile for pure PMMA sample versus temperature

Acknowledgement

CNF was kindly supplied by Prof. Fredrik Lundell. This work was partly supported by the JSPS Core-to-Core Program, the ImPACT Program, IFS collaborative research project, and ELyT lab.

References :

[1] J.-T. Hausmann, *Osteo and Trauma Care*, **14**(2006) 259-264

[2] F. Linde, H.C. Sorensen, *Journal of Biomechanics*, **26**(1993) 1249–1252

[3] W. Lughmani, *et al.*, *Journal of Mechanical behavior of Biomedical Materials*, **42**(2015) 32-42.

[4] Y. Muramoto *et al.*, TFC ELyT Workshop (2016), Tohoku University & Miyagi Zao Royal Hotel, Japan

The PYRAMID project

Project ELyT lab : R32 – study of …

	*Pr. Toshiyuki Takagi Center for Fundamental Research on Nuclear Decommissioning, Tohoku University Tohoku University Institute of Fluid Science*		*Philippe Guy Laboratoire Vivrations Acoustique INSA de Lyon*

OTHER PERSONS INVOLVED:

Yutaka WATANABE, Hiroshi ABE, Shinji EBARA, Tetsuya UCHIMOTO, Takayuki AOKI, Fumio KOJIMA, Ryoichi URAYAMA, Hongjun SUN (Tohoku University), Thomas MONNIER, Jérôme ANTONI , Bernard NORMAND, Julien CHATARD (INSA-Lyon), Nicolas MARY (CNRS/UdL/TU/ELyTMaX), Ryo MORITA, Shun WATANABE (Central Research Institute of Electric Power Industry, Japan) Atsushi IWASAKI (Gunma University, Japan), Pierre CALMON, Christophe REBOUD, Vahan BARONIAN, Xavier ARTUSI, Sylvain CHATILLON, Alain LHEMERY (CEA-LIST),

Abstract :

We aim to develop new tools and techniques to detect and quantify wall thinning due to Flow Assisted Corrosion in piping systems. Corrosion modes and rate will be predicted by numerical simulations at any position for actual layouts of piping systems. These predictions will be validated by electrochemical experiments under controlled mass transfer coefficient. From the previous results, ultrasonic guided modes EMAT networks will be designed. Their performances will be investigated in corrosion test facilities and the adequate signal processing techniques based on Bayesian approach will be developed. To increase the method reliability, simulations will help selecting the best technical solution, based on Probability of Detection and flaw characterization performance. Special ultrasonic imaging techniques will also be applied if necessary. From all the data gathered during the project, an industrial risk evaluation of any kind of piping system subject to corrosion will be performed.

1. Introduction

The PYRAMID project is an International Collaborative Research Project (PRCI), which brings together French public laboratories (MATEIS and LVA at INSA Lyon, and CEA), an International Joint Unit (ELyTMaX), Japanese public laboratories (IFS, and GSE at Tohoku University, GSST at Gunma University), and the Nuclear Technology Research Laboratory at CRIEPI a non profit research foundation, supported by the electrical japanese industries.

PYRAMID project aims to develop new tools and techniques to detect and quantify wall thinning due to Slurry Flow induced Corrosion (SFC) in piping systems. SFC is a special case of Flow Accelerated Corrosion (FAC) in presence of a flow with a high concentration of debris of various kinds (concrete, corrosion, metallic…).

The final goal is to provide a risk management system based on prediction-monitoring of wall thinning due to SFC.

Corrosion modes and rate will be predicted by numerical simulations at any position for actual layouts of piping systems such as elbows. These predictions will be validated by electrochemical experiments under controlled mass transfer coefficient.

Also Ultrasonic Non Destructive Testing (UT) methods will be designed with the help of simulations and their performances will be investigated in corrosion test facilities. The adequate signal processing techniques based on Bayesian approaches will be developed.

UT techniques are widespread in industry because they allow the control in the bulk of the component and help to improve productivity and compliance of products with quality and safety requirements. Among them, Electro-Magnetic Acoustic Transducers (EMAT) allow the generation and sensing of elastic waves in a part without mechanical contact with it; therefore, they can be used at high temperature and in various harsh environments where standard piezoelectric transducers fail. The use of EMAT constitutes a versatile solution adapted to complex cases.

The availability of validated simulation tools to predict the wave field they generate and their sensitivity to an arbitrary wave field is crucial if one wants to benefit of their advantages and limit their drawbacks. Once such tools are developed, they can be efficiently coupled to other tools dedicated to elastic wave propagation and scattering, the complete set of simulation tools allowing the full simulation of non destructive inspections in complex cases.

Elastic Guided Waves (GW) are used in the non-destructive testing of pipes. Numerical study of GW scattering is often computationally expensive because of very short wavelengths compared to the size of the pipe. Furthermore, the number of scattered modes from non-axisymmetric defect (as typical corrosion area, crack…) can be too large for standard finite element method (FE). Accordingly, the simulation platform CIVA deals with models based on a Modal Formalism to simulate non-destructive inspection by GW using the Semi-Analytical Finite Element method (SAFE). Presently, EMAT sources are taken into account in an efficient hybrid SAFE/FE method for computing the scattered modes by an arbitrary complex defect that has been implemented for several years in CIVA NDT simulation platform by CEA.

To increase the method reliability, simulations will help selecting the best technical solution, based on Probability of Detection and flaw characterization performance. Special ultrasonic imaging techniques will also be applied.

This dual approach, which combines simulation and characterization, should make it possible to optimize the inspection process in corroded steel pipes.

From all the data gathered during the project, an industrial risk evaluation of any kind of piping system subject to corrosion will be performed.

The results of the research carried out in the project will be directly applicable to any kind of piping system subject to corrosion that has to be detected, quantified and the subsequent risk evaluated.

2. Impacts and benefits

The PYRAMID project falls under the guidance 15 of French SNR entitled Sensors and Instrumentation and of the Materials and Processes axis (Axis 3) under the challenge of Stimulating Industrial Renewal (Challenge 3).

Firstly, the results of this research will be directly exploitable by the industrial, in particular in the context of the decommissioning of Japanese nuclear plants.

The extension of the simulation tools will contribute to improve the understanding of the FAC phenomena and the performances of the ultrasonic control. The project will therefore have a significant societal impact, as it will meet regulatory requirements on facility safety. From an economic point of view, the different models developed in the project should make it possible to take on new markets in the field of simulation of the NDT, but also in the field of FAC simulation. The implementation of tools to deal with realistic applications with reasonable computational times should appeal industrial sectors whose requirements have not been satisfied so far.

On the NDT side, the objective is to incorporate the achievements into a later version of CIVA and the validity domains associated with the developed simulation tools to be clearly identified.

Integrating the CIVA platform, the developments resulting from the PYRAMID project must make it possible to establish its dominant position in the market for modeling tools for non-destructive methods. The validation phase of the models in the project is therefore particularly important to enhance the capacities of the simulation to reproduce quantitatively the experimental phenomena.

Independently of the developments of the simulation tools, studies carried out in the field of the characterization of FAC in the harshest conditions that can be found constitute subjects of importance for the scientific community on the knowledge of the corrosion processes under slurry flows. Moreover, the knowledge that will be contributed by the project on the ultrasonic control of these corrosion problems are not only interested in nuclear domains but can also be beneficial for other industries (Petroleum Industry, Chemical storage and transport, ...) where an increase in the safety and risk management of piping systems are needed.

By insuring the quality of the NDT of corroded piping systems, in nuclear or chemical plants, and therefore prevent industrial accidents leading to leakage of chemical pollutant, the PYRAMID project will contribute to the industrial and societal values of sustainable development and the safety of people and goods.

In addition, the development of simulation tools will simplify the signal processing, making the inspection technique accessible to a greater number of users. In this way, the increase in control activity will definitely generate new possibilities for creation of employment in the field of the NDT.

The design of new innovative EMAT sensors and integrated sensor networks associated to high performance signal processing algorithms, will also contribute to foster the sensors manufacturing sector.

3. Dissemination and potential interactions with ElytSchool

On a long term scale, the issue of decommissioning nuclear power plants will arise in many countries worldwide, and the results of PYRAMID project will be of a great importance.

Based on the results and methods that will be found to be the most promising, higher education programs could be proposed in order to graduate high level technicians, as well as engineers prepared to handle all the aspects of that challenge.

Finally, beside the publication policy, we would like to organize special sessions focused on FAC modelisation, simulation and characterization, but also on EMAT guided waves NDT methods in the NDT Schools that TU and INSA organize each year in Japan and France alternatively.

Wednesday, March 7th – Afternoon

Sixth session – 16:20-18:00

Experimental Study on Active Control of Protein Mass Flux by Functional Membrane

KOMIYA Atsuki
Institute of Fluid Science,
Tohoku University
2-1-1, Katahira, Aoba-ku, Sendai, 9808577, Japan

LIVI Sébastien
Ingénierie des Matériaux Polymères
UMR CNRS 5223
INSA de Lyon
69621 Villeurbanne Cedex, France

Abstract :

1. Introduction

The diffusion coefficients are one of significant thermophysical properties for the investigation and complete understanding of mass transport phenomena. Conventionally, at a viewpoint of hindered diffusion, the diffusion phenomena of protein have been studied by observing diffusion fields under the conditions of several kinds of gel or membrane system, and effective diffusion coefficients were determined and evaluated [1-3]. As a precursor study by authors [4], a hindered diffusion phenomenon was evaluated by using Poly Lactic Acid (PLA) as a thin membrane. The thin membrane has micro-structured channels and pores, and separates high concentration solution and low concentration one in transient diffusion field. The protein passes through the narrow channels and pores of membrane, and hindered diffusion occurred. In this study, we aim to conduct the diffusion experiments at a view point of active mass transfer control of protein, and quantitative evaluation of mass transport phenomenon by changing the microchannel and pore size of membrane. As same as precursor study, the transient field of Lysozyme in hindered diffusion is carefully visualized with changing the condition such as microchannel and pore size by using optical interferometer in this study. The capability and technique for active control of protein mass transfer are also discussed in this study.

2. Experimentation, discussion

For the visualization of protein mass diffusion field in the vicinity of thin membrane surface, an optical system was applied. In order to attain accurate and reliable measurement of hindered diffusion, we utilized the phase shifting technique, which calculates phase shifted data with 8bit brightness digital data (0 to 255 brightness value) from the obtained interferograms, and gives spatially precise concentration profile. For magnification of the field, a special optical device layout was adopted. The beam was expanded by a convex lens after passing through a test cell. A detector, CCD camera, was settled a position at which an abject was focused. By changing positions of both convex lens and CCD camera, magnification and minification are easily adjusted.

For the formation of small transient diffusion field, a quartz glass cell for optical measurement was applied. The cell is composed of quartz glass, four Teflon blocks and a thin membrane. The four Teflon blocks forms a narrow diffusion channel at the center of quartz glass cuvette, which has dimensions of 4mm in width, 40mm in height and 10mm in depth. A thin membrane, which is exchangeable, is fixed between upper and lower blocks and separates the diffusion channel into two regions. As thin membranes, a series of Polybutyrate Adipate Terephthalate (PBAT) shown in Fig. 1 were used.

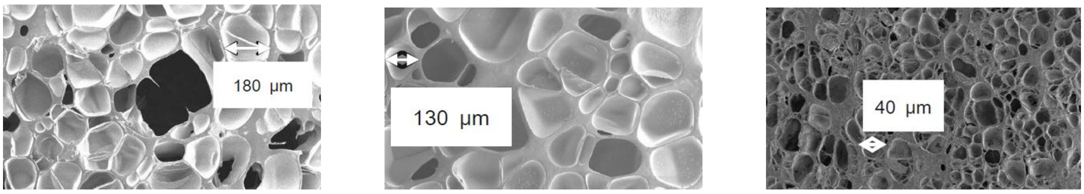

(a) membrane 1: mean dia. 173μm (b) membrane 2 : mean dia. 132μm (c) membrane 3 : mean dia. 18.4μm

Fig.1: Photos of membranes

Each visualization experiment was run in 5 times under same condition for the reduction of measurement error. Under isothermal condition at 25°C in temperature-controlled room. Through the series of experiments in this study, typical protein, Lysozyme (14.3kDa), was applied as target protein. Distilled water was used as solvent in all the solutions. The thickness of the thin membrane was 0.5mm. The experiments were conducted by using Lysozyme solution whose concentration is 5mg/ml. This concentration difference generates analyzable number of fringes in a view area.

Figure 2 shows the visualization results of transient diffusion field of protein by phase shifting interferometer in the vicinity of PBAT membranes 1 and 2 of distilled water side (upper side). The height of field of view is approximately 7.4 mm. As is obvious from Fig. 2, transient diffusion field could be clearly visualized by the interferometer. Figure 2(a) shows a time series of transient diffusion field in the case of membrane 1, and Fig.2 (b) shows those of membrane 2. As is obvious from the comparison of Fig.2 (a) and (b), the PBAT membrane 1 could transport much protein molecules than membrane 2 because Fig.2(a) shows large number of fringes. This is caused by the pore size effect. In both cases, the protein molecules transported from lower region through membrane travel into interior of distilled water area with time advanced, however the travel area (i.e. diffusion area) is not extended with proportional to elapsed time. In case of membrane 1, after 6000 seconds later, fringe pattern shows that the concentration profile keeps stable, and mass flux decreases. From the experimental results, it is suggested that the membrane affects the protein mass transport during pass process of membrane. In Fig. 3, the mass fluxes in the vicinity of thin membrane surface were summarized as a function of cubic value of mean diameter of pore membrane. As is obvious in Fig.3, the mass flux was affected by the pore size, and it is found that there is a proportionality between mass flux and cubic value of pore size only in the range of large pore size. This fact means the mass flux was affected by the volumetric structure of membrane in case of large pore size, however, there is the other effect on mass flux in case of small pore size. The experimental result reveals that there is the other "enhancement" effect between molecule and membrane wall. For more detailed discussion, more experiment is required.

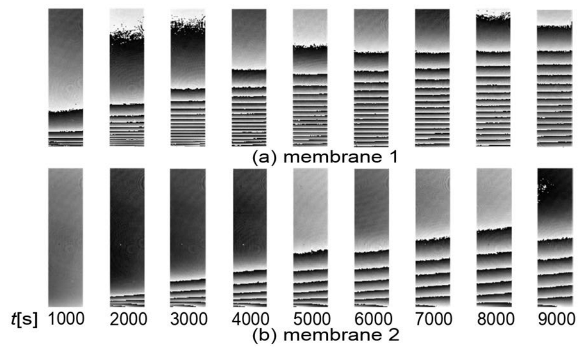

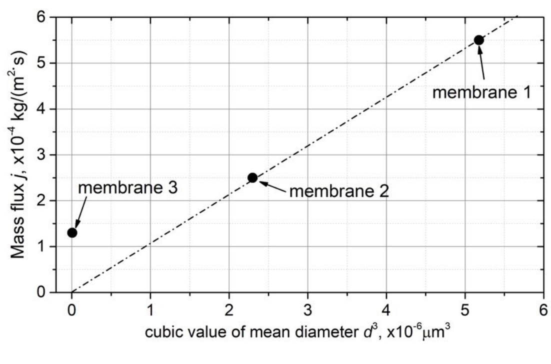

Fig.2: Photos of membranes Fig.3:

References :

[1] T. Varzakas, T. Escurero and I.G. Economou, J. Biotechnol., **72**(1999) 77–83

[2] J. Gutenwik, B. Nilsson and A. Axelsson, Biochem. Eng. J., **19**(2004) 1–7

[3] S. Liang, J. Xu, L. Weng,H. Dai, X. Zhang and L. Zhang, J. Control. Release, **115**(2006) 189–196

[4] A. Komiya, J. Chevalier, S. Pruvost and S. Livi, Proc. of ExHFT8, (2013) USB-447

Nonlinear ultrasonic phased array for imaging closed cracks

	*YOSHIKAZU Ohara Department of Materials Processing, Tohoku University 6-6-02 Aoba, Aramaki-aza, Aoba-ku, Sendai, 980-8579 Japan*		*TOSHIHIRO Tsuji Department of Materials Processing, Tohoku University 6-6-02 Aoba, Aramaki-aza, Aoba-ku, Sendai, 980-8579 Japan*
	*TSUYOSHI Mihara Department of Materials Processing, Tohoku University 6-6-02 Aoba, Aramaki-aza, Aoba-ku, Sendai, 980-8579 Japan*		

Abstract :

1. Introduction

Nondestructive testing is of importance to satisfy the safety and reliability of infrastructure and industrial materials. Within many kinds of nondestructive testing, ultrasonic testing (UT) has the highest sensitivity to cracks, which can significantly weaken material strength. Crack depth can be measured by UT if they are open, since the ultrasound is strongly scattered mainly at tips of cracks, with an air gap between crack faces. Some cracks are however closed because of compressional residual stress or by oxide film generation between crack faces, in which UT may sometimes lead to underestimation or miss detection. This is because ultrasound propagates through the contact parts between crack faces.

To solve this problem, we have focused on the combination of phased array imaging technique with nonlinear ultrasonics, which is a kind of unique technique that is highly sensitive to closed cracks. Nonlinear ultrasonics involves some types of contact vibration of crack faces, which has been referred to contact acoustic nonlinearity (CAN) and non-classical nonlinearity. Thus far, we have developed two kinds of novel imaging methods. The first one is called subharmonic phased array for crack evaluation (SPACE),[1,2]. The fundamental principle that governs SPACE is the subharmonic generation induced by a large-amplitude ultrasonic incidence of which frequency is the order of MHz. It has exhibited a great imaging capability to many closed cracks. Further challenge is to visualize very tightly closed cracks of which the crack closure stress is higher than the large-amplitude incident wave used in SPACE. To overcome this difficulty, we have proposed a combination of thermal stress instead of large-amplitude ultrasonic incidence with phased array imaging technique, and referred to global preheating and local cooling (GPLC)[3,4]. In this study, we will show their unique capability for closed crack imaging.

2. Principles

The schematic of SPACE and GPLC is shown in Fig. 1. SPACE is based on the subharmonic generation by short-burst waves and the phased array algorithm with frequency filtering. It provides fundamental image at the frequency f and subharmonic image at the frequency f/2, visualizing the open and closed parts of cracks, respectively. In GPLC, tensile thermal stress can be applied to closed cracks just by using cooling sprays. Note that its applicable tensile stress is even higher than the stress of large amplitude ultrasonic wave used in SPACE. By temporarily opening closed cracks by GPLC, closed cracks can be imaged by commercially available phased array.

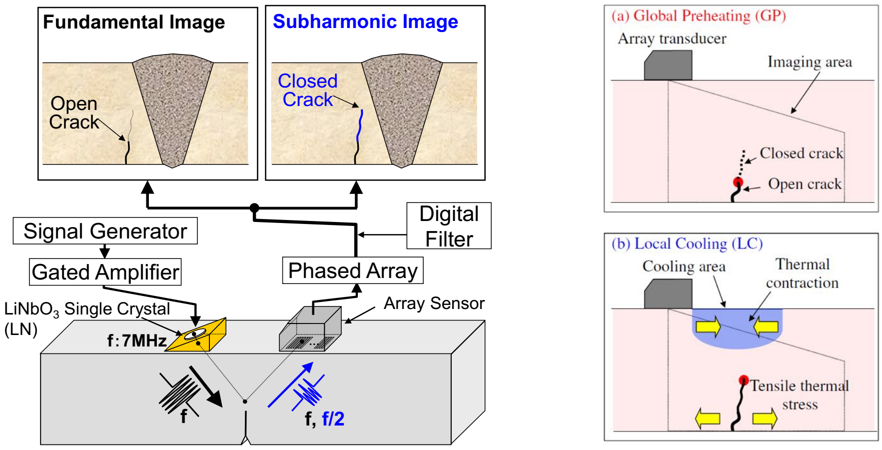

Fig. 1: Schematic of SPACE (left) and GPLC (right) for closed-crack imaging.

3. Experimental results

As typical imaging results obtained by SPACE, the fundamental and subharmonic images of a fatigue crack (aluminum alloy A7075, three-point bending) are shown in Fig. 2. While the fatigue crack was absent in the fundamental image corresponding to conventional ultrasonic phased array image, the subharmonic image clearly indicated the crack tip, which provided an accurate crack depth of 20 mm, which presents the closed-crack imaging capability of SPACE.

Figure 3 is the imaging results obtained by GPLC, where the compact tension specimen (A7075) with a fatigue crack was measured. Before cooling, only the starting notches were imaged, whereas crack responses appeared instantaneously after the cooling. The maximum crack depth was measured to be 11.3 mm at 4 s, which is an excellent agreement with the true crack depth.

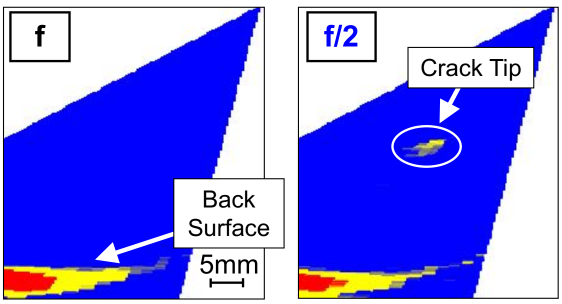

Fig. 2: Imaging results of a fatigue crack (A7075) by SPACE.

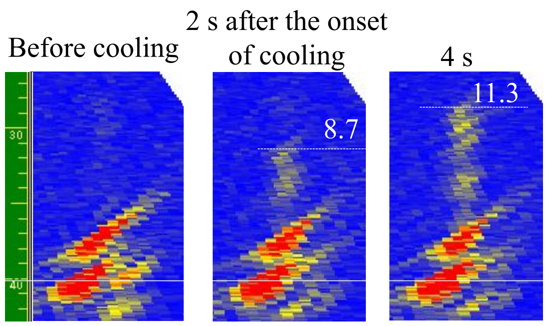

Fig. 3: Imaging results of a fatigue crack by GPLC

References :

[1] Y. Ohara, T. Mihara, R. Sasaki, T. Ogata, S. Yamamoto, Y. Kishimoto and K. Yamanaka, *Appl. Phys. Lett.*, **90** (2007) 011902-1-3.

[2] A. Sugawara, K. Jinno, Y. Ohara and K. Yamanaka, *Jpn. J. Appl. Phys.*, **54** (2015) 07HC08-1-8.

[3] Y. Ohara, K. Takahashi, S. Murai and K. Yamanaka, *Appl. Phys. Lett.*, **103** (2013) 031917-1-5.

[4] Y. Ohara, K. Takahashi, Y. Ino, K. Yamanaka, T. Tsuji and T. Mihara, *NDT & E Int.*, **91** (2017) 139-147.

Surface Integrity and Structural Integrity

Tetsuo Shoji, Professor

Frontier Research Initiative, New Industry Creation Hatchery Center, Tohoku University & National Center for Materials Service Safety
tshoji@fri.niche.tohoku.ac.jp

Abstract :

1. Introduction

Life time prediction and inspection interval optimization are of importance in safe and economical operation of energy conversion plants being operated under the extremely severe environments in temperature, environment and loading. Structural integrity of such energy conversion plants can be degraded by three types of degradation modes such as 1) Material type degradation mode, 2) Surface type degradation mode and 3) Crack type degradation mode. In many cases where the structures are constructed with ductile structural materials such as low carbon wrought steels, stainless steels and nickel base alloys, final stage of failure is cause by the crack propagation to the critical size. Before the crack grows to such a critical size, crack must initiate and propagate some distance as called short crack growth period before behaving a long crack growth as can be evaluated by Fracture Mechanics.

Fig. 1 shows a schematic illustration of the process of crack initiation and growth where six segments of the process is shown in relation to the transition from Surface Integrity to Structural Integrity. There are several stages before crack grow at a rather rapid rate as a long crack behavior where ① Initial condition, ② Precursor, ③ Incubation, ④ Proto-crack and ⑤ and ⑥ Propagation after establishment of crack tip environment and stress field. Surface integrity is strongly affected by the Initial condition before surface is exposed to a service condition where surface is as fabricated, as supplied, surface preparation by mechanical and chemical treatment. In some cases, residual stresses may exist by welding. As a consequence, nature of a surface of a structure can be very different in each component fabricated by different condition such as machining machine and tool, machining speed, cutting depth etc. Therefore, it is very important to characterize the surface based upon microstructure, surface roughness and hardness, In some cases, severe scratch, small tearing crack or heavily deformed slip band can be introduced during a fabrication process and these initial condition may play a crucial role in the following process such as precursor, incubation, initiation and short crack growth. Especially with a focus on the oxidation in high temperature and high pressure waters such as LWR environments, factors which may influence the oxidation kinetics are of great concerns with a special reference to SCC initiation and structural integrity assessment. In order to give an insight to this relevance of surface integrity to structural integrity, some evidences observed in plants and in Lab. are shown below, emphasizing the importance of surface preparation during a fabrication process of strucutures.

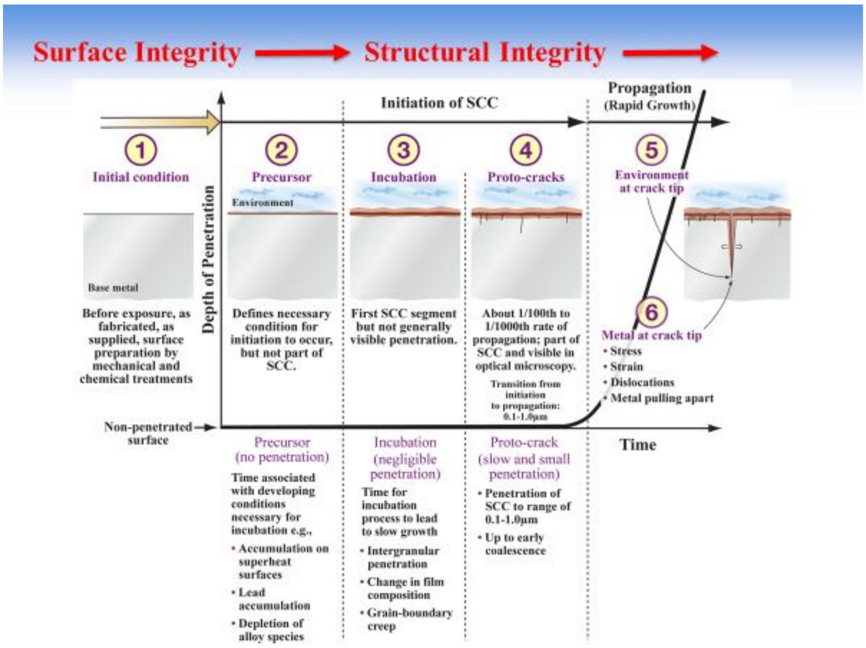

Modified from Roger Staehle, QMN-3 2012, Sun Valley, Idaho, USA

Fig. 1 Transition from Surface Integrity to Structural Integrity in case of SCC

2. Evidences and discussion

Fig. 2 shows example of PWSCC and IGSCC in SG inlet nozzle of PWR M#2 plant. Two type of SCC were observed at the safe end of the inlet nozzle of PWR plant and PWSCC in Ni-base alloy weld and IGSCC in 316 HAZ.

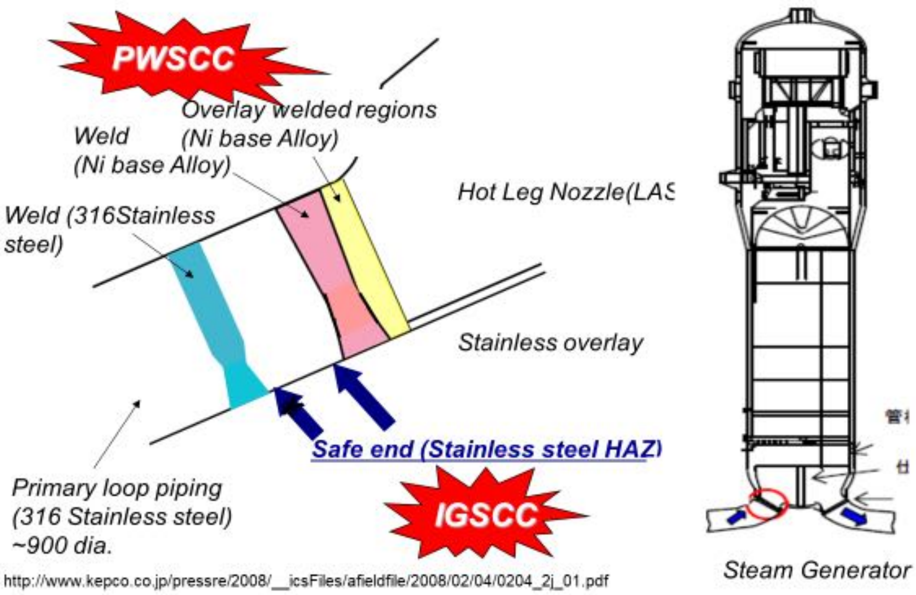

Fig. 2 Field PWSCC and IGSCC events at SG Inlet nozzle of M#2 plant.

After detailed examination of the cracked area of 316 HAZ of the inlet nozzle, preferential oxidation was observed undert the rather uniform oxide film as an oxide intrusion as shown in Fig. 3. There are many slip bands observed at the angle of about 45° to the surface suggesting some shear deformation.

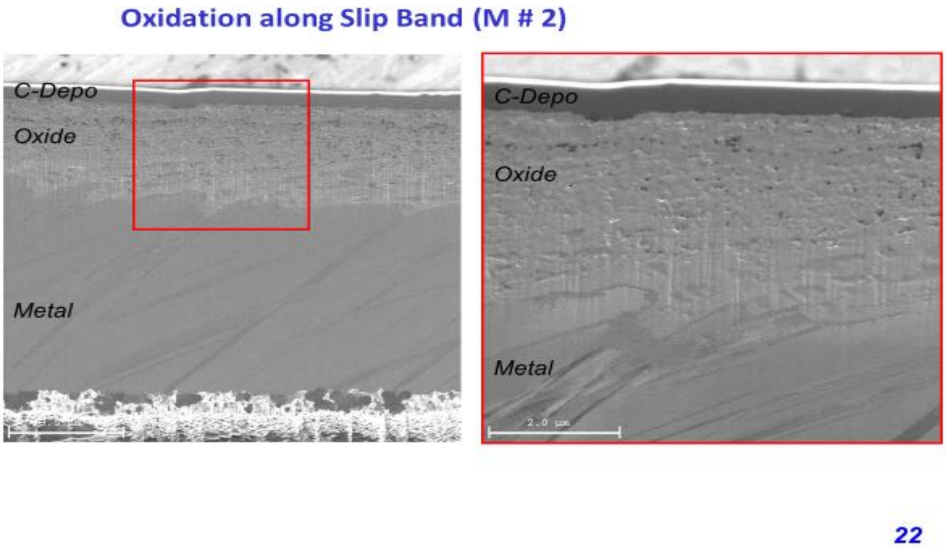

Fig. 3 Surface oxide and oxide intrusion along slip bands

Fig. 4 shows an EDX anlysis of the surafce oxide and oxide intrusion shown in Fig. 3 with an enlargement and the results shows a clear evdence of oxidation along the slip band. It is well known that preferencial dissolution can take place in SSRT in some materials/environments combination but this figure shows a preferential internal oxidation can take place along the slip band. This evidence implies that the slip band formed during the fabrication or contact fatigue/fretting fatigue can also be preferentially oxidized and can play as an intiation site of following SCC. Oxygen mass transport along the slip band by pipe diffussion may affected by the mechanism of hydrogen accelarated oxidation because hydrogen can also diffuse much easily than oxygen by pipe difusion and pre-oxidation by hydrogen may promote the internal oxidation along the slip bands by pipe diffusion.

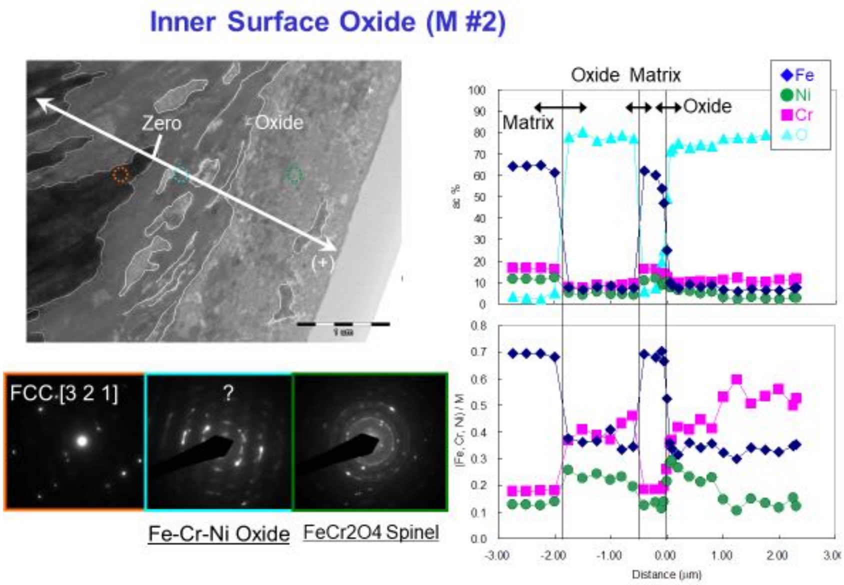

Fig. 4 EDX analysis of oxide of 316 SS at the cracked safe end of the inlet nozzle

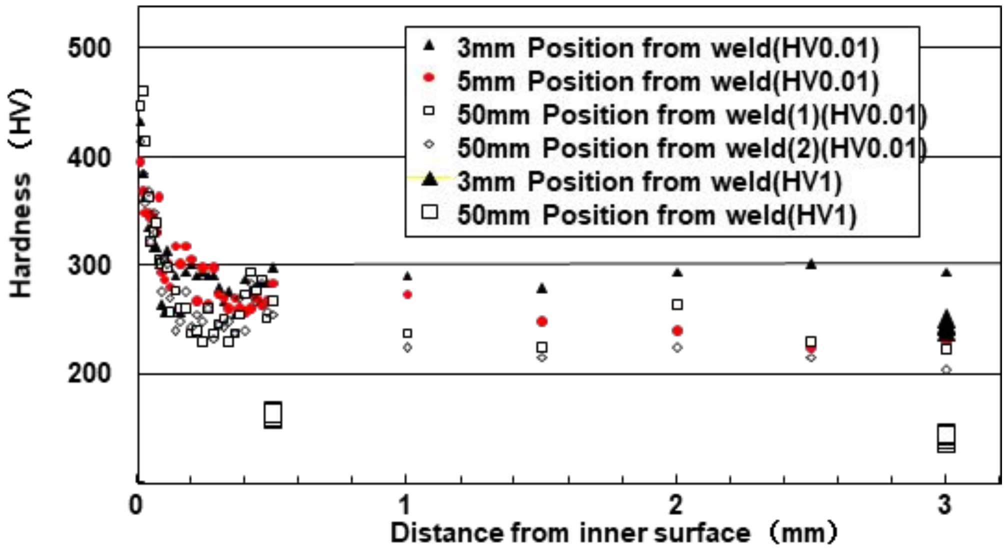

Fig. 5 Surface hardening by machining and SCC initiation relevance

Fig. 5 shows the hardness profile near the surface of the cracked region showing a relevance to SCC initiation. Higher hardness more than 400HV0.01 at closer position of 3 mm from weld is clear where SCC was initiated and propagated. Base metal hardness shows around 150 to 170 HV1. Hardened thickness was around 200 to 400 μm. Importance of surface finish is also observed in the laboratory experiments in relation to the field cracking. Fig. 6 demonstrates the significance of surface finish in oxidation localization of 316L SS in simulated BWR environment. One sample was prepared as mirror polished condition and the other as lathed and then immersed in a simulated BWR water with oxygen of 200 ppb. Oxidation localization was evaluated by the analysis of oxide/metal interface profile analysis. Heavily machined surface shows deeper oxide penetration than those in mirror polished sample.

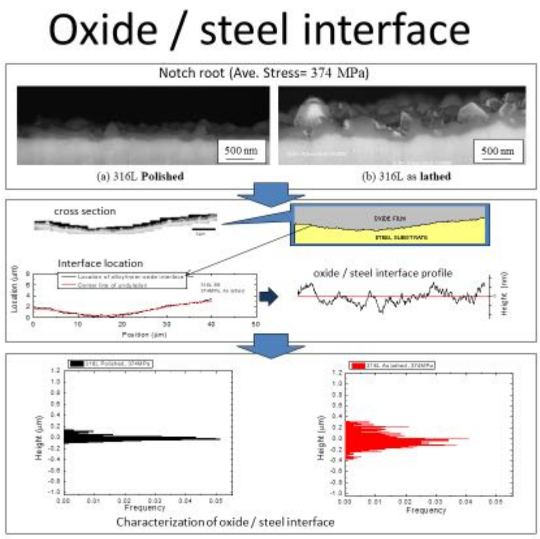

Fig. 6 shows an oxidation localization affected by the surface finish.
One mirror polished and the other lathed finished where deeper oxidation penetration is clear in the histogram of oxide/metal interface profile analysis.

Based upon the interface profile analysis, one parameter as a measure of a depth of localized oxidation penetration has been proposed on these samples and also applied to the samples of the cracked component of PLR piping of BWR and results are summarized in Fig. 7

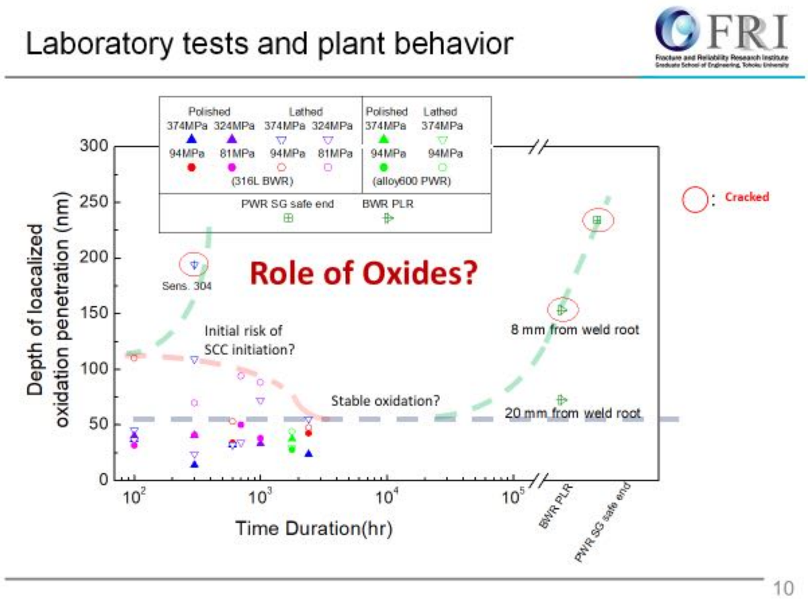

Fig. 7 Sumary of the oxidation penetration parameters obtained in the laboratory tests and also in the field cracking.

Fig. 7 shows a proposed parameter variation with oxidation time and suggests that oxidation localization is more pronounced at the early stage of oxidation and also at the stage of prolonged oxidation time with a strong influence of surface finish. Lathed surface may have a risk of early stage SCC initiation than those of miror polished surface. The results shown inFig. 7 with field cracked data implies that there seems to be a critical number of the proposed parameter for oxidation localization around 100 – 150 nm above which SCC crack may initiate and propagate.

As demonstrated above, surface finish plays a crucial efects of surface oxidation and its localization. There are still a lot of thing have to be done to draw any conclusive statement on this mechanisms but some mechanisms must underlying to promote such a oxidation localization along the slip band. It is interesting to note that similar phenomena is observed in field SCC events in PWR and also in BWR where environmental oxidizing potential is very different and suggesting that such an oxidation localization or oxide intrusion can happen even at the low ECP such as PWR condition. One possible direction to tackle this prolem would be the role of hydrogen in oxidation acceleration through the mechanism of oxidant hydrogen in metal.

References :

[1] Tetsuo Shoji, Kazuhiko Sakaguchi, Zhanpeng Lu, Shinro Hirano, Yukihisa Hasegawa, Taka-aki Kobayashi, Koji Fujimoto, Yuichirou Nomura, International Symposium, Fontevraud 7, September 26 - 30, 2010, Avignon, Popes' Palace, France

[2] Tetsuo Shoji, Zan-Peng Lu, Yoichi Takeda, Nishith Kumar Das, Ismail Tirtom, Chaoyang Fu, Workshop on Detection, Avoidance, Mechanisms, Modeling, and Prediction of SCC Initiation in Water-Cooled Nuclear Reactor Plants, Sept. 7-12., 2008, Beaune, Burgundy, France

[3] Tetsuo Shoji, Quantitative Micro-Nano (QMN) Approach to Predicting SCC of Fe-Cr-Ni Alloys, June 1 – 18, 2010, Sun Valley, Idaho, USA

Magneto-mechanical energy conversion in magneto-rheological elastomers: effect of matrix change

Project ELyT Global “MARECO”

	*SEBALD Gael ELyTMaX UMI 3757, CNRS - Université de Lyon - Tohoku University, International Joint Unit, Tohoku University*		*NAKANO Masami - ELyTMaX UMI 3757, CNRS - Université de Lyon - Tohoku University, - Intelligent Fluid Control Systems Laboratory, Institute of Fluid Science, Tohoku University*
	*CAVAILLE Jean-Yves ELyTMaX UMI 3757, CNRS - Université de Lyon - Tohoku University, International Joint Unit, Tohoku University*		*LALLART Mickael Université de Lyon, INSA-Lyon, LGEF EA682*
	*DIGUET Gildas ELyTMaX UMI 3757, CNRS - Université de Lyon - Tohoku University, International Joint Unit, Tohoku University*		

Abstract :

Applying a shear strain to a magneto-rheological elastomer results in a change in its magnetic permeability, which in turn can be used for electromechanical energy conversion/harvesting. In this work, we present experimental results of pseudo-Villari effect in magneto-rheological elastomers for soft and hard matrix-based composites.

1. Introduction

Vibrational energy harvesting devices offer the capability of converting unnecessary or unavoidable movements or vibrations into electrical energy usable for wireless and self-powered devices. In this framework, magneto-rheological elastomers may offer an attractive alternative thanks to their low stiffness, and very low fabrication cost (similarly to other dielectric polymers [1]). The change of the magnetic permeability with a mechanical stress is known as the Villari effect and finds potential applications as environmental sensors [2]. Conversely, magneto-rheological elastomers, whose mechanical storage and loss moduli can be changed by applied magnetic field, find potential applications for vibration control [3]. In this work, we investigate how magneto-rheological elastomers can also exhibit a pseudo-Villari effect.

2. Experimental results

Magneto-rheological (MR) elastomers are composed of ferro-magnetic particles dispersed in an elastomer matrix. During the curing of the matrix, the particles are aligned in the direction of an external magnetic field to fabricate an anisotropic composite, where the particles form long chains embedded in the elastic matrix. When a shear strain is applied, the chains are twisted from the main direction of the magnetic field, resulting in a decrease of the magnetic permeability. A mechanism of the resulting pseudo-Villari effect was proposed in [4].

At a given shear strain, when a magnetic field is applied, the chains tend to partially re-align in the direction of the main magnetic field, and it might enhance the shear stress as well as dipole-dipole interaction between particles (so-called magneto-rheological effect).

Two types of MR elastomers were experimentally tested. In the first case, silicone rubber (30 wt%) was mixed with carbonyl iron particles (70 wt%) resulting in hard MR elastomer. In the second case, silicon oil (15 wt%) was added to silicone rubber (15 wt%), keeping similar weight fraction of particles in the final composite, resulting in a soft MR elastomer.

Using a dedicated experimental setup, the two MR elastomers were characterized, determining both their MR effect (i.e. change of their mechanical properties as a function of applied magnetic field, Fig. 1), and their pseudo-Villari effect (i.e. change in their magnetic properties under the application of a static shear strain, Fig. 2).

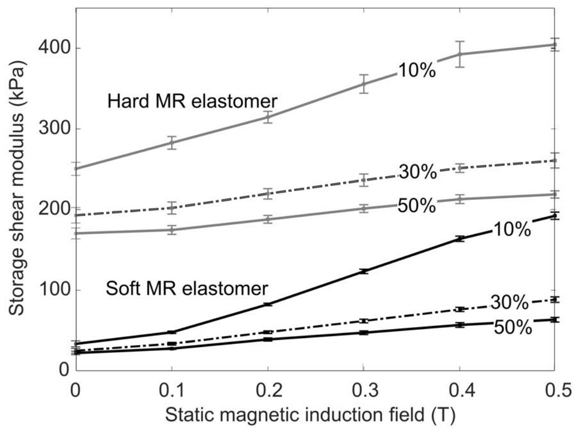

Fig.1: Storage shear modulus for different strain amplitudes as a function of applied magnetic induction field (from [5])

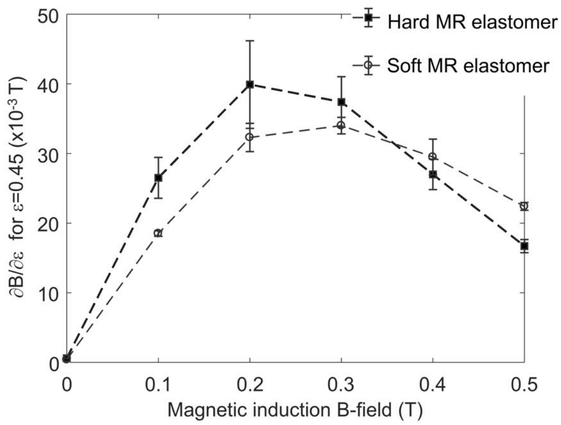

Fig .2. Pseudo-Villari coefficient, as a function of applied magnetic induction field (from [5])

Conclusion

Both soft and hard elastomer matrices exhibit a significant variation of their mechanical properties upon the application of a magnetic induction field. Similar behavior were observed both for their magneto-rheological effect in terms of absolute variation of the modulus (ΔG'~45 for an induction field increasing from 0 to 0.5T) and for their pseudo-Villari effect (ΔB ~10mT for 50% strain and bias magnetic field of 0.3T). Therefore, both magneto-mechanical depends on the particle type and volume fraction only, probably because it comes from the dipole-dipole and induction field - dipole interactions only. As a consequence, the initial properties of the matrix can be adjusted depending on the application (e.g. choosing the resonance frequency of a resonant device by changing the stiffness of the matrix) without any loss of performance in terms of coupling between magnetic and mechanical energies.

References :

[1] M. Lallart, P.-J. Cottinet, D. Guyomar, L. Lebrun, J. Polym. Sci. Part B Polym. Phys. 50 (2012) 523.

[2] C. A. Grimes, C. S. Mungle, K. Zeng, M. K. Jain, W. R. Dreschel, M. Paulose, K. G. Ong, Sensors 2 (2002) 294-313.

[3] S. Sun, H. Deng, J. Yang, W. Li, H. Du, G. Alici, M. Nakano, Smart Mater. Struct. 24 (2015) 045045

[4] M. Lallart, G. Sebald, G. Diguet, J-Y. Cavaille, M. Nakano, Journal of Applied Physics, 122 (2017), 103902

[5] G. Sebald, M. Nakano, M. Lallart, T. Tian, G. Diguet, J-Y. Cavaille, Science and Technology of Advanced Materials, 18 (2017), 766-778

Numerical Analysis for Ultrasonic Testing using EMAT under Extremely High Temperature

Project ELyT lab : R32 – study of …

Fumio Kojima
Institute of Fluid Science, Tohoku University
2-1-1, Katahira, Aoba-ku, Sendai 980-8577 Japan

Abstract : Motivated by ultrasonic test using electromagnetic acoustic transducer (EMAT), an electromagnetic-elastic coupling model is considered under extremely high temperature. Since the mechanism of the producing test signal is quite sensitive with respect to temperature inside the target material, it is very crucial to analyze numerical treatments in such coupling procedures. First, the mechanisms of transmitter-receiver EMAT are described by hybrid use of a transient magnetic potential equation in the subsurface of the target material and a boundary integral equation on the outside material. Secondly, the dynamics of ultrasonic wave propagation is given by an elastic equation with temperature dependent physical parameters. The sensitivities of EMAT based nondestructive testing method are investigated through the computational experiments.

1. Introduction

Casting process simulations have been critical issues on quality control for metal producing process [1]. It is important to collect on-line data related to metal solidification process using in-line measurements. However there have been technical problems on in-line measurements for the casting process due to the very high temperature environment. Ultrasonic testing using electromagnetic acoustic transducer (EMAT, [2]) is a feasible method for steel product monitoring system because of non-contacting device and robustness to high temperature. In this report, we discuss simulation studies on producing test signals by EMAT device. Since the signal strength depends upon electromagnetic parameters, such as magnetic permeability, electrical conductivity of the metal, it is considerably important to simulate the testing mechanism provided with temperature dependencies of those parameters.

2. Simulation Studies

Temperature dependencies on electromagnetic and elastic parameters are given by the empirical curve based on the experimental data. The hybrid use of finite and boundary element method in two spatial dimensions is adopted to our numerical treatment considered here [3]. Figures 1 and 2 depict the electromagnetic elastic propagation domain.

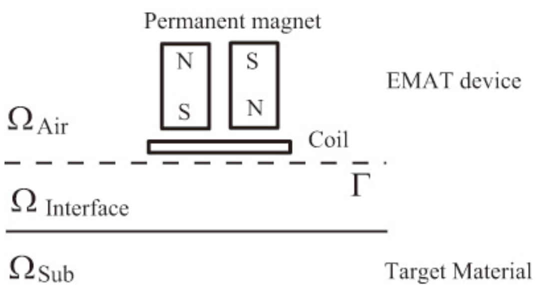

Fig. 1 Geometry in electromagnetic domain

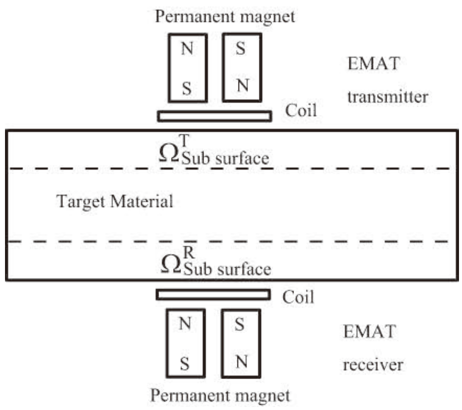

Fig. 2 Geometry in elastic domain

The basic model for eddy current analysis is written by

$$-\left\{\nabla\frac{1}{\mu_0\tilde{\mu}_r(T)}(\nabla A_z)\right\}+\tilde{\sigma}(T)\left(\frac{\partial A_z}{\partial t}+\frac{\partial \Phi}{\partial z}\right)=0 \quad in\ \ \Omega_{Sub}\cup\Omega_{Interface} \qquad \text{1a}$$

$$c(z)A_z+\int_{\Gamma}\left(\frac{\partial A_z}{\partial n}\right)\psi d\Gamma+\int_{\Gamma}A_z\left(\frac{\partial\psi}{\partial n}\right)d\Gamma=\mu_0\int_{C}J_s\psi dx \ \ in\ \Omega_{Air}\cup\partial\Omega_{Interface} \qquad \text{1b}$$

where $\tilde{\mu}_r(T)=1+(\tilde{\mu}_r(T)-1)\chi(\Omega_{Sub}^T)$ and $\tilde{\sigma}(T)=\chi(\Omega_{Sub}^T)\sigma(T)$, respectively. The wave propagation model is represented by

$$\vec{u}=\{u_x,u_y\},\quad \vec{f}_L=\left\{\tilde{\sigma}(T)\left(\frac{\partial A_z}{\partial t}+\frac{\partial\Phi}{\partial z}\right)B_y^M,-\tilde{\sigma}(T)\left(\frac{\partial A_z}{\partial t}+\frac{\partial\Phi}{\partial z}\right)B_x^M\right\}, \qquad \text{2a}$$

$$\rho(T)\frac{\partial^2\vec{u}}{\partial t^2}-\{\nabla(\lambda+2G)(T)(\nabla\cdot\vec{u})\}+\{\nabla\times \mathrm{G}(T)(\nabla\times\vec{u})\}=\vec{f}_L \quad in\ \ \Omega_M\,. \qquad \text{2b}$$

The dynamics of the receiver EMAT is similarly rewritten by

$$-\left\{\nabla\frac{1}{\mu_0\tilde{\mu}_r(T)}(\nabla A_z)\right\}+\tilde{\sigma}(T)\left(\frac{\partial A_z}{\partial t}+\frac{\partial\Phi}{\partial z}\right)=\tilde{\sigma}(T)\left(B_x^M\frac{\partial u_y}{\partial t}-B_y^M\frac{\partial u_x}{\partial t}\right) \qquad \text{3a}$$

$$c(z)A_z+\int_{\Gamma}\left(\frac{\partial A_z}{\partial n}\right)\psi d\Gamma+\int_{\Gamma}A_z\left(\frac{\partial\psi}{\partial n}\right)d\Gamma=0\ . \qquad \text{3b}$$

The temperature dependencies on electromagnetic and elastic parameters used in the experiments are shown in Figs 3 to 6.

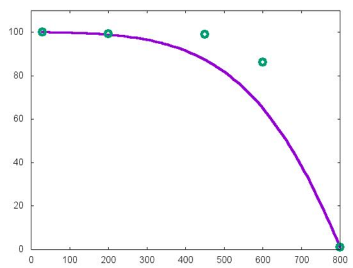

Fig. 3 Magnetic permeability ratio

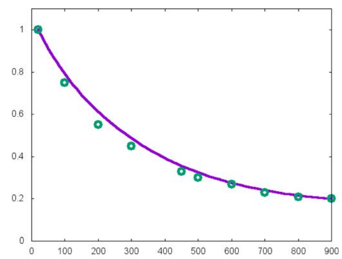

Fig. 4 Electrical conductivity ratio

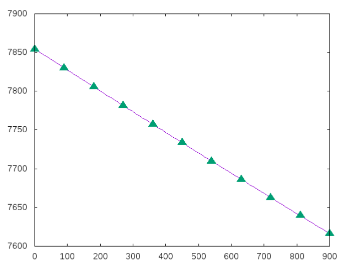

Fig. 5 Material density

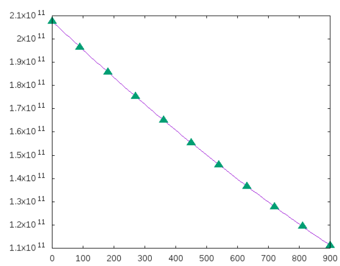

Fig. 6 Young modulus

References :

[1] F. Kojima and N. Kubota : "Void Detection of Steel Products for Process Monitoring System using Electromagnetic Acoustic Transducer", *Electromagnetic Nondestructive Evaluation (XXI), Studies in Applied Electromagnetics and Mechanics*, (2018) to appear

[2] R. B. Thompson : "Physical Principles of Measurements with EMAT Transducers", In *Physical Acoustics*, 19, Academic Press (1990), New York, (1990) 157-200.

[3] F. Kojima : "Defect shape recovering by parameter estimation arising in eddy current testing", *Journal of the Korean Society for Nondestructive Testing*, Vol. 23, No. 6 (2003) 622-634

Thursday, March 8th – Morning

Seventh session – 9:00-10:20

Wall turbulence nature and its control aimed at laminar wing technology

Project ELyT lab :

Aiko YAKENO Ph. D.

Assistant Professor
Aerospace Fluid Engineering Lab.

IFS / Tohoku Univ.
JAPAN

Abstract:

Wall turbulence, such like coherent motions of streamwise roll vortices, associated streaks and their self-sustaining mechanism, have been discussed for decades. Energy conversion performance of fluidic devices such as aircraft, cars, turbine blades and curved pipe will dramatically increase if the turbulence is controlled completely. Wall turbulence nature, the generation and maintenance mechanism of turbulence coherent motion, in other words, laminar-turbulence transition, still attracts attention. With the recent development of computational technology including direct numerical simulation of Navier-Stokes equations, it became possible for us to analyze the detailed flow structure (Fig. 1 and Fig. 2). Obtained new knowledge has given us a new sight to deal with the wall turbulence.

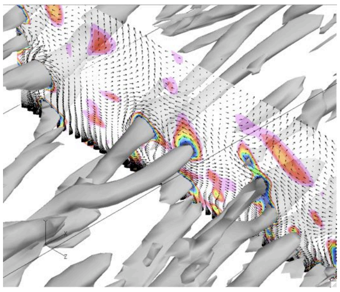

Fig.1: Streamwise vortices visualized with contour surfaces of the 2nd invariant of velocity gradient tensor; $Q = -0.013$.

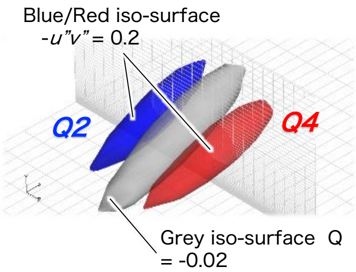

Fig.2: Conditionally sampled streamwise vortex and associated negative Reynolds shear stress; bursting event Q2 (blue) and sweep event Q4 (red) [6].

The opposition control has been one of the most famous flow control technology [1]. It restrains a streamwise vortex rotation by blowing from the wall in its opposite direction. Streamwise roll vortex is responsible for momentum transport to increase friction drag or to suppress flow-separation (Fig. 1). Conventionally-proposed flow control strategies are based on such turbulent motion near the wall. On the other hand, some *predetermined* controls have been known to achieve drastic performance, those control parameters do not depend on the streamwise vortex but the larger length scaled factors. Spanwise wall oscillation control decreases turbulence energy considerably and reduce friction drag as much as 50% [2, 3, 4]. The control is simple and to oscillate the wall in the spanwise direction slowly with the period $T = 100$ in the viscous wall unit. That is corresponds to the streak length scale $l \sim 1000$ more than that of the streamwise vortex [5, 6]. Flow goes through with $T = 100$ and with the convective velocity at $y \sim 10$ to reach $l \sim 1000$ without oscillation. We considered that streak structure is modulated and the self-sustaining mechanism is disturbed under the spanwise wall oscillation. In the presentation, I will introduce some results of non-orthogonal transient growth modes under the oscillation control [7].

On the other hand, several methods for prediction the control effect of the spanwise wall oscillation have been proposed [8, 9,10]. However, both of them can be applied only when the oscillation period is short ($T < 150$), and it is not clear why the proposed index correlates with the turbulence statistics under control. Therefore, I analyzed details of the dynamical process of the multi-scaled turbulence structure consisting of the streamwise vortex and the low speed streak structure. In this study, the flow field of this study is considered to be turbulence of superimposed control oscillation of large time scale and disturbance by streamwise vortex structure of smaller time scale. Therefore, the phase-average statistics based on the frequency of control oscillation and the disturbance component of the deviation therefrom are considered, instead of Reynolds decomposition dealing with time average statistics:

$$f_i(x, y, z, t) = \langle f_i \rangle (y, \phi) + f_i''(x, y, z, t) \qquad 1$$

$$\langle f_i \rangle (y, \phi) = \frac{1}{N} \sum_{n=0}^{N-1} \int_{Lx} \int_{Lz} f_i(x, y, z, \phi + 2\pi n) dxdz \qquad 2$$

At this time, the phase averaged statistic is calculated as above Eq. 2.

Based on the details of phase averaged statistics, a new prediction method was proposed to estimate the drag reduction performance by only the control parameters [6].

References:

(1) H. Choi, P. Moin and J. Kim, Active turbulence control for drag reduction in wall-bounded flows, Journal of Fluid Mechanics, 262: 75-110, 1994.

(2) R. Akhavan and R. D. Kamm and A. H. Shapiro, An investigation of transition to turbulence in bounded oscillatory Stokes flows, Part 1. Experiments, Journal of Fluid Mechanics, 225, 395, 1991.

(3) W. J. Jung, N. Mangiavacchi and R. Akhavan. Suppression of turbulence in wall-bounded flows by high- frequency spanwise oscillations. Physics of Fluids A: Fluid Dynamics, 4(8):1605–1607, 1992.

(4) M. Quadrio and P. Ricco. Critical assessment of turbulent drag reduction through spanwise wall oscillations. Journal of Fluid Mechanics, 521:251–271, 2004.

(5) A. Yakeno, Y. Hasegawa and N. Kasagi, Spatio-temporally periodic control for turbulent friction drag reduction, In proc. of the 6th Turbulence and Shear Flow Phenomena, Seoul, 2007.

(6) A. Yakeno, Y. Hasegawa and N. Kasagi, Modification of quasi-streamwise vortical structure in a drag-reduced turbulent channel flow with spanwise wall oscillation. Physics of Fluids, 26(8):085109, 2014.

(7) A. Yakeno and Kozo Fujii, Transient dynamics and stability of spanwise-oscillatory turbulent channel, In Proc. International Congress of Theoretical and Applied Mechanics (ICTAM), Aug. 2016.

(8) M. R. Dhanak and C. Si. On reduction of turbulent wall friction through spanwise wall oscillations. Journal of Fluid Mechanics, 383(1):175–195, 1999.

(9) J. I. Choi, C. X. Xu, and H. J. Sung. Drag reduction by spanwise wall oscillation in wall-bounded turbulent flows. AIAA journal, 40(5):842–850, 2002.

(10) A. Cimarelli, B. Frohnapfel, Y. Hasegawa, E. D. Angelis, and M. Quadrio. Prediction of turbulent control for arbitrary periodic spanwise wall movement. Physics of Fluids, 25:075102, 2013.

(11) E. Touber and M. A. Leschziner. Near-wall streak modification by spanwise oscillatory wall motion and drag-reduction mechanisms. Journal of Fluid Mechanics, 693:150–200, 2012.

Mechanism Analysis Technique for Fuel Diversification: In-situ Observation of Tribo-chemical Reaction in Methanol Blended Gasoline

Kazuhito Yoshida, Hidenori Hibino, Shinichi Ito,
Ryoichi Hombo, Naruhiko Inayoshi

DENSO Corporation
1-1, Showa-cho, Kariya-shi, Aichi-ken 466-8661, Japan

No abstract

Application of big data analysis to NDT data pool

Tomoya SOMA
NEC Corporation

No abstract

Optimizing surface finish to Prevent SCC initiation in energy industries

Project ELyT lab : New

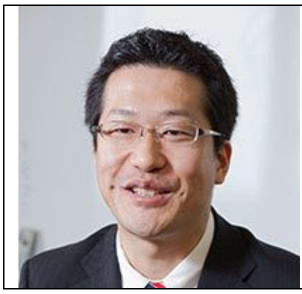

H. Abe[1]
N. Mary[1,2]
T. Miyazaki[1]
Y. Watanabe[1,2]

1: Tohoku University
2: ELyT MaX

B. Ter-Ovanessian[1],
B. Normand[1],
K. Jaffre[1,2]

1: MATEIS INSA Lyon
2: ElyT MaX

Abstract :

The selection of structural materials for applications is usually done from their mechanical properties and adding a safety coefficient to take into account some environmental effect. If this methodology can be used in the most of applications, additional precautions are required in energy industries. Synergistic effects can be activated between the material metallurgy, the environment and mechanical stresses when the material are exposed under extremes conditions (pressure, temperature, strongly aggressive solution, etc.). In various kinds of environments, including boiling water reactor coolant, primary circuit of pressurized water reactor and chloride containing water, the material surface state is the key parameter to control the corrosion and Stress Corrosion Cracking (SCC) susceptibility of alloys. For example, It has been widely accepted that surface machining enhances SCC susceptibility of non-sensitized austenitic stainless steels in a boiling water reactor environment.

Surface finishing operations such as grinding, wire brushing, machining produce surface states that compromise the corrosion resistance of oxidative and passive materials [1]. These processes affect the electrochemical and mechanical stabilities of the material at the microstructure scale and also the passive film properties [2]. A part of our collaborative study (Project ELyT lab: R32 – Understanding and managing stress corrosion cracking) showed that even slight cold work introduced with fine emery finish has significant impact on oxidation properties[3] and cracking susceptibility of Ni base alloys in superheated steam.

Until now, researches focused on the relation between the microstructural modification induced by the surface preparation on the SCC behaviour of material or on the selection of the most suitable treatment [4,5]. However, industries need appropriate surface finish procedures to reasonably minimize SCC susceptibility of alloys. To achieve an effective answer on this demand, new knowledge are required on:

- Physical metallurgy of alloy surface (micro- and nano-structure of surface)

- Electrochemical properties, in particular, stability of passivity (re-passivation kinetic, growth mechanism)

- SCC initiation dynamic (embryo formation, re-passivation, coalescence of micro-cracks).

All those properties need to be linked each other to understand the effect of surface finish on SCC susceptibility of alloys.

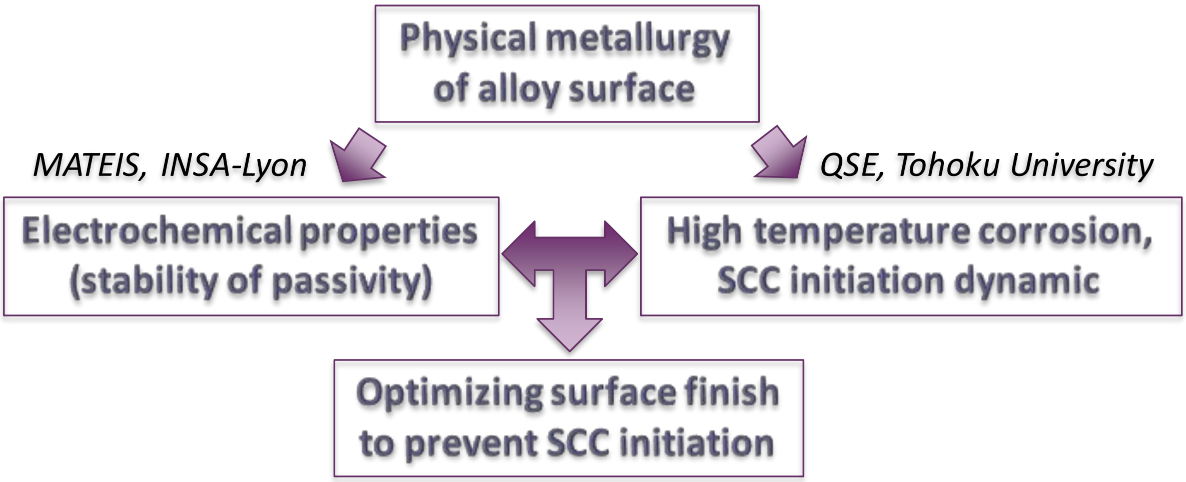

Figure 1 : Frame of the project

References :

[1] M. Moine, N. Mary, B. Normand, L. Peguet, A. Gaugain, H.N. Evin, Tribo electrochemical behavior of ferrite and ferrite–martensite stainless steels in chloride and sulfate media, Wear. 292–293 (2012) 41–48. doi:10.1016/j.wear.2012.06.001.

[2] B. Ter-Ovanessian, N. Mary, B. Normand, Passivity Breakdown of Ni-Cr Alloys: From Anions Interactions to Stable Pits Growth, J. Electrochem. Soc. 163 (2016) C410–C419. doi:10.1149/2.0381608jes.

[3] F. Hamdani, H. Abe, B. Ter-Ovanessian, B. Normand, Y. Watanabe, Effect of Chromium Content on the Oxidation Behavior of Ni-Cr Model Alloys in Superheated Steam, Metall. Mater. Trans. A. 46 (2015) 2285–2293. doi:10.1007/s11661-015-2786-7.

[4] S. Ghosh, V. Kain, Microstructural changes in AISI 304L stainless steel due to surface machining: Effect on its susceptibility to chloride stress corrosion cracking, J. Nucl. Mater. 403 (2010) 62–67. doi:10.1016/j.jnucmat.2010.05.028.

[5] S.J. Lennon, F.P.A. Robinson, G.G. Garrett, The Influence of Applied Stress and Surface Finish on the Pitting Susceptibility of Low Alloy Turbine Disk Steels in Wet Steam, CORROSION. 40 (1984) 409–413. doi:10.5006/1.3593946.

Thursday, March 8th – Morning

Eighth session – 10:50-12:00

Thermofluid characteristics of a flow channel with finger-stacked structure

Shinji Ebara
Graduate school of Engineering, Tohoku University, 6-6-01-2 Aramaki-Aza-Aoba, Aoba-ku, Sendai, Miyagi, 980-8579, Japan

Hidetoshi Hashizume
Graduate school of Engineering, Tohoku University, 6-6-01-2 Aramaki-Aza-Aoba, Aoba-ku, Sendai, Miyagi, 980-8579, Japan.

Abstract : For the first wall cooling in Flibe blanket of a fusion reactor, a flow channel with finger-stacked structure has been proposed. In this study, a flow visualization experiment was conducted in order to optimize the channel structure. And then, a heat transfer experiment using the channel optimized was performed to investigate its heat transfer characteristics precisely.

1. Introduction

The Flibe blanket has been proposed and studied as one of the advanced blanket systems for nuclear fusion reactors [1]. Although the blanket has several favorable features, Flibe has poor heat transfer performance due to its high Plandtl number. In addition, the blanket system is under strong magnetic field generated by superconductor magnet, corrosive F_2 gas generates from Flibe due to electrolysis by MHD effect when the flow velocity becomes high. For these reasons, it is necessary to develop heat transfer enhancement to realize high heat transfer performance under low flow velocity. As heat transfer promoter for Flibe flow, a flow channel with finger-stacked structure (FSS) was proposed [2]. The channel comprises of a number of circular cylinders with hemispheres on the tops (referred to as ‘fingers’) as turbulent promoters. The fingers are set so as to have spatial gap between their tops and a channel wall, which is heated by core plasma, to avoid the flow stagnations and hot spots. Heat transfer characteristic of the channel with FSS, of course, depends on its structure such as finger arrangement, the gap width between the fingers and the heated wall, finger dimensions and so on. In this study, we conducted a flow visualization experiment using 2-dimensional PIV measurement to optimize the channel structure. Subsequently, a heat transfer experiment using the flow channel optimized was performed to scrutinize its heat transfer characteristics.

2. Flow visualization experiment

In the experiment, the refractive indices of the channel material and working fluid were matched by using sodium iodide solution as a working fluid to visualize the complex inner flow in the channel with FSS precisely in the 2-dimensional PIV measurement. The detail dimensions of a test section is shown in Fig. 1. In this study, two different FSS arrangements (staggered and in-line), three different gap widths, C_g, (0, 1, and 2 mm), and three different finger lengths, H, (14, 28, and 54 mm) were investigated. To understand the 3-dimentional internal flow field, visualization for 3 coordinate planes (XY, YZ and ZX as shown in Fig. 1) was conducted. Particle Reynolds number based on the finger diameter, d, and the superficial velocity was set to be from 4200 to 4600 as turbulent flow regime in this experiment. As typical results, Figs. 2 show the time-averaged flow fields and distributions of turbulent kinetic energy in FSS channels with three gap widths, finger length of 54 mm, and staggered finger layout in ZX plane 2 mm away from the bottom channel wall. It is found that it can be seen in the case of C_g= 1 mm thatl ow velocity areas behind fingers are reduced largely and velocity fluctuation almost halves compared to the case with no gap. After considerations about the experimental results of the flow visualizaiton, the channel with FSS in the staggered layout having 1 mm gap width with *d*/*H* = 0.5 or 1 was chosen as one of the optimized channel structures for heat transfer enhancement.

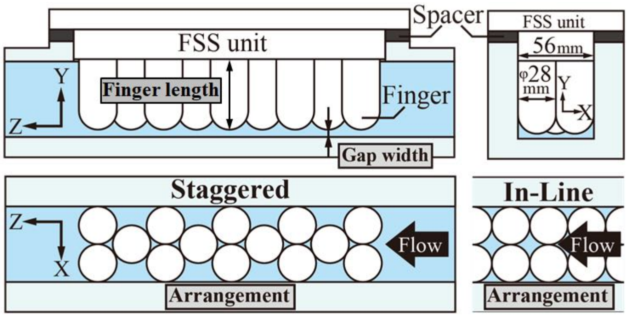

Fig. 1: Detail dimensions of test section

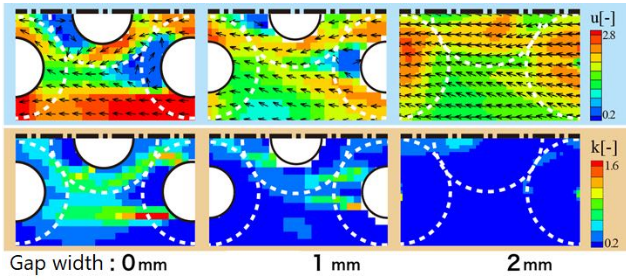

Fig. 2: Effect of gap width in ZX plane

(*H*=54 mm, staggered layout)

3. Heat transfer experiment

For the channel with optimized FSS parameter, a heat transfer experiment was conducted using 7/10-scale model of FSS channel and silicon oil as a simulant of Flibe in terms of high Prandtl number fluid. Heat transfer characteristic obtained from the experiment is shown in Fig. 3. In the figure, the solid line indicated by SPP shows the correlation equation obtained from the reference 3 using a sphere-packed pipe as a heat transfer promoter. When C_g= 0.7 mm, corresponding to the case of C_g= 1 mm in the visualization experiment, heat transfer performance is the most enhanced and almost equal to that of the sphere-packed pipe.

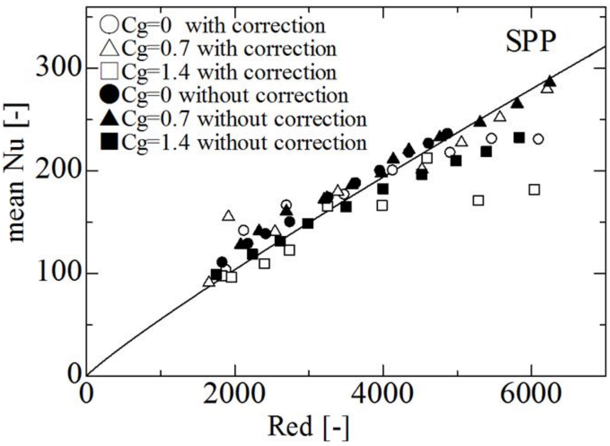

$$Nu_d = 0.1094\,\mathrm{Re}_d^{0.902}\,\mathrm{Pr}^{0.327}\left(\frac{\mu_b}{\mu_w}\right)^{0.144}$$

Fig. 3: Relation between space-averaged Nusselt number and Reynolds number

4. Conclusion

In this study, the structure of cooling channel with FSS was optimized by the flow visualization experiment and its heat transfer characteristic was investigated. It was found that the channel with a slight clearance gap between finger top and heat transfer wall could attain good heat transfer performance with hot spot mitigation.

References :

[1] A. Sagara, Y. Igitkhanov, F. Najmabadi, *Fusion Eng. Des.*, **85** (2010) 1336-1341
[2] S.Ebara, M. Nematollahi, H. Hashizume, *Fusion Eng. Des.*, **89** (2014) 1251–1256
[3] A. Watanabe, S. Ebara, A. Sagara, H. Hashizume, *Fusion Eng. Des.*, **88** (2013) 2357–2360

Thermomechanical modelling of High Molecular Weight semi-crystalline polymers

Project ELyT lab: R6 –Resilient Polymeric cold spray coating

C. A. Bernard[1,2,3], T. Deplancke[4], O. Lame[4], K. Ogawa[2,3], J.-Y. Cavaillé[3]




[1]Frontier Research Institute for Interdisciplinary Sciences, Tohoku University, Sendai, Japan
[2]Fracture and Reliability Research Institute, Tohoku University, Sendai, Japan
[3]ELyTMax, UMI 3757, CNRS—Université de Lyon—Tohoku University International Joint Unit, Tohoku University, Sendai, Japan
[4]MATEIS, INSA LYON, Lyon, France

Abstract:

High molecular weight semi-crystalline polymers are difficult to shape due to their very long chains and strong visco-elastic behavior. Processing these materials required to sinter them (powder)by pressing at high temperature and/or high speed. Even for these loading conditions, the efficiency of the process is far from being optimal. To improve it, we developed numerical models to represent the mechanical behavior of these materials.

1. Introduction

Semi-crystalline polymers exhibit complex microstructure involving crystal network, with crystalline lamellaes and tie molecules, and macromolecular network. In the case of high molecular weight semi-crystalline polymers, they exhibit very long chains, which participate at the same time in the construction of the crystalline lamellae, tie molecules, and macromolecular network [1,2]. These materials are often used for structural and protective applications; however, their behavior is still not well understood and modelled. Therefore, to improve the numerical prediction of such material, it is needed to physically describe the relationship between its microstructure.

For high molecular weight semi-crystalline polymers, Deplancke et al. [3] developed a one-dimensional model based on the evolution of structure between crystals and fibrils within the crystal network. The model assumes that, at room temperature, the amorphous chains (tie molecules, fibrils and macromolecular network) are in their rubbery state. Thus, their behavior, assumed to be hyperelastic, is represented by the 8-chain model [4]. The crystalline structure is represented by an elastic-perfectly-plastic model. On the other hand, they established a relationship between fibrils and crystals through the stress concentration:

$$\sigma_c = k\sigma_f \tag{1}$$

where σ_c is the stress of the crystal, σ_f is the stress of the fibrils and *k* represent the mechanical coupling between fibrils and crystal. Moreover, the stress-strain within the crystal network is represented by the relationships:

$$\begin{cases} \sigma = \varphi\sigma_c + (1-\varphi)\sigma_f \\ \varepsilon = \varphi\varepsilon_c + (1-\varphi)\varepsilon_f \end{cases} \tag{2}$$

This model provides good prediction of the material behavior; however, a three-dimensional model is needed to extend this model to further application.

2. Three-dimensional constitutive model

From the one-dimensional model developed by Deplancke et al. [3], we developed a three-dimensional model based on the polymer physics. The difficulty of the model lies in the consideration of the mechanical coupling with respect of the crystalline ratio. Using the finite strain formalism, we express the total deformation gradient related to crystal network $\mathbb{F}_{CN}$ through:

$$\mathbb{F}_{CN} = \mathbb{F}_f^{1-\varphi}\mathbb{F}_c^{\varphi} \text{ with } \begin{cases} \mathbb{F}_f = \mathbb{F}_f^e\mathbb{F}_f^p \\ \mathbb{F}_c = \mathbb{F}_c^e\mathbb{F}_c^p \end{cases} \quad (3)$$

where φ is the crystalline ratio, subscript 'c' represents the contribution of the crystal lamellae and subscript 'f' represents the contribution of the fibrils within the crystal network. Moreover, each structure can be deformed elastically, defined by superscript 'e', and visco-plastically, defined by superscript 'p'.

The evolutive mechanical coupling between crystal lamellae and fibrils also need to be considered in the three-dimensional model. Unlike Deplancke et al. [3], we propose to introduce the mechanical coupling in the formulation of the deformation gradients instead of stress tensors. Thus, the relationship between fibrils and crystal lamellae is described by ζ parameter through:

$$\mathbb{F}_c = \left(\mathbb{F}_f\right)^{\zeta}. \quad (4)$$

From these constitutive equations, we simulate the mechanical behavior of Ultra High Molecular Weight PolyEthylene (UHMWPE). The numerical predictions are compared with uniaxial compression tests in Figure 1. Fairly good agreement is observed between experimental results and numerical predictions. The next step of this modelling is to introduce these constitutive equations into a finite element software to simulate dynamic applications such as the impact of a polymer particle onto a substrate (ie. Cold-spray process).

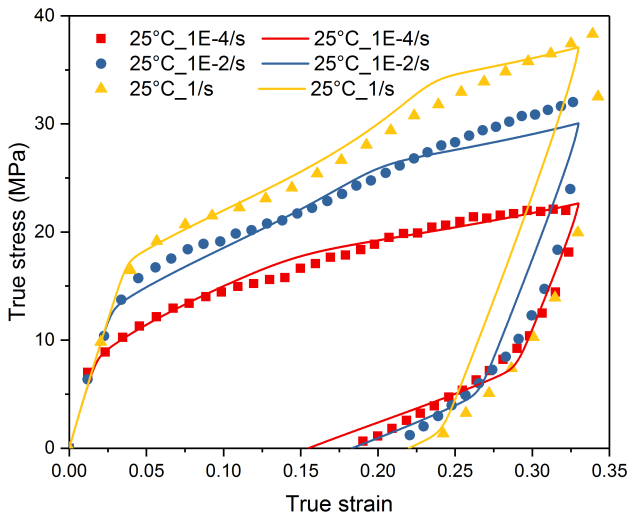

Figure 1: Compressive thermomechanical behavior of UHMWPE. Comparison between experimental results (dot) from Deplancke et al. [3] and 3D numerical predictions (solid).

References:

[1] J. Defebvin et al., *Polymer* **84**, 148-157 (2016).
[2] S. Humbert et al., *Polymer*, **52**(21), 4899-4909 (2011)
[3] T. Deplancke et al., submitted to *Int. J. Plasticity*, (2017)
[4] E.M. Arruda and M.C. Boyce, *J. Mech. Phys. Solids*, **41**(2), 389-412 (1993)

List of Participants

Abdouni	Abdenaceur	LTDS, Ecole Centrale de Lyon	*abde-naceur.abdouni@doctorant.ec-lyon.fr*
Abe	Hiroshi	GSE, Tohoku University	*hiroshi.abe@qse.tohoku.ac.jp*
Adachi	Koshi	GSE, Tohoku University	*koshi@tribo.mech.tohoku.ac.jp*
Arai	Hirokazu	JTEKT	*hirokazu_arai@jtekt.co.jp*
Baulin	Oriane	MATEIS, INSA-Lyon	*oriane.baulin@insa-lyon.fr*
Belin	Michel	LTDS, CNRS	*michel.belin@ec-lyon.fr*
Bernard	Chrystelle	ELyTMaX, Tohoku University	*chrystelle.bernard@rift.mech.tohoku.ac.jp*
Besset	Sébastien	LTDS, Ecole Centrale de Lyon	*sebastien.besset@ec-lyon.fr*
Boulon	Georges	iLM, UCBL	*georges.boulon@univ-lyon1.fr*
Cavaillé	Jean-Yves	ELyTMaX, INSA-Lyon	*jean-yves.cavaille@cnrs.fr*
Chevalier	Jérôme	MATEIS, INSA-Lyon	*jeromechevalier@me.com*
Chiba	Akihiko	IMR, Tohoku University	*a.chiba@imr.tohoku.ac.jp*
Coativy	Gildas	MATEIS, INSA-Lyon	*gildas.coativy@insa-lyon.fr*
Coffigniez	Marion	MATEIS, INSA-Lyon	*marion.coffigniez@insa-lyon.fr*
De Barros Bouchet	Maria Isabel	LTDS, Ecole Centrale de Lyon	*maria-isabel.de-barros@ec-lyon.fr*
Diguet	Gildas	ELyTMaX, Tohoku University	*gildas.diguet.d4@tohoku.ac.jp*
Djaghloul	Mehdi	LTDS, Ecole Centrale de Lyon	*mehdi.djaghloul@ec-lyon.fr*
Ducharne	Benjamin	LGEF, INSA-Lyon	*benjamin.ducharne@insa-lyon.fr*
Ebara	Shinji	GSE, Tohoku University	*shinji.ebara@qse.tohoku.ac.jp*
Fabrègue	Damien	MATEIS, INSA-Lyon	*damien.fabregue@insa-lyon.fr*
Fontaine	Julien	LTDS, CNRS	*julien.fontaine@ec-lyon.fr*
Fridrici	Vincent	LTDS, Ecole Centrale de Lyon	*vincent.fridrici@ec-lyon.fr*
George	Daniel	ICube, Université de Strasbourg	*george@unistra.fr*
Gillot	Frédéric	LTDS, Ecole Centrale de Lyon	*frederic.gillot@ec-lyon.fr*
Gupta	Bhaawan	ELyTMaX, INSA-Lyon/Tohoku University	*bhaawan.gupta@insa-lyon.fr*
Guy	Philippe	LVA, INSA-Lyon	*philippe.guy@insa-lyon.fr*
Hartmann	Daniel	MATEIS, UCBL	*daniel.hartmann@univ-lyon1.fr*
Hemette	Sylvain	LTDS, Ecole Centrale de Lyon	*sylvain.hemette@doctorant.ec-lyon.fr*
Iwasaki	Atsushi	Gunma University	*aiwasaki@gunma-u.ac.jp*
Jay	Laura	LTDS, Ecole Centrale de Lyon	*laura.jay@ec-lyon.fr*
Joly-Pottuz	Lucile	MATEIS, INSA-Lyon	*lucile.joly-pottuz@insa-lyon.fr*
Kada	Tomoyasu	JTEKT	*tomoyasu.kada@jtekt.eu*
Kapsa	Philippe	LTDS, CNRS	*philippe.kapsa@ec-lyon.fr*
Kohl	Manfred	Karlsruhe Institute of Technology	*manfred.kohl@kit.edu*
Kojima	Fumio	Tohoku University	*kojima@koala.kobe-u.ac.jp*
Komiya	Atsuki	IFS, Tohoku University	*komiya@tohoku.ac.jp*
Kosukegawa	Hiroyuki	IFS, Tohoku University	*kosukegawa@wert.ifs.tohoku.ac.jp*
Kubo	Momoji	IMR, Tohoku University	*momoji@imr.tohoku.ac.jp*
Kunishima	Takeshi	JTEKT	*takeshi_kunishima@jtekt.co.jp*
Lallart	Mickaël	LGEF, INSA-Lyon	*mickael.lallart@insa-lyon.fr*

Lame	Olivier	MATEIS, INSA-Lyon	*olivier.lame@insa-lyon.fr*
Long	Yun	LTDS, Ecole Centrale de Lyon	*yun.long@ec-lyon.fr*
Martin	Jean Michel	LTDS, Ecole Centrale de Lyon	jean-michel.martin@ec-lyon.fr
Mary	Nicolas	ELyTMaX, INSA-Lyon	nicolas.mary@insa-lyon.fr
Miki	Hiroyuki	FRIS, Tohoku University	miki@fris.tohoku.ac.jp
Minfray	Clotilde	LTDS, Ecole Centrale de Lyon	clotilde.minfray@ec-lyon.fr
Mohanasundaram	Pradeep	LTDS, Ecole Centrale de Lyon	pradeep.mohanasundaram@ec-lyon.fr
Mokhtari	Morgane	MATEIS, INSA-Lyon	morgane.mokhtari@insa-lyon.fr
Muramoto	Yuta	IFS, Tohoku University	yuta.muramoto@biofluid.ifs.tohoku.ac.jp
Nakamoto	Hiroyuki	INSA-Lyon/Kobe University	nakamoto@panda.kobe-u.ac.jp
Nishi	Yoshitake	Tokai University	*am026429@keyaki.cc.u-tokai.ac.jp*
Ogawa	Kazuhiro	GSE, Tohoku University	*kogawa@rift.mech.tohoku.ac.jp*
Ohara	Yoshikazu	GSE, Tohoku University	*ohara@material.tohoku.ac.jp*
Ohira	Takeyuki	GSE, Tohoku University	*takeyuki.ohira@rbm.qse.tohoku.ac.jp*
Ohta	Makoto	IFS, Tohoku University	*ohta@biofluid.ifs.tohoku.ac.jp*
Rieu	Jean-Paul	iLM, UCBL	*jean-paul.rieu@univ-lyon1.fr*
Rodney	David	iLM, UCBL	*david.rodney@univ-lyon1.fr*
Sebald	Gael	ELyTMaX, INSA-Lyon	*gael.sebald@insa-lyon.fr*
Shimoyama	Koji	IFS, Tohoku University	*shimoyama@tohoku.ac.jp*
Shirai	Atsushi	IFS, Tohoku University	*shirai@ifs.tohoku.ac.jp*
Shoji	Tetsuo	NICHe, Tohoku University	*tshoji@fri.niche.tohoku.ac.jp*
Soma	Tomoya	NEC	*t-soma@cq.jp.nec.com*
Takagi	Toshiyuki	IFS, Tohoku University	*takagi@ifs.tohoku.ac.jp*
Takeda	Sho	IFS, Tohoku University	*takeda@wert.ifs.tohoku.ac.jp*
Tanno	Kanako	ELyTMaX, Tohoku University	*kanako.tanno.a5@tohoku.ac.jp*
Tene Deffo	Yves Armand	LGEF, INSA-Lyon	*ytenedeffo@yahoo.com*
Ter-Ovanessian	Benoît	MATEIS, INSA-Lyon	*benoit.ter-ovanessian@insa-lyon.fr*
Tokumasu	Takashi	IFS, Tohoku University	*tokumasu@ifs.tohoku.ac.jp*
Tupin	Simon	IFS, Tohoku University	*simon@biofluid.ifs.tohoku.ac.jp*
Uchimoto	Tetsuya	IFS, Tohoku University	*uchimoto@ifs.tohoku.ac.jp*
Unoura	Sayaka	ELyTMaX, Tohoku University	*sayaka.unoura.a8@tohoku.ac.jp*
Wada	Naoto	IFS, Tohoku University	*naotowada2011@gmail.com*
Watanabe	Yutaka	GSE, Tohoku University	*yutaka.watanabe@qse.tohoku.ac.jp*
Yakeno	Aiko	IFS, Tohoku University	*yakeno@edge.ifs.tohoku.ac.jp*
Yamanaka	Kenta	IMR, Tohoku University	*k_yamanaka@imr.tohoku.ac.jp*
Yoshida	Kazuito	DENSO Corporation	*kazuhito_yoshida@denso.co.jp*
Yoshimi	Kyosuke	GSE, Tohoku University	*yoshimi@material.tohoku.ac.jp*